Title:

Nicotinic acetylcholine receptors in a songbird brain

Norman Chinweike Asogwa[1#], Noriyuki Toji[2#], Ziwei He[1], Chengru Shao[1], Yukino Shibata[1], Shoji Tatsumoto[3], Hiroe Ishikawa[3], Yasuhiro Go[3,4,5], and Kazuhiro Wada[1, 2*]

[1]Graduate School of Life Science, Hokkaido University, Sapporo, Japan
[2] Faculty of Science, Hokkaido University, Sapporo, Japan
[3]Cognitive Genomics Research Group, Exploratory Research Center on Life and Living Systems, National Institutes of Natural Sciences, Okazaki, Japan
[4]School of Life Science, SOKENDAI (The Graduate University for Advanced Studies), Okazaki, Japan
[5]Department of Physiological Sciences, National Institute for Physiological Sciences, Okazaki, Japan

[#] These authors contributed equally to this work.

*Correspondence
Kazuhiro Wada, MD, PhD
Faculty of Science, Hokkaido University,
Room 910, Building No.5,
North 10, West 8, Kita-ku, Sapporo, Hokkaido
060-0810, Japan,
Email: wada@sci.hokudai.ac.jp

Abstract

Nicotinic acetylcholine receptors (nAChRs) are ligand-gated ion channels that mediate fast synaptic transmission and cell signaling, which contribute to learning, memory, and the execution of motor skills. Birdsong is a complex learned motor skill in songbirds. Although the existence of 15 nAChR subunits has been predicted in the avian genome, their expression patterns and potential contributions to song learning and production have not been comprehensively investigated. Here we cloned all the 15 nAChR subunits (ChrnA1–10, B2–4, D, and G) from the zebra finch brain and investigated the mRNA expression patterns in the neural pathways responsible for the learning and production of birdsong during a critical period of song learning. Although there were no detectable hybridization signals for ChrnA1, A6, A9, and A10, the other 11 nAChR subunits were uniquely expressed in one or more major subdivisions in the song nuclei of the songbird brain. Of these 11 subunits, ChrnA3–5, A7, and B2 were differentially regulated in the song nuclei compared with the surrounding anatomically related regions. ChrnA5 was upregulated during the critical period of song learning in the lateral magnocellular nucleus of the anterior nidopallium. Furthermore, single-cell RNA sequencing revealed ChrnA7 and B2 to be the major subunits expressed in neurons of the vocal motor nuclei HVC and robust nucleus of the arcopallium, indicating the potential existence of ChrnA7-homomeric and ChrnB2-heteromeric nAChRs in limited cell populations. These results suggest that relatively limited types of nAChR subunits provide functional contributions to song learning and production in songbirds.

Keywords

acetylcholine, nicotinic receptors, sensorimotor learning, zebra finch, vocal learning

Abbreviations

A, arcopallium; **AA**, anterior arcopallium; **AD**, dorsal arcopallium; **AI**, intermediate arcopallium; **AId**, dorsal part of AI; **AIv**, ventral part of AI; AMVi, intermediate part of the medial ventral arcopallium; **AP**, posterior arcopallium; **Area X**, striatum song nucleus Area X; **B**, nucleus basorostralis; **Cb**, cerebellum; **CMM**, caudomedial mesopallium; **DLM**, dorsolateral nucleus of medial thalamus; **DM**, dorsal medial nucleus of the midbrain; **dn**, deep nuclei of the cerebellum; **E**, entopallium; **g**, granular layer of the cerebellar cortex; **Gp**, globus pallidus; **H**, hyperpallium; **Hp**, hippocampus; **HVC**, acronym as proper name used for the song nucleus; **IPc**, nucleus isthmi pars parvocellularis; **L**, field L subdivision of nidopallium; **LMAN**, lateral magnocellular nucleus of the anterior nidopallium; **MMAN**, medial magnocellular nucleus of the anterior nidopallium; **M**, mesopallium; m, molecular layer of the cerebellar cortex; **MLd**, nucleus mesencephalicus lateralis pars dorsalis; **N**, nidopallium; **NCM**, caudomedial nidopallium; **P**, pallidum; **p**, Purkinje cell layer of the cerebellar cortex; **Pt**, nucleus pretectalis; **RA**, robust nucleus of the arcopallium; **Rt**, nucleus rotundus; **SP**, nucleus subpretectalis; **Spl**, nucleus spiriformis lateralis; **Str**, striatum; **TeO**, tectum opticum; **Tha**, thalamus; **TnA**, nucleus taenia; **w**, white matter layer in the cerebellum

Introduction

In the CNS, acetylcholine receptors (AChRs) mediate acetylcholine (ACh) function in the arousal-related enhancement of sensory processing (Fu et al., 2014; Herrero et al., 2008; Shea, Koch, Baleckaitis, Ramirez, & Margoliash, 2010), cognition and memory (Anagnostaras et al., 2003; Hasselmo, 2006; Wallace & Bertrand, 2013), motor skill acquisition (Conner, Culberson, Packowski, Chiba, & Tuszynski, 2003; H. Q. Li & Spitzer, 2020; Thouvarecq, Protais, Jouen, & Caston, 2001), and selective attention (Noudoost & Moore, 2011; Parikh, Kozak, Martinez, & Sarter, 2007; Sarter, Bruno, & Turchi, 1999). These AChR-mediated physiological processes are likely shared among vertebrate species because of the high conservation of AChR protein sequences and their related signaling pathways (Dajas-Bailador & Wonnacott, 2004; Gotti & Clementi, 2004; Pedersen, Bergqvist, & Larhammar, 2019). However, except for the extensively studied species of mammals, fundamental knowledge about the expression of AChRs in the CNS is limited in vertebrates, including avian species.

AChRs comprise two major classes: muscarinic and nicotinic receptors (Gotti & Clementi, 2004; Kruse et al., 2014). Nicotinic AChRs (nAChRs) are ligand-gated ion channels that are permeable to Na^+, K^+, and Ca^{2+} ions. Hence, nAChRs mediate not only fast synaptic transmission but also intracellular signaling via Ca^{2+}-dependent signaling machinery (Dajas-Bailador & Wonnacott, 2004; Gotti et al., 2009; Wonnacott, 1997; M. Zoli, Pucci, Vilella, & Gotti, 2018). Functional nAChRs exist in either homo- or hetero-pentameric configurations formed from α subunits (ChrnAs) as the ligand binding subunits and β subunits (ChrnBs) as structural subunits (Couturier et al., 1990; Gotti et al., 2009; N. Le Novere, Corringer, & Changeux, 2002; M. Zoli, Pistillo, & Gotti, 2015). To date, the existence of 15 nAChR subunits (ChrnA1–10, B2–4, D, and G) is predicted in the genome of avian species. In comparison, mammals do not retain ChrnA8 but express two additional subunits, ChrnB1 and ChrnE. Although the number and types of nAChR subunits are not perfectly conserved between avian and mammalian species, the phylogenetic relationship between homologous subunit genes is highly conserved (Lovell et al., 2020; Pedersen et al., 2019; Sargent, 1993; Wada et al., 1988) (**Figure 1(a)**).

Based on their pharmacological and structural properties, nAChR subunits are divided into three major functional groups: muscle subunits (ChrnA1, B1, D, E, and G), standard neuronal subunits that form heteromeric receptors with pairwise α (ChrnA2–6) and β (ChrnB2–4)

subunit combinations, and other neuronal subunits (ChrnA7–10) that can form homomeric nAChRs (Gotti et al., 2009; M. Zoli et al., 2015). These different combinations are associated with specific physiological and developmental features (Gotti et al., 2009; Role & Berg, 1996; Michele Zoli, Le Novere, Hill, & Changeux, 1995). Some neuronal nAChR subunits are selectively expressed in specific subregions of the CNS in vertebrates, including mammals (Dineley-Miller & Patrick, 1992; Han et al., 2000; Wada et al., 1988; Winzer-Serhan & Leslie, 1997; Michele Zoli et al., 1995) and birds (Halvorsen & Berg, 1990; Lovell, Huizinga, Friedrich, Wirthlin, & Mello, 2018; Morris et al., 1990; Whiting et al., 1991). However, at the single-cell level, the combinations of nAChR subunits that are coexpressed in the CNS have not yet been fully elucidated.

Oscine songbirds learn birdsong, a complex vocal skill, during a critical period that comprises the sensory and sensorimotor learning phases (Brenowitz & Beecher, 2005; Doupe & Kuhl, 1999; Marler & Slabbekoorn, 2004). During the sensory learning phase, a juvenile bird listens to and memorizes a copy of the tutor song, while during the sensorimotor learning phase, the pupil bird practices singing repeatedly and refines its vocal outputs to mimic the memorized tutor song model through auditory feedback. Song acquisition is shaped by singing subsong, plastic song, and crystallized song. The learning and production of birdsong are controlled by specialized neural circuits known as song pathways (**Figure 1(b)**). These song pathways are organized into two anatomically and functionally distinct neural circuits called the anterior pathway (AFP) and vocal motor pathway (VMP), with interconnecting song nuclei. The AFP consists of a pallial–basal ganglia–thalamic connection with three song nuclei: the lateral magnocellular nucleus of the anterior nidopallium (LMAN), nucleus Area X in the striatum, and anterior part of the medial nucleus of the dorsolateral thalamus (aDLM, the part of DLM that receives afferent input from Area X and sends output projection to LMAN) (Luo, Ding, & Perkel, 2001). The VMP comprises the HVC (acronym as proper name) and robust nucleus of the arcopallium (RA). Although the VMP participates in song production, the AFP is not required for singing but is a crucial neural circuit for song learning and maintenance by generating vocal fluctuations (Andalman & Fee, 2009; Bottjer, Miesner, & Arnold, 1984; Brainard & Doupe, 2000; Kao, Doupe, & Brainard, 2005; Nottebohm, Stokes, & Leonard, 1976; Scharff & Nottebohm, 1991).

In songbirds, ACh and associated enzymes such as acetylcholinesterase (AChE) and choline acetyltransferase (ChAT) exist in several song nuclei (Ryan & Arnold, 1981;

Sakaguchi & Saito, 1989; Zuschratter & Scheich, 1990). Song nucleus HVC receives cholinergic afferents from the ventral pallidum of the basal forebrain, a brain region homologous to the nucleus basalis of Meynert in mammals (R. Li & Sakaguchi, 1997; Reiner et al., 2004). In addition, the concentration of ACh increases in the song nuclei HVC, RA, and LMAN of male zebra finches during the early critical period of song learning (Sakaguchi & Saito, 1989). Similarly, AChE is highly enriched in the song nuclei HVC, RA, and LMAN during this critical period (Ryan & Arnold, 1981; Sadananda, 2004; Sakaguchi & Saito, 1991). These findings suggest the expression of AChRs in the song nuclei that mediates cholinergic functions during song learning and production. Our previous investigation revealed developmental regulation and inter- and intra-specific differences in the expression of muscarinic AChR subunits (mAChRs) in the song pathways (Asogwa, Mori, Sanchez-Valpuesta, Hayase, & Wada, 2018). In contrast to mAChRs, only a limited number of nAChR subunits have been reported to be expressed in the songbird brain (Lovell, Clayton, Replogle, & Mello, 2008; Lovell et al., 2018; Watson, Adkins‐Regan, Whiting, Lindstrom, & Podleski, 1988). ZEBrA, the online public repository of gene expression in the zebra finch brain (http://www.zebrafinchatlas.org/), currently provides *in situ* hybridization information for nAChR subunits ChrnA3–5, A7, B2, and B3 (Lovell et al., 2020). However, the precise number of nAChR subunits involved and their expression levels and patterns, particularly in the song nuclei, during song development have not been fully investigated.

Here, we cloned 15 nAChR subunits from the zebra finch brain; however, no detectable signal was obtained in the brain sections by *in situ* hybridization for four subunits. The remaining 11 subunits were expressed to varying levels in at least one brain subdivision (pallium, hippocampus, subpallium, midbrain, or cerebellum). Specifically, the expression of ChrnA3–5, A7, and B2 revealed unique specializations in one or more song nuclei. In addition, the single-cell transcriptional analysis revealed the potential existence of ChrnA7-homomeric and ChrnB2-heteromeric nAChRs in the vocal motor nuclei.

Materials and Methods

Animals

Male zebra finches (*Taeniopygia guttata*) were used for this study at the three stages of song development: subsong (30–45 post-hatching day [phd], n = 6), plastic song (50–65 phd, n = 6), and the crystallized song (>120 phd, n = 6). Because of the limited number of brain sections available in one of six brains, only five birds at the subsong stage were utilized for *in situ* hybridization with ChrnA4, A5, and A10 probes. For that same reason, *in situ* hybridization for ChrnA4 and A10 probes was performed with five birds at the plastic song stage. The birds were used from our breeding colonies at Hokkaido University, Sapporo, Japan. Photoperiod was maintained at 13h light/11 hr dark cycle with free access to food and water. Song developmental stages were confirmed by the probability density distribution of syllable duration in songs (Aronov, Veit, Goldberg, & Fee, 2011). All animal-based procedures complied with the regulations of the Committee on Animal Experiments of Hokkaido University. These regulations are requirements of the National Regulations for Animal Welfare in Japan (Law for the Humane Treatment and Management of Animals, partial amendment number No.105, 2011).

RT-PCR and cloning of nAChR subunits

Attempts were made to clone, from the zebra finch brain, all 15 nAChR subunits identified or predicted in birds (Pedersen et al., 2019; Sargent, 1993). The ChrnA7-like subunit in the National Centre for Biotechnology Information (NCBI, accession # XM_002187662) was labeled as ChrnA8. RT-PCR was performed on total RNA collected from adult male zebra finch brains before light-ON in the morning. Total RNA was extracted by TRIzol Reagent (Thermo Fisher), treated with DNaseI to digest contamination from genome DNA, and transcribed to complementary DNA (cDNA) using Superscript Reverse Transcriptase (Invitrogen) with oligo(dT) primers. In the first attempt to clone the targeted subunits, we designed PCR oligo-primers to target protein regions that are conserved between mammals, birds, reptiles, and amphibians (**Table 1**). When the initial cloning failed, we used putative mRNA sequences predicted by the NCBI for primer design. Partial DNA fragment of each targeted nAChR subunit was amplified by PCR (Ex Taq polymerase, Takara Bio) using the synthesized cDNA template and cloned into pGEM-T easy plasmids (Promega) based on a previous method (Asogwa et al., 2018; Wada, Sakaguchi, Jarvis, & Hagiwara, 2004). The cloned cDNA fragments were verified by DNA sequencing. The sequence identities of cloned cDNA fragments and their predicted amino acids were authenticated by comparison

with the transcripts of nAChR subunits in the zebra finch, chicken, and human in the NCBI, using Nucleotide and Protein BLASTs. The cloned partial cDNA sequences of 15 nAChR subunits were assigned in GenBank with accession numbers OL679454–OL679467 and OM201170 (**Table 1**).

Radioisotope *in situ* hybridization and quantification of mRNA expression

Brain tissues were sampled from birds in dark, silent, and non-singing conditions. To ensure that mRNA expression was not due to singing or hearing songs, the birds were kept in a sound-attenuation box under these conditions for at least 10 hr prior to euthanasia and sacrifice. Brain tissues were put in plastic molds with tissue-compounding medium (Tissue-Tek, Sakura) and immediately transferred onto crushed dry ice. Subsequently, they were stored at ‑80℃ until sectioning. The brain tissues were sectioned at 12 µm-thickness on the sagittal plane and mounted on silane-coated slides. The radioisotope *in situ* hybridization and quantification of expressed mRNA levels were conducted according to previous studies (Asogwa et al., 2018). Using specific T7 or SP6 RNA polymerases (Roche) to the inserted sense-/antisense direction of nAChR subunits, ^{35}S-labeled riboprobes were synthesized from the T7 or SP6 promoter sites of pGEM-T. Fresh frozen brain sections were fixed in 3% paraformaldehyde/1×phosphate-buffered saline (PBS, pH 7.0), washed three times in 1×PBS, acetylated, washed three times in 2×SSPE, dehydrated in ascending ethanol concentrations (50, 70, 90, and 100%), and then air-dried. Each Riboprobe (10^6 cpm) was mixed with 150 µl of hybridization buffer (50% formamide; 10% dextran sulfate; 1×Denhart's solution; 12 mM EDTA, pH 8.0; 10 mM Tris–HCl, pH 8.0; 30 mM NaCl; 0.5 µg/µl yeast tRNA; and 10 mM dithiothreitol. Hybridization was performed in an oil bath for 14 hr at 65℃. Slides were next washed stepwise in two changes of chloroform, in 2×SSPE/0.1% 2β-mercaptoethanol for 30 min, in 50% formamide/0.1% 2β–mercaptoethanol for 60 min, twice in 2×SSPE/0.1% 2β-mercaptoethanol for 30 min each, and twice in 0.1× SSPE/0.1% 2β-mercaptoethanol for 15 min each. For ChrnA2, because of the high %GC contents (65% GC) of its probe, hybridization and washing temperatures were set at 68.5℃. The slides were dehydrated in ascending ethanol concentrations (50, 70, 90, and 100%), air-dried, and exposed to BioMax MR Films (Kodak) for 4–5 days before development. mRNA signals were quantified from X-ray films by digitally scanning them under a microscope (Z16 Apo, Leica, Buffalo Grove, IL) that was connected to a CCD camera (DFC490, Leica), with Leica Application Suite, version 3.3.0 (Leica). Light and camera settings were maintained constant for all images to avoid biased comparisons. Images were converted to a 256-gray scale. mRNA expression

levels were quantified as mean pixel intensities using Adobe Photoshop (CS2, Adobe Systems, San Jose, CA, RRID: SCR_014199). After X-ray film exposure, brain slides were Nissl-stained with Cresyl violet acetate solution (Sigma, St Louis, MO, USA) to aid visual evaluation of anatomical subregions. For the figure presenting mRNA expression in the brain, images of *in situ* hybridization taken in sagittal sections were oriented with the rostral side to the right and the dorsal side upward, and the black-and-white negatives were inverted, so that white represents mRNA signal. Based on careful comparison of *in situ* hybridization images taken from 10 birds, we were able to distinguish real signals from artifacts. Apparent artifacts from *in situ* hybridization images were identified as shown in Figures 2, 3, and 4, and were removed in Photoshop using The Spot Healing Brush Tool function.

Single-cell RNA sequencing

The brain of an adult male zebra finch was used for single-cell RNA sequencing (scRNA-seq) experiment. The bird was placed in a sound-attenuating box overnight under silent and dark conditions. The next morning before light onset, the bird under deep anesthesia was perfused with ice-cold Cutting Buffer (Saunders et al., 2018). Then, the telencephalon was removed and kept in ice-cold Cutting Buffer until sectioning. Brain sections were cut at 400 µm in the sagittal plane in ice-cold Cutting Buffer with a microslicer (DTK-1000, DOSAKA EM). HVC and RA tissues were punched out with Miltex Biopsy Punch (1 mm diameter; Ted-pella Inc.), frozen in sample storage buffer with 0.2 U/mL RNase inhibitor (Takara), and 10% DMSO in 1xPBS and stored at –80 ℃ until nuclei isolation. Punched tissues were homogenized in 750 µl of ice-cold Nuclei PURE Lysis Buffer using a glass Dounce tissue grinder (Wheaton) (40 times with tight pestle), centrifuged at 500x g for 10 minutes at 4 ℃, washed with 1 mL of Nuclei Wash and Resuspension Buffers. After centrifugation, the supernatant was removed, while the nuclei were suspended in 120 µL of Nuclei Wash and Resuspension Buffers with DAPI and filtered with 40 µm cell strainers. Isolated cell nuclei were purified with a cell sorter (SH800, Sony) using DAPI fluorescence. The 10× Chromium libraries were prepared using Chromium Single Cell Library Kit v3 (PN-1000092, 10x Genomics) according to the manufacturer's protocol. cDNA along with cell barcode identifiers were PCR-amplified, while sequencing libraries were prepared. The constructed library was sequenced on MGI DNBSEQ-G400 (150 bp Paired-end) platform. The Cell Ranger Software Suite (v4.0.0) was used to perform sample de-multiplexing, barcode processing, and single-cell 3' unique molecular identifier (UMI) counting. Splicing-aware aligner STAR was used in FASTQs alignment with a zebra finch reference genome

(bTaeGut1_v1.p, GCF_003957565.1 based custom reference genome). Cell barcodes were determined based on the distribution of UMI counts automatically.

Cell cluster Analysis

The R package Seurat v.3 was used for the following data filtering and analyses (Stuart et al., 2019). Filtering criteria applied to the data, using 'CreateSeuratObject,' included min.cells = 3, and min.features = 200. After filtering, a total of 6,510 and 6,977 cells in HVC and RA, respectively, were left for further analysis. The filtered gene-barcode matrix was first normalized using "LogNormalize" methods with default parameters. The top 2,000 variable genes were then identified using the "vst" method in Seurat FindVariableFeatures function. Principal component analysis (PCA) was performed using the top 2,000 variable genes. UMAP was performed on 27 to 31 principal components for visualizing the cells. Meanwhile, graph-based clustering was performed on the PCA-reduced data for clustering analysis with Seurat v.3. Clusters were determined using FindNeighbors (with 27 to 31 principal components) and FindClusters (resolution=1). The expression of established marker genes was used to assign identities for each cluster: SLC17A6 for glutamatergic neurons; GAD1 and GAD2 for GABAergic neurons; SOX4 and SOX11 for neuronal precursors; SLC15A2, SLC1A2, and ASPA for astrocytes; PDGFRA and NKX2.2 for oligodendrocyte precursor cells (OPCs); PLP1 and ST18 for oligodendrocytes; and CSF1R and IKZF1 for microglia (Saunders et al., 2018; Tasic et al., 2016; Tasic et al., 2018; Zhang et al., 2014). Subclusters in glutamatergic neurons in HVC were identified based on a previous report (Colquitt, Merullo, Konopka, Roberts, & Brainard, 2021) and *in situ* hybridization database, ZEBrA (Lovell et al., 2020): GFRA1 and UTS2B were used as marker genes for $HVC_{(RA)}$ neurons projecting to RA (Bell et al., 2019); NTS and SCUBE1 for $HVC_{(X)}$ neurons projecting from HVC to Area X and RA neurons projecting to the nucleus of cranial nerve XII; GRIA4, GRM1, and CACNA2D1 for surrounding caudal nidopallium (cN) neurons; and CACNA1H, MGAT4C, and ADYAP1 for RA surrounding arcopallial neurons. Three unknown clusters with no specific marker gene and several small clusters (less than 60 cells in each) were filtered out. Each neural cell-type was isolated and re-clustered based on the expression of ChrnA3–5, A7, and B2 and two to four other genes specifically expressed in each using PCA implemented in the RunPCA function of Seurat. Subtype specific genes included KCNH1 and ROBO2 for $HVC_{(RA)}$ neurons; SRD5A2 and SLIT3 for $HVC_{(X)}$ neurons; SRD5A2 and SLC4A11 for RA projection neurons; GPC6, FOXP2, MAF, and VSTM2A for interneurons; and CELF2, DACH2, LOC115498355, and SDCCAG8 for HVC progenitor neurons. Then

UMAP was performed on all principal components in each cell type for visualizing cell clusters formation based on CHRN family gene expression patterns.

Statistical analyses

Data obtained on the developmental regulation of different AChR subunits were analyzed with statistical software SPSS (IBM Statistics, Armonk, NY). Differences in mRNA expression levels of ChrnA3–5, A7, and B2 in the song nuclei were analyzed after a test for homogeneity of variance, using one-way analyses of variance (ANOVA) followed, when appropriate, by Scheffe's *F* tests.

Results

nAChR subunits expressed in zebra finches

Using cDNAs synthesized from the brain tissues of an adult male zebra finch and oligo-primers specific to protein-coding regions of nAChR, we cloned partial cDNA fragments of all 15 nAChR subunits (ChrnA1–10, B2–4, D, and G) predicted in avian species using RT-PCR (**Table 1**). The partial cDNAs and the corresponding translated amino acid sequences of the 15 cloned nAChRs were verified by comparing each nAChR subunit transcript predicted for the zebra finch with those previously identified in chicken and human. We confirmed that the match between each cloned partial nAChR subunit and the predicted full-length mRNA of the targeted subunits in the zebra finch was ≥98.6% at nucleotide level and ≥99.3% at protein level (**Tables 1** and **2**). This result was consistent with the NCBI database prediction of nAChR transcripts from the zebra finch genome and indicated that 15 nAChR subunits were expressed in the zebra finch brain.

To evaluate the confounding cross-hybridization potential of *in situ* hybridization probes, we calculated the fraction (as a percentage) of sequence identities between each cloned subunit fragment and all non-targeted nAChR subunit protein-coding regions (**Table 2**). This analysis revealed that while the cloned partial cDNAs had near perfect match (≥98.6% similarity highlighted in red on the diagonal) with their targeted subunit sequences (as described above), the match with any non-targeted cross-nAChR subsequence was ≤76.8% (off-diagonal similarity values). Only 21 (10%) of the 210 off-diagonal values were greater that 50% (entries in various shades of pink). We speculated that this level of mismatch was sufficient to avoid confounds from cross-hybridization with non-targeted nAChR subunits.

The cloned partial fragments of ChrnA1–10, B2–4, D, and G was used in *in situ* hybridization experiments to reveal the distribution of nAChR subunit expression in the brain tissues of adult male zebra finches. Eleven (ChrnA2–5, A7, A8, B2–4, D, and G) of the 15 cloned subunits were expressed in unique patterns in at least one of the following brain regions: pallium, thalamus, midbrain, and cerebellum (**Figures 2, 3, 4**). In contrast, the four remaining receptor subunits, ChrnA1, A6, A9, and A10, exhibited few or no detectable mRNA signals throughout the whole brain. Therefore, no further investigations into mRNA expression were conducted for these four subunits.

Expression of nAChR subunits in telencephalic subregions

The pattern of mRNA expression and amount of each nAChR subunit available were evaluated in the following five major pallial telencephalic brain subdivisions: hyperpallium, mesopallium, nidopallium, arcopallium, and hippocampus. ChrnA4 and A7 were highly expressed in the mesopallium, arcopallium, and hippocampus compared with the other pallial subdivisions (**Figures 2, 3, 5**). In contrast, ChrnA2, A5, and B2 showed consistent but relatively low-level expression within all telencephalic subdivisions. As distinct exceptions, ChrnA3 and B4 showed similar expression patterns, strictly restricted to the mesopallium. Taken together, the mRNA for ChrnA3, A4, A7, and B4 exhibited a higher level of expression in the mesopallium than in the other pallial subdivisions (**Figure 5**).

Consistent with the pattern of nAChR subunit expression in the nidopallium, mRNAs of ChrnA2, A7, and B2 were uniformly throughout the caudomedial nidopallium (NCM), which is known as the avian secondary auditory area (**Figure 6**). Conversely, ChrnA5 expression was more restricted to the rostral portion of NCM, where its expression was higher than in the anterior nidopallium. ChrnA3, A4, and B4 were expressed at very low or undetectable levels in NCM as in most of the other nidopallial regions.

Subunits ChrnA4 and ChrnA7 showed differential expression in the subdomains (Mello, Kaser, Buckner, Wirthlin, & Lovell, 2019) of the arcopallium (**Figure 7(a)**). ChrnA4 was intensely expressed in most arcopallial subdomains except in the dorsal part of AI (AId), where it was almost fully suppressed. ChrnA7 distinctly showed higher expression in the caudal areas, including AD and the ventral part of AP, than in all other subdomains. ChrnA2, A5, and B2 were expressed with nearly uniform intensities at low-to-moderate levels throughout the subdomains of the arcopallium. ChrnA3 and B4 expressions were undetectable. Quite uniquely, ChrnA8 mRNA expression was well-defined and confined in the intermediate part of the medial ventral arcopallium (AMVi), so-called nucleus taenia (TnA) (**Figure 7(b)**).

The primary sensory input regions located within the nidopallium, including field L (auditory), entopallium (visual), and nucleus basorostralis (somatosensory/trigeminal), are anatomically defined in Nissl-stained tissue by a higher cell density relative to the surrounding nidopallium. While ChnrA2 mRNA was lightly expressed with near uniform intensity in each surrounding region of the nidopallium, expression of all other nAChR subunits was apparently absent in the primary sensory input regions (**Figures 2, 3, 4**).

Similarly, ChrnA3, A5, and B4 expressions were suppressed in the subpallial striatum and globus pallidus. In contrast, ChrnA4 was uniquely expressed in the striatal region, with small dots, suggesting its selective expression in a specific cell type (**Figure 2**). The cells labeled for ChrnA4 expression, seen as intense isolated small dots, were clearly identified as a sparse cell population in the striatum by the Zebra Finch Expression Brain (ZEBrA) atlas based on digoxigenin-based labeling *in-situ* hybridization method. Similarly, ChrnB3 mRNA expression was observed specifically in the lateral pallium (**Figure 4**). In contrast, ChrnA2, A7, and B2 expressions in the striatum and pallidum were similar to those in pallial regions.

In the hippocampus, we observed a unique form of nAChR subunit specialization that was further portrayed according to the delineation of the hippocampus into dorsal and ventral subdivisions (**Figure 8**) with ChrnA3 expression occurring dorsally and ChrnA4 and A7 ventrally, suggesting a potential distinction of ACh function between the proximal and distal parts. Furthermore, ChrnA4 and A7 were even more expressed in the mesopallium, exhibiting seamless expression from the mesopallium to the ventral hippocampus. Notably, the expression of ChrnA3 was also confined to the medial caudal part of the hippocampus (**Figure 2**). In contrast to these selective expressions of ChrnA3, A4, and A7 subunits, ChrnA2 and B2 were expressed equally in the dorsal and ventral hippocampus. However, ChrnA5 and B4 expression levels were nearly undetectable in the hippocampus.

Expression of nAChR subunits in the midbrain and cerebellum

Further investigation revealed more specializations for ChrnA2–5, A7, A8, and B2–B4 in the nuclei/parts of the midbrain (**Figure 9**). Specifically, the nucleus pretectalis (Pt) and spiriform lateralis (Spl) were strongly labeled by ChrnA2, A4, A5, A7, and B2. While ChrnA4 and A5 were more intensely expressed both in Pt and Spl than in other midbrain nuclei, ChrnA7 was selectively expressed only in Pt. Conversely, ChrnA2 and B2 mRNA expressions were higher in Spl than in Pt. However, the expression of these subunits was almost completely suppressed below signal detection in the nucleus rotundus (Rt). There were exceptions, suggesting a selective cell type expression in Rt: ChrnA2 and B2 were observed with low-to-moderate expression, and ChrnA8, with sporadic expression. ChrnA2, A5, and B2 showed low-level expression in the dorsomedial nucleus of the midbrain (DM), namely, the midbrain vocal center, and the nucleus mesencephalicus lateralis pars dorsalis (MLd), which forms the avian homologue of the central nucleus of the mammalian inferior colliculus (Boord, 1968; Woolley & Portfors, 2013). In addition, ChrnA7 mRNA was

selectively expressed in the ventral part of MLd (near the 3rd ventricle). However, most nAChR subunits were undetected in these regions. The nuclei subpretectalis (SP) and isthmi pars parvocellularis (IPc) play crucial roles in the regulation of visual figure-ground discrimination (Schryver & Mysore, 2019; Scully, Acerbo, & Lazareva, 2014). Here, ChrnB4 showed clear and specific expression in SP, while in contrast, IPc was labeled with high levels of ChrnA4, A5, and B3 expression (but ChrnA4 expression was suppressed in the lateral part of IPc; **Figure 2**). Overall, these results indicated that nAChR subunits are expressed differently in various combinations in the subnuclei/parts of the midbrain.

The layers of tectum opticum (TeO) also revealed distinct patterns of nAChR subunit distribution. According to Cajal's definition (Ramon y Cajal, 1911), there are about 15 histologically identifiable layers in the avian TeO (Wylie, Gutierrez-Ibanez, Pakan, & Iwaniuk, 2009). In this study, five layers (layers 4, 6, 8, 10, and 13) were clearly differentiated according to the labeling patterns/intensities of ChrnA2, A4, A5, A7, A8, B2, and B3 mRNAs (**Figure 9**). Unlike ChrnA3 and B4, whose expression is clear in the mesopallium, these subunits were completely downregulated in all identified layers and subnuclei of TeO. ChrnA4, A7, A8, and B3 were more highly expressed in the deeper layers (layers 8–13) than in the more peripheral layers (layers 4–6), although their downregulation was not as great as that of ChrnA3 and B4. However, ChrnA2, A5, and B2 showed moderate-to-high levels of expression in all of the identified tectal layers.

We further examined the expression patterns of ChrnA2–5, A7, B2–4, D, and G in four anatomical layers of the cerebellum (the molecular, Purkinje cell, granular, and white matter layers). However, even though ChrnA2, D, and G were expressed in the granular layer, their mRNA signals were very weak (**Figure 10**), and those for ChrnA3 and B4 mRNA were almost undetectable. Moreover, whereas ChrnA4 and B2 were clearly expressed in the granular layer, ChrnA7 was selectively expressed in Purkinje cell layer. The expression of ChrnA5 was intense in both the granular and Purkinje cell layers, while ChrnB3 showed selective stronger expression at the top and bottom parts of the granular layer than in other parts of the cerebellum.

Overall, the expressions of 4 of the 15 cloned AChR subunits (ChrnA1, A6, A9, and A10) were very low or below detectable levels throughout the entire brain. However, expression of 11 subunits (ChrnA2–5, A7, A8, B2–4, D, and G) showed unique combinations of spatial

patterns and intensities in at least one subregion of the pallium, thalamus, midbrain, and cerebellum (**Figure 11**).

Differential expression of nAChR subunits in song nuclei

Of the 15 nAChR subunits cloned from the male zebra finch, 6 (ChrnA2–5, A7, and B2) were expressed in the following song nuclei at the adult stage: HVC and RA in the VMP; and LMAN, Area X, and aDLM in the AFP (Figures 2, 3, 4). Expression of ChrnA2 in these song nuclei was not differentially regulated against the surrounding regions, but the five other subunits showed differential expression in one or more song nuclei compared with their surrounding regions.

Four of these differentially regulated subunits, ChrnA3, A5, A7, and B2, were expressed at higher levels in the premotor song nucleus HVC than the surrounding caudal nidopallium (**Figure 12**). In particular, ChrnA3 mRNA was expressed in limited HVC cells, whereas the other subunits showed a uniform expression pattern throughout HVC. In addition, the expression of ChrnA5 and B2 was clearly higher in LMAN relative to the surrounding rostral nidopallium. Although ChrnA7 was certainly expressed in LMAN, its expression was not specialized in comparison with that in the surrounding area (**Figure 12 (a)**). In addition, ChrnA5, B2, and other subunits were not differentially expressed in the shell subregion of LMAN (Bottjer & Altenau, 2010) relative to the surrounding nidopallium.

Conversely, the expression of ChrnA4 was lower in RA than in the surrounding arcopallium. Although none of the nAChR subunits exhibited higher levels of expression in RA and Area X relative to the surrounding arcopallium and striatum, respectively, low to moderate expression was observed in RA (for ChrnA7 and B2) and Area X (for ChrnA4 and B2) compared with the respective surrounding brain areas. In aDLM, only ChrnA5 showed a higher differential expression level than the surrounding DLM.

Although differences in the expression of glutamate receptors are observed between the lateral and the medial parts of the AFP song nuclei (Wada et al., 2004), two nAChR subunits that were expressed with higher levels in LMAN (ChrnA5 and B2) and in aDLM (ChrnA5) relative to their respective surrounding area did not show differential expressions in the medial MAN and dorsomedial nucleus of the posterior thalamus.

Developmental regulation of nAChR subunits during the critical period of song learning

To examine a potential developmental change in expression of nAChR subunits in the song nuclei (HVC, RA, LMAN, Area X, and aDLM) through the critical period of song learning, we quantified the mRNA expression levels of ChrnA3–5, A7, and B2. Male zebra finches at the subsong (35–45 phd), plastic song (50–65 phd), and crystallized song (120–140 phd) stages were used. Although nAChR subunits were expressed to varying degrees among the song nuclei, only ChrnA5 showed significantly different regulation in the song nucleus LMAN, with its expression level increased from subsong to crystallized stages (one-way ANOVA followed by Scheffe's F tests, $*p = 0.031$) (**Figure 12 (b)**). However, even though the shell subregion of LMAN is implicated in song learning in juvenile zebra finches (Bottjer & Altenau, 2010), the expressions of ChrnA5 and other subunits were not differentially regulated through the critical period of song learning. In addition, although the expression levels of ChrnA5 in Area X increased gradually from the subsong to crystallized song stage, the difference was not statistically significant due to individual variability in the mRNA expression level at the plastic and crystallized song stages. These results indicate that the expression of most nAChR subunits was consistently regulated in the song nuclei throughout song development.

Cell type-specific expression of nAChR subunit in the song nuclei

To elucidate the expression of nAChR subunits in different cell types of the vocal motor nuclei HVC and RA, in which the ACh content and related enzyme activity change markedly during the critical period for song learning (Sakaguchi & Saito, 1989), we performed single-cell RNA sequencing (scRNA-seq) with the two song nuclei from an adult male zebra finch. Based on the data obtained, we analyzed the expression of ChrnA1–10, B2–4, and D, and G mRNAs in different cell types, including glutamatergic excitatory neurons (including $HVC_{(X)}$, $HVC_{(RA)}$, and RA projecting neurons), GABAergic neurons, progenitor neurons, astrocytes, microglia, oligodendrocytes, OPC, and surrounding excitatory neurons in the nidopallium and arcopallium (**Figures 13, 14, 15, 16**). Consistent with earlier *in situ* hybridization results, the scRNA-seq data revealed that ChrnA1, A9, B3, B4, and D were expressed only in a few cells in both HVC and RA, while ChrnA6 mRNA was not detected. An exceptional discrepancy in mRNA detection was observed between *in situ* hybridization and snRNA-seq for ChrnA2 and ChrnA10. Although *in situ* hybridization revealed adequate expression of ChrnA2 mRNA throughout the entire brain, including HVC and RA, scRNA-seq showed no

ChnrA2 (+) cells in both HVC and RA. Conversely, ChrnA10 expression level was almost undetectable by *in situ* hybridization, whereas snRNA-seq showed several excitatory and inhibitory neurons and astrocytes labeled as expressing ChnrA10. Despite our best effort to carefully evaluate the specificity of the *in situ* hybridization probe and gene annotation information used for scRNA-seq analysis, the inconsistent detection of ChrnA2 and A10 mRNAs remains unclear.

In contrast to those subunits with low or undetectable expression levels, ChrnA3–5, A7, A8, B2, and G were expressed in at least one cell type in these song nuclei at varying levels and in different numbers of cells (**Figures 14 and 16**). In particular, ChrnA7 and B2 were expressed in most cell types of HVC and RA. As for the results from *in situ* hybridization (**Figure 12 (a)**), ChrnA3 expression was biased in selective cell populations of $HVC_{(RA)}$ and $HVC_{(X)}$ projecting neurons and in a few RA projecting neurons. Although very few glutamatergic projecting neurons in HVC and RA expressed ChrnA4, progenitor neurons for HVC and OPC in both HVC and RA showed clear and intense expression of this subunit. ChrnA8 was selectively expressed in a subtype of astrocytes in HVC but not in RA, while ChrnG was selectively expressed in a few oligodendrocyte populations in these song nuclei. In addition, *in situ* hybridization signals for ChnrA8 and G mRNA were very subtle. Taken together, the scRNA-seq analysis revealed both nonspecific expressions of ChrnA7 and B2 among various cell types and much selective expression of ChrnA3–5, A8, and G in limited cell types, suggesting that there are potentially unique nAChR subunit combinations at the single-cell level in the vocal motor song nuclei HVC and RA.

Since nAChR subunits form heteromeric or homomeric pentamers, which possess different physiological and pharmacological properties (Albuquerque, Pereira, Alkondon, & Rogers, 2009; Gotti et al., 2009; M. Zoli et al., 2015), we further investigated the potential combinations of nAChR subunits coexpressed in neuronal cell types of HVC and RA by focusing on ChrnA3–5, A7, and B2 (**Figure 17**), which were detected in the song nuclei by *in situ* hybridization. The results revealed that limited populations of each neuron type expressed only specific nAChR subunits. For instance, although ChrnA3, A5, A7, and B2 were expressed in $HVC_{(RA)}$ neurons, 55% of $HVC_{(RA)}$ neurons showed no expression of nAChR subunits. In addition, most of the remaining $HVC_{(RA)}$ neurons expressed only a single type of nAChR subunit. The selective expression of nAChR subunits was similarly observed in other neuron types in HVC and RA: $HVC_{(X)}$ neurons, interneurons, and progenitor neurons

in HVC and projecting neurons and interneurons in RA. ChrnA7 subunits are known to form homomeric nAChRs, while other α subunits (ChrnA2–6) combine with β subunits to form heteromeric receptors (Gotti et al., 2009; M. Zoli et al., 2015). Indeed, we found that ChrnA7 was expressed in some populations of all neuron types in HVC and RA (29% of $HVC_{(RA)}$, 62% of $HVC_{(X)}$, 12% of HVC interneurons, 5% of HVC progenitor neurons, 32% of RA projecting neurons, and 10% of RA interneurons), suggesting the potential existence of ChrnA7-homomeric receptors in these neural cell types. Because the expressions of ChrnB3 and B4 were detected only in a few cells in HVC and RA (**Figures 4, 14, 16**), ChrnB2 must be the main β subunit of heteromeric nAChRs in the song nuclei. Our snRNA-seq data revealed that 10%–22% of the neural cell types in HVC and RA expressed ChrnB2 (**Figure 17 (a), (b)**). It is necessary to recognize potential technical limitations of scRNA-seq in detecting the transcribed mRNAs at low levels; even though we counted at least 1 UMI of the scRNA-seq reads as a positive expression of each nAChR subunit, cells coexpressing ChnB2 and other α subunits comprised only a 2%–20% fraction of each neural cell type in HVC and RA. When we focused especially on ChrnB2-expressing cells, ChrnA7 was the main α subunit coexpressed with ChrnB2 in 31%, 66%, and 33% of ChrnB2(+)-$HVC_{(RA)}$, -$HVC_{(X)}$, and -RA projecting neurons, respectively (arrowheads in **Figure 17 (a)-(c)**). This information on coexpression suggests the presence of a ChrnA7/B2 heteromeric receptor, which was recently found in rodent and human brains (Qiang Liu, Huang, Shen, Steffensen, & Wu, 2012; Q. Liu et al., 2009; Thomsen et al., 2015). These findings demonstrated that nAChR subunits were expressed in a limited cell population of each cell type in the vocal motor nuclei HVC and RA. Furthermore, nAChR may form ChrnA7-homomeric or ChrnB2-containing heteromeric receptors in these cell populations. However, compared with the more abundant expression of ChrnA7-homomeric receptors, far fewer neuronal cells expressed ChrnB2-containing receptors.

Discussion

To comprehensively investigate the expression of nAChR subunits in an oscine songbird brain, including the neural circuits for acquiring and producing birdsong, we cloned 15 nAChR subunits, ChrnA1–10, B2–4, D, and G, from the zebra finch brain and highlighted their unique expression patterns in the telencephalon, thalamus, midbrain, and cerebellum. Whether the developmental origin of the hyperpallium is distinct or similar to regions below it remains an unsolved problem in avian pallial organization (Jarvis et al., 2005; Medina & Reiner, 2000; Reiner et al., 2004). The results of this study have shown that all 6 nAChR subunits expressed in the telencephalon were similarly expressed in both the hyperpallium and nidopallium across the mesopallium. The concordant expression of these nAChRs between the hyperpallium and nidopallium is consistent with the hypothesis that these two pallium subdivisions have a common origin (Gedman et al., 2021; Jarvis et al., 2013).

Five of the subunits (ChrnA3–5, A7, and B2) were expressed at varying levels in one or more song nuclei in the zebra finch brain. Of these, only ChrnA5 mRNA was differently regulated in the AFP song nucleus LMAN throughout the critical period of song development. These findings indicated that, in contrast to the change in ACh concentration and the activity of ChAT and AChE in the song nuclei through the critical period of song learning (Sakaguchi & Saito, 1989, 1991), the expression of most nAChR subunits was consistently maintained in the song nuclei during song acquisition. Furthermore, scRNA-seq analysis revealed the potential expression of ChrnA7-homomeric and ChrnB2-containing heteromeric nAChRs in limited cell populations of most neuronal cell types in the vocal premotor nuclei HVC and RA.

Comparison of nAChR subunit expression between avian and mammalian species

A similar number of nAChR subunits are expressed in the CNS of avian and mammalian species (Han et al., 2000; Nicolas Le Novere, Zoli, & Changeux, 1996; Lein et al., 2007; Lovell et al., 2018; Morris et al., 1990). However, the expression patterns and levels of nAChRs in the brain are not conserved between them. For example, the pattern of expression of four nAChR subunits (ChrnA1–3, A5) was apparently different in the pallium of zebra finches and the cortex of the mouse (**Figures 2, 3, 4, 18**). Specifically, ChrnA3 and ChrnA5 were expressed in the mesopallium and entire pallial subregions, of the zebra finch, respectively (**Figures 2, 5**). In contrast, there was no detectable expression of the mRNAs of these subunits in the mouse cortex (**Figure 18**). Conversely, ChrnA1 and ChrnA2 were

consistently expressed throughout the entire mouse brain, the expression levels of these two α subunits were undetectable in the zebra finch brain. Furthermore, some of the nAChR subunits, such as ChnrA2 and A4, were differentially expressed in the cortical layers of the mice and marmoset (**Figure19**), suggesting that nAChRs expression in the telencephalic regions is species-specifically diversified. The discrepancies thus identified in the pattern of expression of nAChR subunits are in sharp contrast to highly conserved expression patterns of the glutamate and dopamine receptor subunits between the avian pallium and mammalian cortical regions (Kubikova, Wada, & Jarvis, 2010; Wada et al., 2004).

The potential functional contribution of nAChR subunits in the vocal motor nuclei

Multiple lines of studies in songbirds have suggested potential contributions of the cholinergic system to vocal learning and production. For example, stimulating the cholinergic basal forebrain, a region homologous to the nucleus basalis of Meynert in mammals (R. Li & Sakaguchi, 1997; Reiner et al., 2004), suppresses auditory responses to the bird's own song in HVC and RA neurons in anesthetized zebra finches (Shea & Margoliash, 2003). Furthermore, the direct injection of nicotine into HVC produces a strong and consistent suppression of auditory responses in HVC neurons. Arousal state-dependent changes in auditory responses in HVC are an essential modulator of auditory input to the vocal motor region during song learning (Cardin & Schmidt, 2003; Schmidt & Konishi, 1998; Shea & Margoliash, 2003, 2010). However, the precise HVC neuron type responsible for nicotine-induced auditory suppression has not been determined physiologically.

Our scRNA-seq analysis revealed that in HVC, ChrnA3, A5, A7, and B2 were expressed in three neuron types in HVC: $HVC_{(RA)}$ neurons, $HVC_{(X)}$ neurons, and interneurons (**Figure 14**). However, the populations of cells that expressed these nAChR subunits differed among the neural cell-type classes in HVC. We found that 45% of $HVC_{(RA)}$ neurons and 30% of HVC interneurons expressed at least one type of nAChR subunits, mainly ChrnA7 or B2. In contrast, 77% of $HVC_{(X)}$ neurons expressed one or more of the ChrnA3, A5, A7, and B2 subunits. In particular, 63% of $HVC_{(X)}$ neurons expressed ChrnA7 subunits, which can form functional homomeric receptors. Thus, ChrnA7 subunits may play an important role in modulating the activity of $HVC_{(X)}$ neurons in an arousal state-dependent manner. Further gene manipulation studies of these nAChR subunits at the cell-type level will be crucial to investigate the direct functional contribution of nAChRs in HVC to song learning and production.

In RA, the chronic infusion of a mixture of mAChR and nAChR antagonists during the critical period of song learning induces abnormal song development, characterized by the absence of stereotyped syllable sequences (Puzerey, Maher, Prasad, & Goldberg, 2018). Acute infusion of the AChR antagonist mixture into RA of juvenile zebra finches does not affect the syllable acoustics or the timing of early plastic songs, suggesting that not cholinergic modulation of fast synaptic transmission but rather cell signaling in RA is crucial for normal song learning (Puzerey et al., 2018). In addition, tetanic stimulation of LMAN to RA axon fibers induces long-term potentiation (LTP) in RA in the presence of nicotine; however, without nicotine it does not produce LTP (Salgado-Commissariat, Rosenfield, & Helekar, 2004). This nicotine-mediated LTP in RA is blocked by selective antagonists to ChrnA7-homomeric and ChrnA4/B2-heteromeric nAChRs. Our scRNA-seq findings revealed that ChrnA7 was identified in approximately 30% of RA projecting neurons, which could be a sensitive site to ChrnA7 homomeric receptor-specific antagonists in RA. However, although 15% of RA projecting neurons expressed ChrnB2, cells coexpressing ChrnB2 and other α subunits including ChrnA4 accounted for only 0.1%–1.2% of RA projecting neurons. These expression data are contrary to the observed pharmacological effect of ChrnA4/B2 heteromeric nAChR antagonists in RA. Although ChrnA4/B2 coexpression in RA was sparse, we found that 5% of RA projecting neurons coexpressed ChrnA7 and B2. Thus, instead of a ChrnA4/B2 combination, ChrnA7/B2 heteromeric receptors may contribute to the induction of nicotine-mediated LTP. Notably, approximately half of RA projecting neurons did not express any nAChR subunits. Thus, concerning nAChRs, RA projecting neurons are composed of heterogeneous populations, which may elicit differential responses to nAChR activation by nicotine (Meng, Wang, Yao, Zhang, & Li, 2017; Salgado-Commissariat et al., 2004).

The potential functional contribution of nAChR subunits in the AFP nuclei

Similar to the VMP song nuclei, we found that limited nAChR subunits were expressed in the AFP song nuclei, Area X (ChrnA2–5, A7, and B2), aDLM (ChrnA2, A4, A5, A7, and B2), and LMAN (ChrnA2, A5, A7, and B2). Particularly, the expressions of ChrnA5 and B2 were higher in LMAN than in the surrounding nidopallium. Furthermore, ChrnA5 was the only subunit that showed a significant difference in expression during the critical period of song learning. Although physiological and pharmacological analyses of these subunits have not been performed in the AFP nuclei, our findings suggest that ChrnA7-homomeric and

ChrnB2-containing heteromeric nAChRs exist in the AFP song nuclei, as speculated for HVC and RA. The AFP is a crucial neural circuit in the regulation of song learning and maintenance by generating vocal variability (Andalman & Fee, 2009; Aronov, Andalman, & Fee, 2008; Brainard & Doupe, 2000; Kao et al., 2005; Ölveczky, Andalman, & Fee, 2005). The concentration of ACh and the activity of ChAT and AChE are increased and maintained in LMAN during the critical period of song learning (Sakaguchi & Saito, 1989, 1991). Thus, specific agonists/antagonists of ChrnA7-homomeric and ChrnB2-containing heteromeric nAChRs could be used to examine whether vocal variability can be modulated during song development. Further studies focusing on particular cell types and nAChR subtype combinations in the song nuclei will be crucial to elucidating cholinergic contributions via the nAChRs involved in neural plasticity and song learning.

Table 1. Cloned partial cDNA information of nAChR subunits in this study[1]

[1] The primers listed were used for cloning the cDNA fragments. Accession numbers are for record in GenBank. The last three columns list the similarity of amino acid sequences, expressed as percentages between cloned fragments and the corresponding nAChRs in zebra finch, chicken, and human, respectively. Human chrnA8 does not exist.

Table 2. Sequence similarities between cDNAs and the protein-coding regions of 15 nAChR subunits in the zebra finch[1]

1Matching base-pair sequences as a fraction of the length of cDNAs are shown as percentages. High similarity values (≥98.5%) on the diagonal (cells highlighted in red) shown on-target identity. Perfect dissimilarity with off-target subunits is represented by a zero in an off-diagonal entry. Because the full-length transcript is expected to be expressed in cells, non-zero off-diagonal similarity values indicate the potential for *in situ* cross-hybridization of each subunit cDNA fragment to 14 off-target subunits. The low off-diagonal similarity values (≤76.8%) indicate that the potential for such confounds was low.

Acknowledgments

We appreciate Mrs. Keiko Sumida for her great contribution toward breeding our experimental birds. This research was supported by the Ministry of Education, Culture, Sports, Science and Technology Scholarship #153033 to C. N. A., and MEXT/JSPS KAKENHI Grant Number #4903-JP17H06380, JP19H04888, JP21H02456, JP21K18265, and the Takeda Science Foundation to K.W.

Availability of data and materials

The authors confirm that all of the data underlying the reported findings are included in the manuscript. All raw data are available to the corresponding author on request.

Authors' contributions

NCA and KW designed the research. NCA, NT, ZH, and KW performed the experiments. NCA, NT, and KW performed the analysis. CS, YS, ST, HI, and YG contributed to critical support for experiments and analysis. NCA, NT, and KW wrote the paper. The authors declare no competing financial interests. All authors read and approved the final manuscript.

Figures & Figure Legends

Figure 1. Phylogram of nicotinic acetylcholine receptor subunits and brain diagram of the neural circuits for song learning and production

(**a**) Phylogenetic relationship of nAChR subunits in the zebra finch, chicken, and human, generated with full-length protein-coding sequences using Molecular Evolutionary Genetics Analysis software (https://www.megasoftware.net/). Local bootstrap probabilities from the maximum-likelihood analysis are shown for branches below the terminals. All subunit types show closer homologies to each other across species than they do to different receptor types within species.

(**b**) The vocal motor circuit and the anterior forebrain pathway (pallial–basal ganglia–thalamic loop circuit) are represented as solid and dotted black lines, respectively. HVC (proper name); RA, robust nucleus of the arcopallium; Area X, Area X of the striatum; aDLM, anterior dorsal lateral nucleus of the medial thalamus; LMAN, lateral magnocellular nucleus of the anterior nidopallium; nXIIts, the tracheosyringeal part of the 12th cranial nerve nuclei; H, hyperpallium; M, mesopallium; N, nidopallium; A, arcopallium; L, field L; St, Striatum; P, pallidum; Hp, hippocampus.

Figure 2. Expression of nicotinic acetylcholine receptor A subunits (ChrnA1–5) in the male zebra finch brain

Expression images for each subunit are in a different row, and within rows, images of parasagittal brain sections are organized by medial (left) to lateral (right) progression. Sections are oriented with rostral side to the right, and dorsal side up. Levels of brightness represents levels of the mRNA signal. A camera lucida drawing at the top of each column identifies the brain areas represented in the sections in the column below. Scale bar = 1 mm.

Figure 3. Expression of nicotinic acetylcholine receptor A subunits (ChrnA6–10) in the male zebra finch brain

Expression images are arranged as in Figure 2. Scale bar = 1 mm.

Figure 4. Expression of nicotinic acetylcholine receptor B (ChrnB2–4), D, and G subunits in the male zebra finch brain

Expression images are arranged as in Figure 2. Scale bar = 1 mm.

Figure 5. Expression of nAChR subunits in subdivisions of the anterior pallial regions

In situ hybridization images for ChrnA2–5, A7, B2, and B4. Camera lucida drawing (bottom right panel) shows boundaries of the major subdivisions (H, hyperpallium; M, mesopallium; N, nidopallium; Str, Striatum) of these brain regions in exact correspondence to the orange dotted lines in the ChrnB4 image, and approximately for all others. Scale bar = 3 mm, for all images.

Figure 6. Expression of nAChR subunits in subdivisions of the posterior medial pallial regions

In situ hybridization images for ChrnA2–5, A7, B2, and B4. Bottom right: camera lucida drawing showing major subdivisions (Hp, hippocampus; NCM, caudomedial nidopallium; CMM, caudomedial mesopallium of the brain) of these brain regions. Scale bar = 3 mm.

Figure 7. Expression of nAChR subunits in subdivisions of the arcopallium

(a) *In situ* hybridization images for ChrnA2–5, A7, B2, and B4 in the lateral arcopallial regions. Camera lucida drawing (lower right) shows major subdivisions of this region of the brain. Orange dotted lines represent the borders of brain subdivisions: the anterior, posterior, dorsal, and intermediate arcopallium denoted by AA, AP, AD, and AI, respectively. AId and AIv: dorsal and ventral subdivisions of AI, respectively. cN: caudal nidopallium.

(b) Specific expression of ChrnA8 in the intermediate part of the medial ventral arcopallium (AMVi), also called nucleus taenia (TnA).

Figure 8. Expression of nAChR subunits in subdivisions of the hippocampus

In situ hybridization images for ChrnA2–5, A7, B2, and B4. Camera lucida drawing (lower right panel) shows the dorsal (Hpd) and ventral (Hpv) subdivisions of the hippocampus. cN: caudal nidopallium. Scale bar = 3 mm.

Figure 9. Expression of nAChR subunits in the midbrain

In situ hybridization images for ChrnA2–5, A7, A8, and B2–4. Orange dotted lines show the borders of nuclei/parts in the midbrain. Right bottom: Nissl-stained brain image showing midbrain nuclei: Pt, nucleus pretectalis; Spl, nucleus spiriform lateralis; Rt, nucleus rotundus; DM, nucleus dorsomedialis of the midbrain; MLd, nucleus mesencephalicus lateralis, pars dorsalis; SP, nucleus; IPc, nucleus isthmi pars parvocellularis. Arabic numerals represent clearly identified layers of the tectum opticum. Scale bar = 3 mm.

Figure 10. Expression of nAChR subunits in the cerebellum

In situ hybridization images for ChrnA2–5, A7, B2–4, D, and G. Camera lucida showing sublayers of the cerebellum; p = Purkinje layer, m = molecular layer, g = granular layer, w = white matter, dn = deep nucleus. Scale bar = 3 mm.

Figure 11. Heatmap summarizing the expression of nAChR subunits in subregions of the zebra finch brain

Levels of expression were measured by image pixel intensity and represented in the heatmap by 5-grading colors (color bar).

Figure 12. Expression of nAChR subunits in the song nuclei of adult male zebra finches

(**a**) ChrnA3–5, A7, and B2 expression in song nuclei, HVC, RA, LMAN, Area X, and aDLM. Brains are sagittal, white color represents mRNA signal. Right panels: Camera lucida drawings depicting each song nucleus. Dotted dark lines show the borders of the song nuclei. (**b**) nAChR subunit expression in the song nuclei during song development. ChrnA3–5, A7, and B2 expression in HVC, RA, LMAN, Area X, and aDLM during the subsong (35–45 phd, orange), plastic song (50–65 phd, blue), and crystallized song (120–140 phd, red) stages of song development. Bars: mean ± SEM. n = 6 birds/each stage. One-way analysis of variance, ANOVA, $*p < 0.05$.

Figure 13. Expression of marker genes at each cell-type in HVC

Violin (left side panel) and UMAP (right side panel) plots of cell clusters expressing major cell type marker genes **(a)** and sub-type marker of glutamatergic neuron **(b)**.

Figure 14. Expression of nAChR subunits in various cell types in HVC

UMAP (Uniform Manifold Approximation and Projection) plots of cells expressing ChrnA1–5, A7–10, B2–4, D, and G in HVC (n = 6,510 cells). Red dots in each panel represent cells expressing the subunit indicated at the top left. The color gradation represents the intensity of expression. In the reference UMAP panel at the top, each color represents a class of cell types.

Figure 15. Expression of marker genes at each cell-type in RA

Violin (left side panel) and UMAP (right side panel) plots of cell clusters expressing major cell type marker genes **(a)** and sub-type marker of glutamatergic neuron **(b)**.

Figure 16. Expression of nAChR subunits in various cell types in RA

UMAP (Uniform Manifold Approximation and Projection) plots of cells expressing ChrnA1–5, A7–10, B2–4, D, and G in RA (n = 6,977 cells). Red dots in each panel represent cells expressing the subunit indicated at the top left. The color gradation represents the intensity of expression. In the reference UMAP panels (upper), each color represents a class of cell types.

Figure 17. Expression of nAChR subunits in various neuron types in HVC and RA

UMAP plots of neuronal cell types (organized by row) expressing each of the ChrnA3–5, A7, and B2 subunits (organized by column) in HVC (**a**) and RA (**b**). Each colored dot represents one neuron expressing the corresponding subunit gene. The color gradation represents the intensity of expression. $HVC_{(RA)}$ and $HVC_{(X)}$ are projecting neurons from HVC to RA and Area X, respectively. $HVC_{(RA)}$, $HVC_{(X)}$, and RA projecting neurons are glutamatergic excitatory neurons. $HVC_{(RA)}$ = 1,715 cells; $HVC_{(X)}$ = 326 cells; interneurons in HVC and RA = 896 and 959 cells, respectively; HVC progenitor cells = 275 cells; and RA projecting neurons = 892 cells. Arrowheads indicate cells coexpressing ChrnA7 and B2 subunits. Percentage at the bottom of each UMAP plot is the fraction of the total cell population expressing the corresponding nAChR subunit in the corresponding neural cell type. (**c**) Coexpression rates of ChrnB2 (+) neurons with ChrnA3 (green), A4 (light blue), A5 (cream-yellow), and A7 (pink). Gray represents negatives (no expression of any of the ChrnA3–5, and A7 subunits.

Figure 18. nAChRs mRNA expression in the mouse brain

All images are adapted from Allen Brain Atlas mouse *in situ* hybridization data (https://mouse.brain-map.org/search/index).

Figure 19. Differential expressions of ChrnA2 and A4 between mouse and marmoset cortices

(**a**) ChrnA2 expression in the mouse (left) and marmoset (right) cortices. (**b**) ChrnA4 expression in the mouse (left) and marmoset (right) cortices. Panels below are enlarged

857 from enclosed dotted square parts in the above panels. *In situ* hybridization images are
858 adapted from Allen Brain Atlas mouse ISH data (https://mouse.brain-map.org/search/index)
859 and the Marmoset Gene Atlas (https://gene-atlas.brainminds.riken.jp/).
860

References

Albuquerque, E. X., Pereira, E. F., Alkondon, M., & Rogers, S. W. (2009). Mammalian nicotinic acetylcholine receptors: from structure to function. *Physiol Rev, 89*(1), 73-120. doi:10.1152/physrev.00015.2008

Anagnostaras, S. G., Murphy, G. G., Hamilton, S. E., Mitchell, S. L., Rahnama, N. P., Nathanson, N. M., & Silva, A. J. (2003). Selective cognitive dysfunction in acetylcholine M1 muscarinic receptor mutant mice. *Nat Neurosci, 6*(1), 51-58. doi:10.1038/nn992

Andalman, A. S., & Fee, M. S. (2009). A basal ganglia-forebrain circuit in the songbird biases motor output to avoid vocal errors. *Proc Natl Acad Sci U S A, 106*(30), 12518-12523. doi:10.1073/pnas.0903214106

Aronov, D., Andalman, A. S., & Fee, M. S. (2008). A specialized forebrain circuit for vocal babbling in the juvenile songbird. *Science, 320*(5876), 630-634. doi:10.1126/science.1155140

Aronov, D., Veit, L., Goldberg, J. H., & Fee, M. S. (2011). Two distinct modes of forebrain circuit dynamics underlie temporal patterning in the vocalizations of young songbirds. *J Neurosci, 31*(45), 16353-16368. doi:10.1523/JNEUROSCI.3009-11.2011

Asogwa, N. C., Mori, C., Sanchez-Valpuesta, M., Hayase, S., & Wada, K. (2018). Inter- and intra-specific differences in muscarinic acetylcholine receptor expression in the neural pathways for vocal learning in songbirds. *J Comp Neurol, 526*(17), 2856-2869. doi:10.1002/cne.24532

Bell, Z. W., Lovell, P., Mello, C. V., Yip, P. K., George, J. M., & Clayton, D. F. (2019). Urotensin-related gene transcripts mark developmental emergence of the male forebrain vocal control system in songbirds. *Sci Rep, 9*(1), 816. doi:10.1038/s41598-018-37057-w

Boord, R. L. (1968). Ascending projections of the primary cochlear nuclei and nucleus laminaris in the pigeon. *Journal of Comparative Neurology, 133*(4), 523-541.

Bottjer, S. W., & Altenau, B. (2010). Parallel pathways for vocal learning in basal ganglia of songbirds. *Nat Neurosci, 13*(2), 153-155. doi:10.1038/nn.2472

Bottjer, S. W., Miesner, E. A., & Arnold, A. P. (1984). Forebrain lesions disrupt development but not maintenance of song in passerine birds. *Science, 224*(4651), 901-903.

Brainard, M. S., & Doupe, A. J. (2000). Interruption of a basal ganglia-forebrain circuit prevents plasticity of learned vocalizations. *Nature, 404*(6779), 762-766. doi:10.1038/35008083

Brenowitz, E. A., & Beecher, M. D. (2005). Song learning in birds: diversity and plasticity, opportunities and challenges. *Trends Neurosci, 28*(3), 127-132. doi:10.1016/j.tins.2005.01.004

Cardin, J. A., & Schmidt, M. F. (2003). Song system auditory responses are stable and highly tuned during sedation, rapidly modulated and unselective during wakefulness, and suppressed by arousal. *J Neurophysiol, 90*(5), 2884-2899.

Colquitt, B. M., Merullo, D. P., Konopka, G., Roberts, T. F., & Brainard, M. S. (2021). Cellular transcriptomics reveals evolutionary identities of songbird vocal circuits. *Science, 371*(6530). doi:10.1126/science.abd9704

Conner, J. M., Culberson, A., Packowski, C., Chiba, A. A., & Tuszynski, M. H. (2003). Lesions of the basal forebrain cholinergic system impair task acquisition and abolish cortical plasticity associated with motor skill learning. *Neuron, 38*(5), 819-829.

Couturier, S., Bertrand, D., Matter, J.-M., Hernandez, M.-C., Bertrand, S., Millar, N., . . . Ballivet, M. (1990). A neuronal nicotinic acetylcholine receptor subunit (α7) is developmentally regulated and forms a homo-oligomeric channel blocked by α-BTX. *Neuron, 5*(6), 847-856.

Dajas-Bailador, F., & Wonnacott, S. (2004). Nicotinic acetylcholine receptors and the regulation of neuronal signalling. *Trends Pharmacol Sci, 25*(6), 317-324. doi:10.1016/j.tips.2004.04.006

Dineley-Miller, K., & Patrick, J. (1992). Gene transcripts for the nicotinic acetylcholine receptor subunit, beta4, are distributed in multiple areas of the rat central nervous system. *Molecular Brain Research, 16*(3), 339-344. doi:https://doi.org/10.1016/0169-328X(92)90244-6

Doupe, A. J., & Kuhl, P. K. (1999). Birdsong and human speech: common themes and mechanisms. *Annu Rev Neurosci, 22*, 567-631. doi:10.1146/annurev.neuro.22.1.567

Fu, Y., Tucciarone, J. M., Espinosa, J. S., Sheng, N., Darcy, D. P., Nicoll, R. A., . . . Stryker, M. P. (2014). A cortical circuit for gain control by behavioral state. *Cell, 156*(6), 1139-1152. doi:10.1016/j.cell.2014.01.050

Gedman, G., Haase, B., Durieux, G., Biegler, M. T., Fedrigo, O., & Jarvis, E. D. (2021). As above, so below: Whole transcriptome profiling demonstrates strong molecular similarities between avian dorsal and ventral pallial subdivisions. *J Comp Neurol*. doi:10.1002/cne.25159

Gotti, C., & Clementi, F. (2004). Neuronal nicotinic receptors: from structure to pathology. *Prog Neurobiol, 74*(6), 363-396. doi:10.1016/j.pneurobio.2004.09.006

Gotti, C., Clementi, F., Fornari, A., Gaimarri, A., Guiducci, S., Manfredi, I., . . . Zoli, M. (2009). Structural and functional diversity of native brain neuronal nicotinic receptors. *Biochem Pharmacol, 78*(7), 703-711. doi:10.1016/j.bcp.2009.05.024

Halvorsen, S. W., & Berg, D. K. (1990). Subunit composition of nicotinic acetylcholine receptors from chick ciliary ganglia. *Journal of Neuroscience, 10*(6), 1711-1718.

925 Han, Z.-Y., Le Novère, N., Zoli, M., Hill Jr, J. A., Champtiaux, N., & Changeux, J.-P. (2000). Localization
926 of nAChR subunit mRNAs in the brain of Macaca mulatta. *European Journal of Neuroscience,*
927 *12*(10), 3664-3674. doi:https://doi.org/10.1046/j.1460-9568.2000.00262.x
928 Hasselmo, M. E. (2006). The role of acetylcholine in learning and memory. *Curr Opin Neurobiol, 16*(6),
929 710-715. doi:10.1016/j.conb.2006.09.002
930 Herrero, J. L., Roberts, M. J., Delicato, L. S., Gieselmann, M. A., Dayan, P., & Thiele, A. (2008).
931 Acetylcholine contributes through muscarinic receptors to attentional modulation in V1.
932 *Nature, 454*(7208), 1110-1114. doi:10.1038/nature07141
933 Jarvis, E. D., Gunturkun, O., Bruce, L., Csillag, A., Karten, H., Kuenzel, W., . . . Butler, A. B. (2005).
934 Avian brains and a new understanding of vertebrate brain evolution. *Nat Rev Neurosci, 6*(2),
935 151-159. doi:10.1038/nrn1606
936 Jarvis, E. D., Yu, J., Rivas, M. V., Horita, H., Feenders, G., Whitney, O., . . . Wada, K. (2013). Global
937 view of the functional molecular organization of the avian cerebrum: mirror images and
938 functional columns. *J Comp Neurol, 521*(16), 3614-3665. doi:10.1002/cne.23404
939 Kao, M. H., Doupe, A. J., & Brainard, M. S. (2005). Contributions of an avian basal ganglia-forebrain
940 circuit to real-time modulation of song. *Nature, 433*(7026), 638-643.
941 doi:10.1038/nature03127
942 Kruse, A. C., Kobilka, B. K., Gautam, D., Sexton, P. M., Christopoulos, A., & Wess, J. (2014). Muscarinic
943 acetylcholine receptors: novel opportunities for drug development. *Nat Rev Drug Discov,*
944 *13*(7), 549-560. doi:10.1038/nrd4295
945 Kubikova, L., Wada, K., & Jarvis, E. D. (2010). Dopamine receptors in a songbird brain. *J Comp Neurol,*
946 *518*(6), 741-769. doi:10.1002/cne.22255
947 Le Novere, N., Corringer, P. J., & Changeux, J. P. (2002). The diversity of subunit composition in
948 nAChRs: evolutionary origins, physiologic and pharmacologic consequences. *J Neurobiol,*
949 *53*(4), 447-456. doi:10.1002/neu.10153
950 Le Novere, N., Zoli, M., & Changeux, J. P. (1996). Neuronal nicotinic receptor a6 subunit mRNA is
951 selectively concentrated in catecholaminergic nuclei of the rat brain. *European Journal of*
952 *Neuroscience, 8*(11), 2428-2439.
953 Lein, E. S., Hawrylycz, M. J., Ao, N., Ayres, M., Bensinger, A., Bernard, A., . . . Jones, A. R. (2007).
954 Genome-wide atlas of gene expression in the adult mouse brain. *Nature, 445*(7124), 168-
955 176. doi:10.1038/nature05453
956 Li, H. Q., & Spitzer, N. C. (2020). Exercise enhances motor skill learning by neurotransmitter
957 switching in the adult midbrain. *Nat Commun, 11*(1), 2195. doi:10.1038/s41467-020-16053-
958 7

959 Li, R., & Sakaguchi, H. (1997). Cholinergic innervation of the song control nuclei by the ventral
960 paleostriatum in the zebra finch: a double-labeling study with retrograde fluorescent tracers
961 and choline acetyltransferase immunohistochemistry. *Brain Res, 763*(2), 239-246.
962 Liu, Q., Huang, Y., Shen, J., Steffensen, S., & Wu, J. (2012). Functional α7β2 nicotinic acetylcholine
963 receptors expressed in hippocampal interneurons exhibit high sensitivity to pathological
964 level of amyloid β peptides. *BMC Neurosci, 13*(1), 155. doi:10.1186/1471-2202-13-155
965 Liu, Q., Huang, Y., Xue, F., Simard, A., DeChon, J., Li, G., . . . Wu, J. (2009). A novel nicotinic
966 acetylcholine receptor subtype in basal forebrain cholinergic neurons with high sensitivity
967 to amyloid peptides. *J Neurosci, 29*(4), 918-929. doi:10.1523/JNEUROSCI.3952-08.2009
968 Lovell, P. V., Clayton, D. F., Replogle, K. L., & Mello, C. V. (2008). Birdsong "transcriptomics":
969 neurochemical specializations of the oscine song system. *PLoS One, 3*(10), e3440.
970 doi:10.1371/journal.pone.0003440
971 Lovell, P. V., Huizinga, N. A., Friedrich, S. R., Wirthlin, M., & Mello, C. V. (2018). The constitutive
972 differential transcriptome of a brain circuit for vocal learning. *BMC Genomics, 19*(1), 231.
973 doi:10.1186/s12864-018-4578-0
974 Lovell, P. V., Wirthlin, M., Kaser, T., Buckner, A. A., Carleton, J. B., Snider, B. R., . . . Mello, C. V. (2020).
975 ZEBrA: Zebra finch Expression Brain Atlas-A resource for comparative molecular
976 neuroanatomy and brain evolution studies. *J Comp Neurol, 528*(12), 2099-2131.
977 doi:10.1002/cne.24879
978 Luo, M., Ding, L., & Perkel, D. J. (2001). An avian basal ganglia pathway essential for vocal learning
979 forms a closed topographic loop. *J Neurosci, 21*(17), 6836-6845.
980 Marler, P., & Slabbekoorn, H. (2004). *Nature's Music: The Science of Birdsong*: Elsevier Academic
981 Press.
982 Medina, L., & Reiner, A. (2000). Do birds possess homologues of mammalian primary visual,
983 somatosensory and motor cortices? *Trends Neurosci, 23*(1), 1-12.
984 Mello, C. V., Kaser, T., Buckner, A. A., Wirthlin, M., & Lovell, P. V. (2019). Molecular architecture of
985 the zebra finch arcopallium. *J Comp Neurol*. doi:10.1002/cne.24688
986 Meng, W., Wang, S., Yao, L., Zhang, N., & Li, D. (2017). Muscarinic Receptors Are Responsible for the
987 Cholinergic Modulation of Projection Neurons in the Song Production Brain Nucleus RA of
988 Zebra Finches. *Front Cell Neurosci, 11*, 51. doi:10.3389/fncel.2017.00051
989 Morris, B. J., Hicks, A. A., Wisden, W., Darlison, M. G., Hunt, S. P., & Barnard, E. A. (1990). Distinct
990 regional expression of nicotinic acetylcholine receptor genes in chick brain. *Molecular Brain*
991 *Research, 7*(4), 305-315. doi:https://doi.org/10.1016/0169-328X(90)90081-N

992 Nottebohm, F., Stokes, T. M., & Leonard, C. M. (1976). Central control of song in the canary, Serinus
993 canarius. *J Comp Neurol, 165*(4), 457-486. doi:10.1002/cne.901650405
994 Noudoost, B., & Moore, T. (2011). The role of neuromodulators in selective attention. *Trends Cogn*
995 *Sci, 15*(12), 585-591. doi:10.1016/j.tics.2011.10.006
996 Ölveczky, B. P., Andalman, A. S., & Fee, M. S. (2005). Vocal Experimentation in the Juvenile Songbird
997 Requires a Basal Ganglia Circuit. *PLoS Biol., 3*(5), e153.
998 doi:10.1371/journal.pbio.0030153.g001
999 Parikh, V., Kozak, R., Martinez, V., & Sarter, M. (2007). Prefrontal acetylcholine release controls cue
1000 detection on multiple timescales. *Neuron, 56*(1), 141-154.
1001 Pedersen, J. E., Bergqvist, C. A., & Larhammar, D. (2019). Evolution of vertebrate nicotinic
1002 acetylcholine receptors. *BMC Evol Biol, 19*(1), 38. doi:10.1186/s12862-018-1341-8
1003 Puzerey, P. A., Maher, K., Prasad, N., & Goldberg, J. H. (2018). Vocal learning in songbirds requires
1004 cholinergic signaling in a motor cortex-like nucleus. *J Neurophysiol, 120*(4), 1796-1806.
1005 Ramon y Cajal, S. (1911). Histologie du système nerveux de l'homme et des vertébrés. *Maloine, Paris,*
1006 *2*, 153-173.
1007 Reiner, A., Perkel, D. J., Bruce, L. L., Butler, A. B., Csillag, A., Kuenzel, W., . . . Avian Brain
1008 Nomenclature, F. (2004). Revised nomenclature for avian telencephalon and some related
1009 brainstem nuclei. *J Comp Neurol, 473*(3), 377-414. doi:10.1002/cne.20118
1010 Role, L. W., & Berg, D. K. (1996). Nicotinic Receptors in the Development and Modulation of CNS
1011 Synapses. *Neuron, 16*(6), 1077-1085. doi:10.1016/s0896-6273(00)80134-8
1012 Ryan, S. M., & Arnold, A. P. (1981). Evidence for cholinergic participation in the control of bird song;
1013 acetylcholinesterase distribution and muscarinic receptor autoradiography in the zebra
1014 finch brain. *J Comp Neurol, 202*(2), 211-219. doi:10.1002/cne.902020207
1015 Sadananda, M. (2004). Acetylcholinesterase in central vocal control nuclei of the zebra finch
1016 (Taeniopygia guttata). *J Biosci, 29*(2), 189-200.
1017 Sakaguchi, H., & Saito, N. (1989). The acetylcholine and catecholamine contents in song control
1018 nuclei of zebra finch during song ontogeny. *Developmental Brain Research, 47*(2), 313-317.
1019 Sakaguchi, H., & Saito, N. (1991). Developmental change of cholinergic activity in the forebrain of
1020 the zebra finch during song learning. *Developmental Brain Research, 62*(2), 223-228.
1021 Salgado-Commissariat, D., Rosenfield, D. B., & Helekar, S. A. (2004). Nicotine-mediated plasticity in
1022 robust nucleus of the archistriatum of the adult zebra finch. *Brain Res, 1018*(1), 97-105.
1023 doi:10.1016/j.brainres.2004.05.051
1024 Sargent, P. B. (1993). The diversity of neuronal nicotinic acetylcholine receptors. *Annual Review of*
1025 *Neuroscience, 16*(1), 403-443.

Sarter, M., Bruno, J. P., & Turchi, J. (1999). Basal forebrain afferent projections modulating cortical acetylcholine, attention, and implications for neuropsychiatric disorders. *Ann N Y Acad Sci, 877*, 368-382.

Saunders, A., Macosko, E. Z., Wysoker, A., Goldman, M., Krienen, F. M., de Rivera, H., . . . McCarroll, S. A. (2018). Molecular Diversity and Specializations among the Cells of the Adult Mouse Brain. *Cell, 174*(4), 1015-1030 e1016. doi:10.1016/j.cell.2018.07.028

Scharff, C., & Nottebohm, F. (1991). A comparative study of the behavioral deficits following lesions of various parts of the zebra finch song system: implications for vocal learning. *J Neurosci, 11*(9), 2896-2913.

Schmidt, M. F., & Konishi, M. (1998). Gating of auditory responses in the vocal control system of awake songbirds. *Nat Neurosci, 1*(6), 513.

Schryver, H. M., & Mysore, S. P. (2019). Spatial dependence of stimulus competition in the avian nucleus isthmi pars magnocellularis. *Brain Behav Evol, 93*(2-3), 137-151.

Scully, E. N., Acerbo, M. J., & Lazareva, O. F. (2014). Bilateral lesions of nucleus subpretectalis/interstitio-pretecto-subpretectalis (SP/IPS) selectively impair figure-ground discrimination in pigeons. *Vis Neurosci, 31*(1), 105-110. doi:10.1017/S0952523813000424

Shea, S. D., Koch, H., Baleckaitis, D., Ramirez, J. M., & Margoliash, D. (2010). Neuron-specific cholinergic modulation of a forebrain song control nucleus. *J Neurophysiol, 103*(2), 733-745. doi:10.1152/jn.00803.2009

Shea, S. D., & Margoliash, D. (2003). Basal forebrain cholinergic modulation of auditory activity in the zebra finch song system. *Neuron, 40*(6), 1213-1226. doi:10.1016/s0896-6273(03)00723-2

Shea, S. D., & Margoliash, D. (2010). Behavioral state-dependent reconfiguration of song-related network activity and cholinergic systems. *J Chem Neuroanat, 39*(2), 132-140. doi:10.1016/j.jchemneu.2009.10.002

Stuart, T., Butler, A., Hoffman, P., Hafemeister, C., Papalexi, E., Mauck, W. M., 3rd, . . . Satija, R. (2019). Comprehensive Integration of Single-Cell Data. *Cell, 177*(7), 1888-1902 e1821. doi:10.1016/j.cell.2019.05.031

Tasic, B., Menon, V., Nguyen, T. N., Kim, T. K., Jarsky, T., Yao, Z., . . . Zeng, H. (2016). Adult mouse cortical cell taxonomy revealed by single cell transcriptomics. *Nat Neurosci, 19*(2), 335-346. doi:10.1038/nn.4216

Tasic, B., Yao, Z., Graybuck, L. T., Smith, K. A., Nguyen, T. N., Bertagnolli, D., . . . Zeng, H. (2018). Shared and distinct transcriptomic cell types across neocortical areas. *Nature, 563*(7729), 72-78. doi:10.1038/s41586-018-0654-5

Thomsen, M. S., Zwart, R., Ursu, D., Jensen, M. M., Pinborg, L. H., Gilmour, G., . . . Mikkelsen, J. D. (2015). alpha7 and beta2 Nicotinic Acetylcholine Receptor Subunits Form Heteromeric Receptor Complexes that Are Expressed in the Human Cortex and Display Distinct Pharmacological Properties. *PLoS One, 10*(6), e0130572. doi:10.1371/journal.pone.0130572

Thouvarecq, R., Protais, P., Jouen, F., & Caston, J. (2001). Influence of cholinergic system on motor learning during aging in mice. *Behav Brain Res, 118*(2), 209-218.

Wada, K., Ballivet, M., Boulter, J., Connolly, J., Wada, E., Deneris, E. S., . . . Patrick, J. (1988). Functional expression of a new pharmacological subtype of brain nicotinic acetylcholine receptor. *Science, 240*(4850), 330-334. doi:10.1126/science.2832952

Wada, K., Sakaguchi, H., Jarvis, E. D., & Hagiwara, M. (2004). Differential expression of glutamate receptors in avian neural pathways for learned vocalization. *J Comp Neurol, 476*(1), 44-64. doi:10.1002/cne.20201

Wallace, T. L., & Bertrand, D. (2013). Importance of the nicotinic acetylcholine receptor system in the prefrontal cortex. *Biochem Pharmacol, 85*(12), 1713-1720. doi:10.1016/j.bcp.2013.04.001

Watson, J. T., Adkins‐Regan, E., Whiting, P., Lindstrom, J. M., & Podleski, T. R. (1988). Autoradiographic localization of nicotinic acetylcholine receptors in the brain of the zebra finch (Poephila guttata). *Journal of Comparative Neurology, 274*(2), 255-264.

Whiting, P., Schoepfer, R., Conroy, W., Gore, M., Keyser, K., Shimasaki, S., . . . Lindstrom, J. (1991). Expression of nicotinic acetylcholine receptor subtypes in brain and retina. *Molecular Brain Research, 10*(1), 61-70.

Winzer-Serhan, U. H., & Leslie, F. M. (1997). Codistribution of nicotinic acetylcholine receptor subunit α3 and β4 mRNAs during rat brain development. *Journal of Comparative Neurology, 386*(4), 540-554. doi:https://doi.org/10.1002/(SICI)1096-9861(19971006)386:4<540::AID-CNE2>3.0.CO;2-2

Wonnacott, S. (1997). Presynaptic nicotinic ACh receptors. *Trends Neurosci, 20*(2), 92-98. doi:https://doi.org/10.1016/S0166-2236(96)10073-4

Woolley, S. M., & Portfors, C. V. (2013). Conserved mechanisms of vocalization coding in mammalian and songbird auditory midbrain. *Hear Res, 305*, 45-56. doi:10.1016/j.heares.2013.05.005

Wylie, D. R., Gutierrez-Ibanez, C., Pakan, J. M., & Iwaniuk, A. N. (2009). The optic tectum of birds: mapping our way to understanding visual processing. *Can J Exp Psychol, 63*(4), 328-338. doi:10.1037/a0016826

Zhang, Y., Chen, K., Sloan, S. A., Bennett, M. L., Scholze, A. R., O'Keeffe, S., . . . Wu, J. Q. (2014). An RNA-sequencing transcriptome and splicing database of glia, neurons, and vascular cells of

the cerebral cortex. *J Neurosci, 34*(36), 11929-11947. doi:10.1523/JNEUROSCI.1860-14.2014

Zoli, M., Le Novere, N., Hill, J. A., & Changeux, J.-P. (1995). Developmental regulation of nicotinic ACh receptor subunit mRNAs in the rat central and peripheral nervous systems. *Journal of Neuroscience, 15*(3), 1912-1939.

Zoli, M., Pistillo, F., & Gotti, C. (2015). Diversity of native nicotinic receptor subtypes in mammalian brain. *Neuropharmacology, 96*(Pt B), 302-311. doi:10.1016/j.neuropharm.2014.11.003

Zoli, M., Pucci, S., Vilella, A., & Gotti, C. (2018). Neuronal and Extraneuronal Nicotinic Acetylcholine Receptors. *Curr Neuropharmacol, 16*(4), 338-349. doi:10.2174/1570159X15666170912110450

Zuschratter, W., & Scheich, H. (1990). Distribution of choline acetyltransferase and acetylcholinesterase in the vocal motor system of zebra finches. *Brain Res, 513*(2), 193-201. doi:https://doi.org/10.1016/0006-8993(90)90457-M

(a)

Zebra finch ChrnA2 (XP 041571428)
Chicken ChrnA2 (NP 990146)
Human ChrnA2 (NP 000733)
Human ChrnA4 (NP 000735)
Zebra finch ChrnA4 (XP 012425694)
Chicken ChrnA4 (NP 001384279)
Zebra finch ChrnA3 (XP 012424533)
Chicken ChrnA3 (NP 989747)
Human ChrnA3 (NP 000734)
Human ChrnA6 (NP 000736)
Zebra finch ChrnA6 (XP 002188874)
Chicken ChrnA6 (NP 990695)
Zebra finch ChrnA5 (XP 030137058)
Chicken ChrnA5 (NP 989746)
Human ChrnA5 (NP 000736)
Human ChrnB3 (NP 000740)
Zebra finch ChrnB3 (XP 002189048)
Chicken ChrnB3 (NP 990143)
Human ChrnA1 (NP 000070)
Zebra finch ChrnA1 (XP 002199082)
Chicken ChrnA1 (NP 990147)
Zebra finch ChrnA7 (XP 030136897)
Chicken ChrnA7 (NP 989512)
Human ChrnA7 (NP 000737)
Zebra finch ChrnA8 (7-like) (XP 002187698)
Chicken ChrnA8 (7-like) (NP 990532)
Zebra finch ChrnA9 (XP 030126824)
Chicken ChrnA9 (NP 990091)
Human ChrnA9 (NP 060051)
Human ChrnA10 (NP 065135)
Zebra finch ChrnA10 (XP 030140591)
Chicken ChrnA10 (NP 001094506)
Zebra finch ChnrB2 (XP 030147527)
Chicken ChrnB2 (NP 990144)
Human ChrnB2 (NP 000739)
Human ChrnB4 (NP 000741)
Zebra finch ChrnB4 (XP 030137055)
Chicken ChrnB4 (NP 990150)
Zebra finch ChrnD (XP 030136510)
Chicken ChrnD (NP 001026488)
Human ChrnD (NP 001298125)
Human ChrnG (NP 005190)
Zebra finch ChrnG (XP 030136509)
Chicken ChrnG (NP 001026739)

0.20

(b)

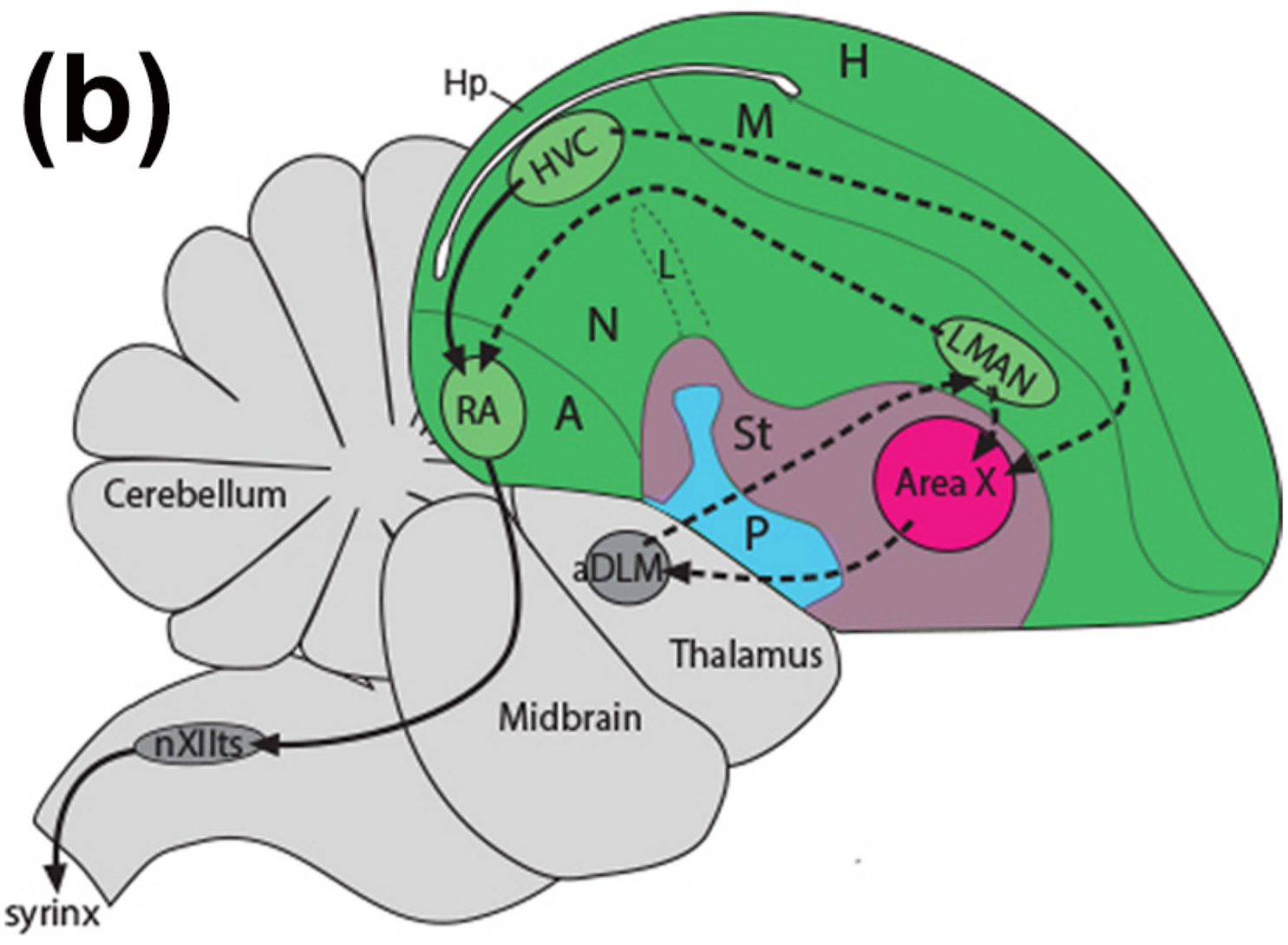

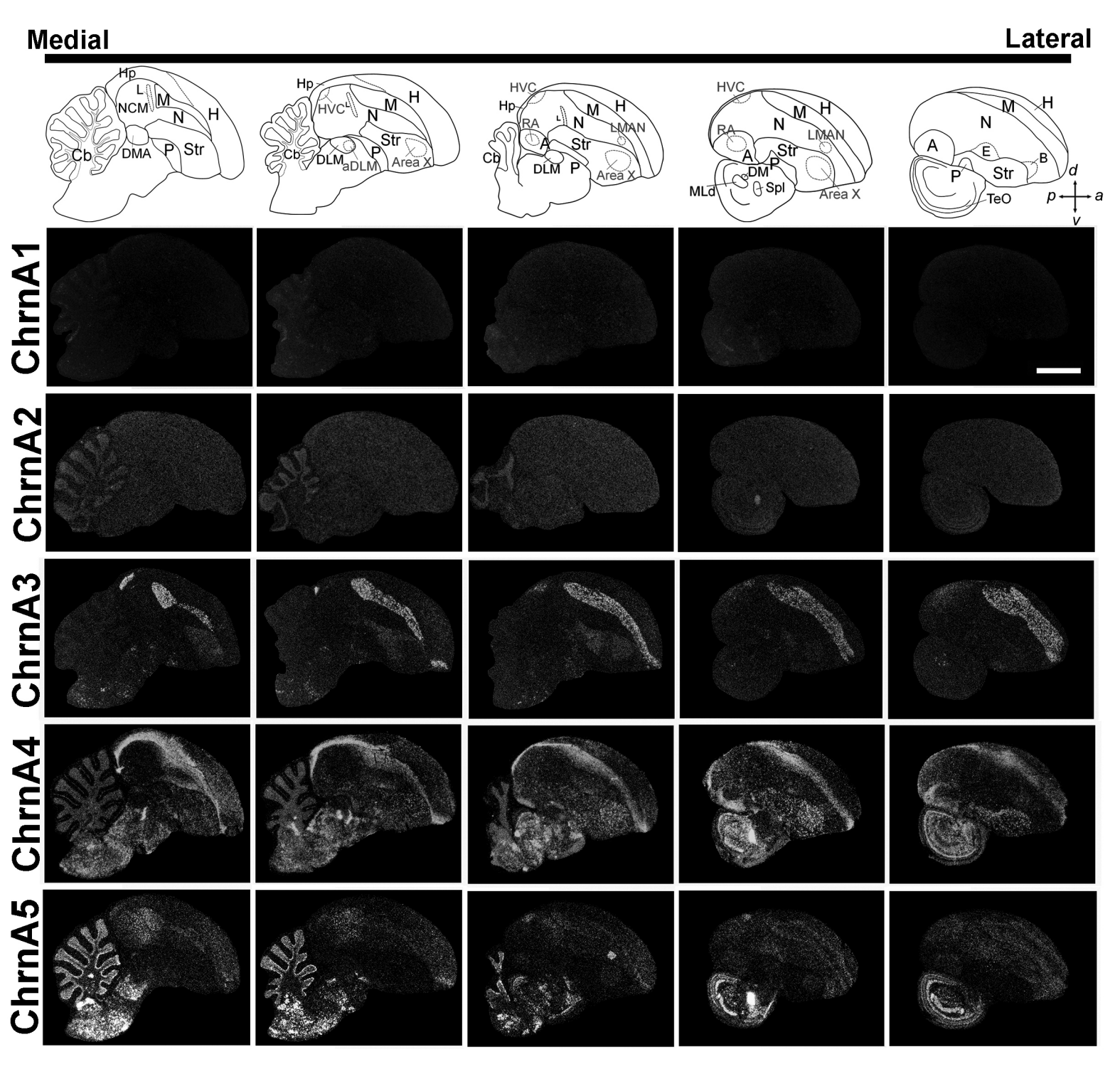
Medial
Lateral
Hp
L
NCM
M
N
H
Cb
DMA
P
Str
HVC
RA
LMAN
A
DLM
aDLM
Area X
DM
MLd
Spl
E
B
TeO
d
p
a
v
ChrnA1
ChrnA2
ChrnA3
ChrnA4
ChrnA5

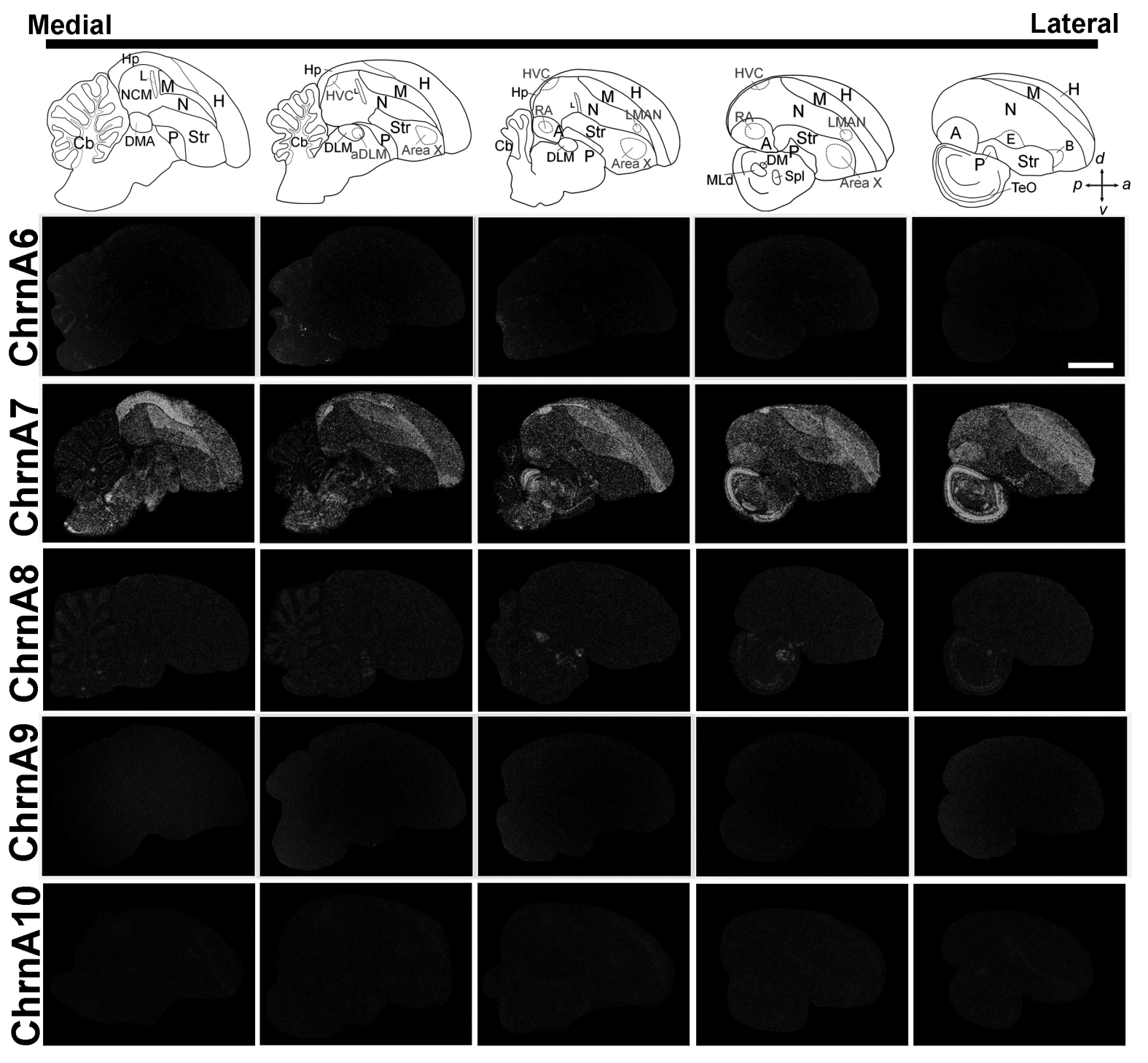
Medial
Lateral
Hp
L
NCM
M
N
H
Cb
DMA
P
Str
HVC
RA
LMAN
A
DLM
aDLM
Area X
MLd
Spl
E
B
TeO
d
p
a
v
ChrnA6
ChrnA7
ChrnA8
ChrnA9
ChrnA10

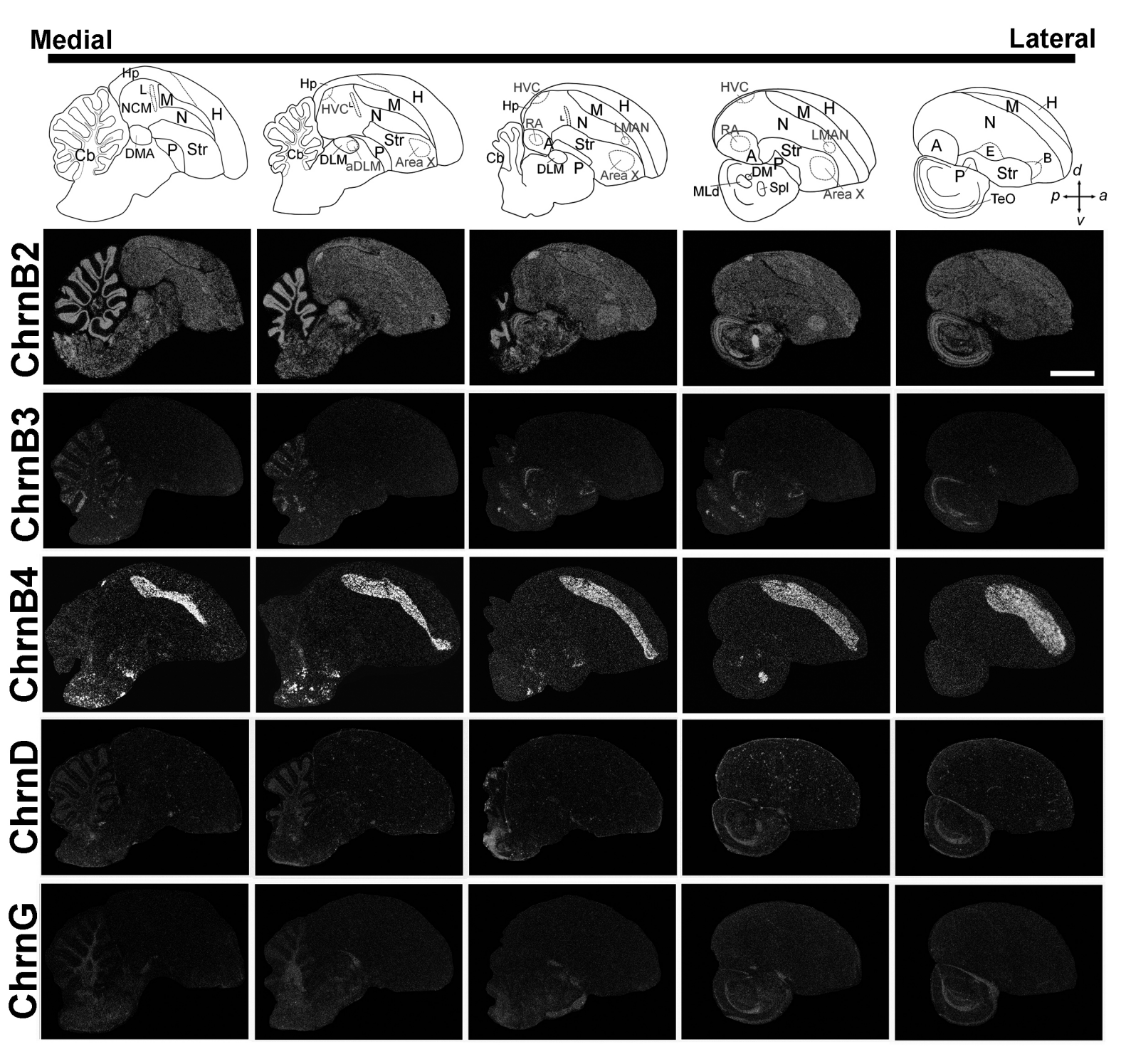
Medial
Lateral
Hp
L
NCM
M
N
H
Cb
DMA
P
Str
HVC
RA
LMAN
A
DLM
aDLM
Area X
DM
MLd
Spl
E
B
TeO
d
p
a
v
ChrnB2
ChrnB3
ChrnB4
ChrnD
ChrnG

ChrnA2

ChrnA3

ChrnA4

ChrnA5

ChrnA7

ChrnB2

ChrnB4

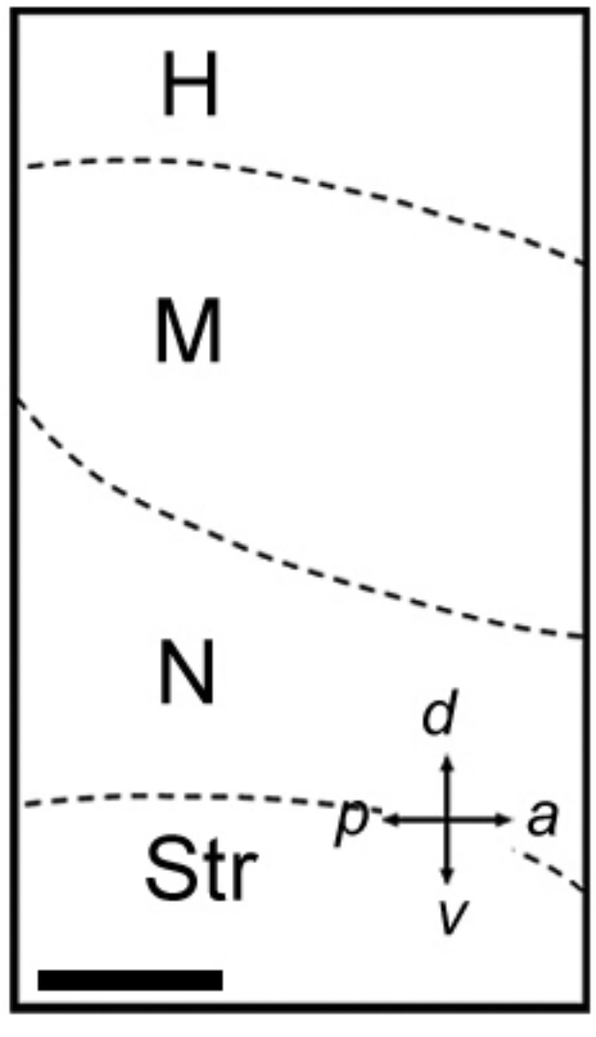

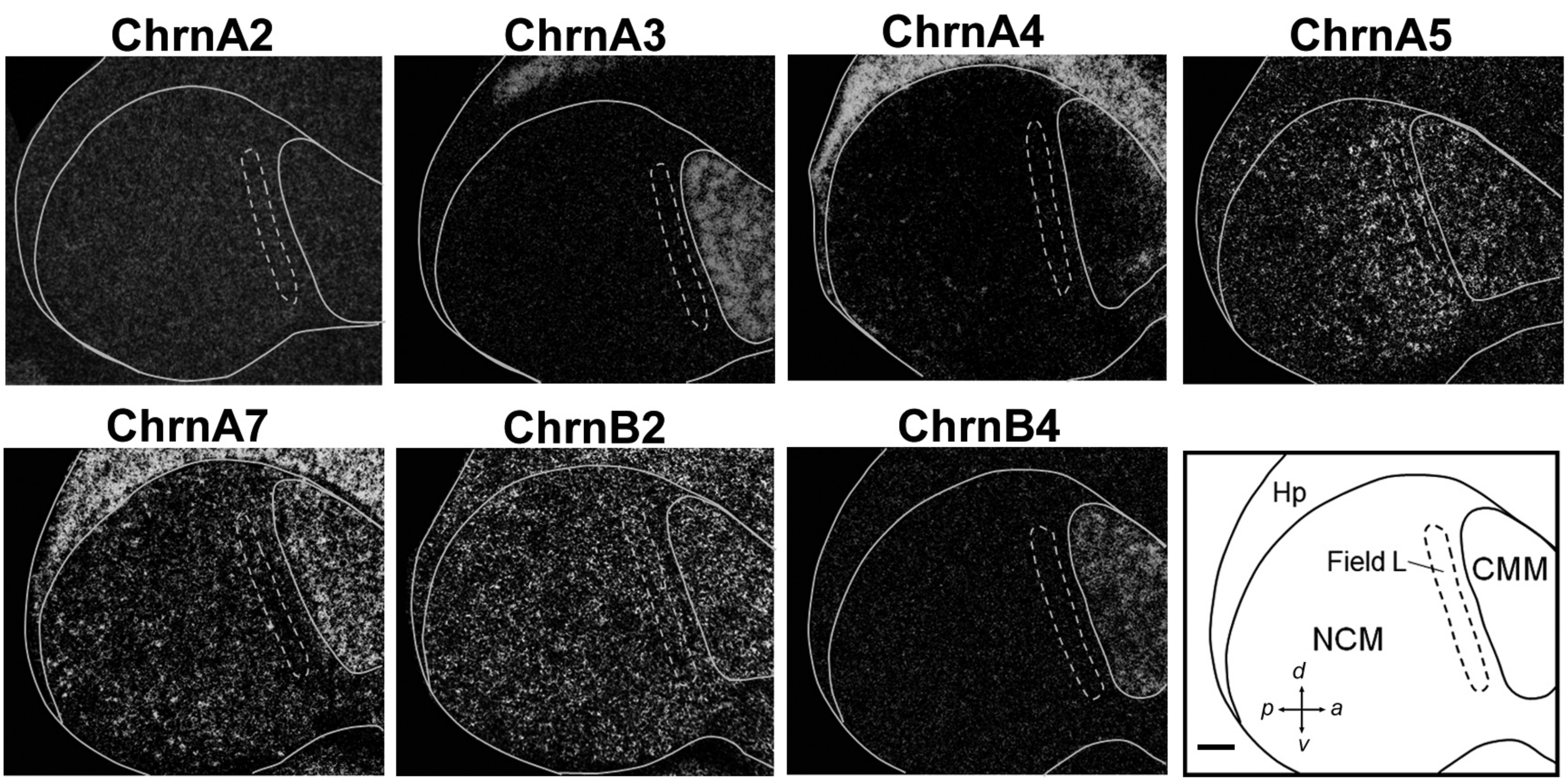
ChrnA2
ChrnA3
ChrnA4
ChrnA5
ChrnA7
ChrnB2
ChrnB4
Hp
Field L
CMM
NCM
d
p
a
v

(a)

ChrnA2

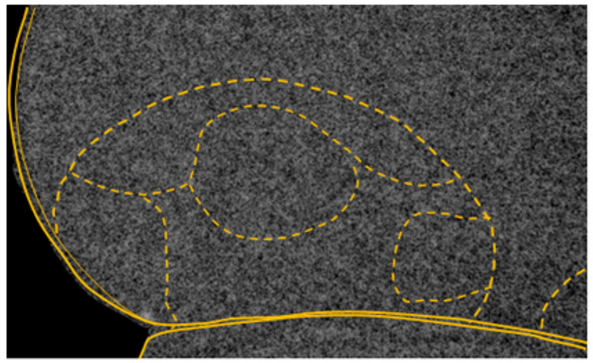

ChrnA3

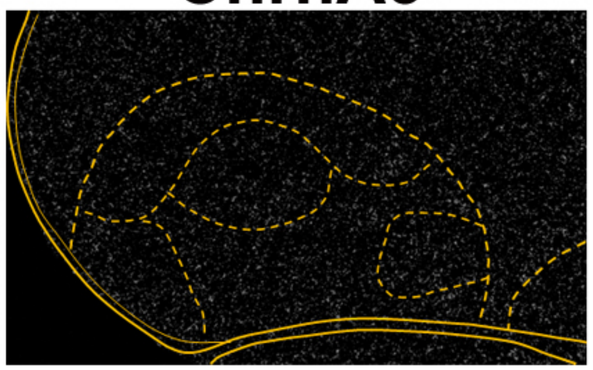

ChrnA4

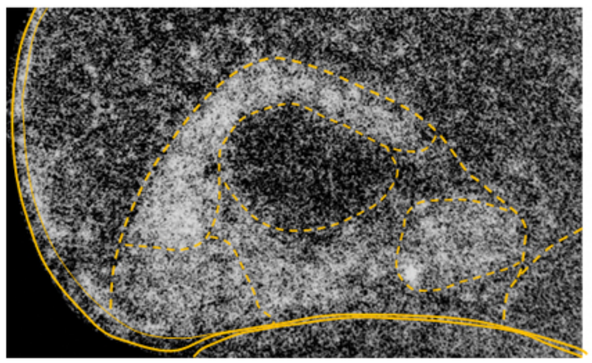

ChrnA5

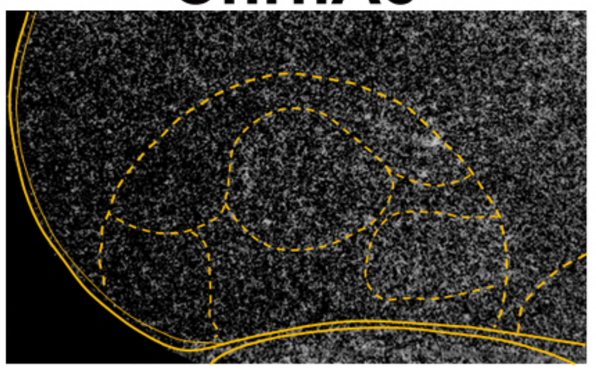

ChrnA7

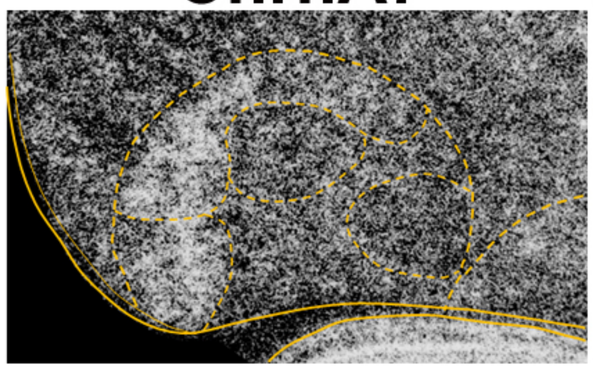

ChrnB2

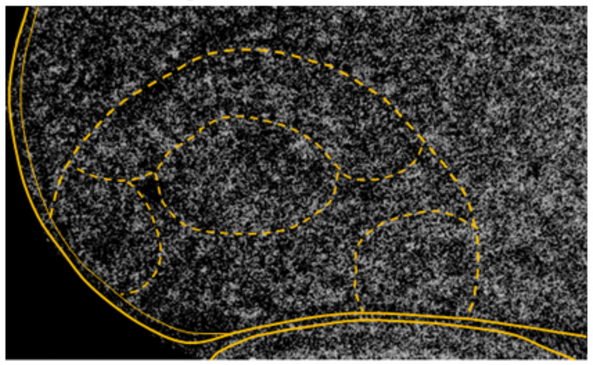

ChrnB4

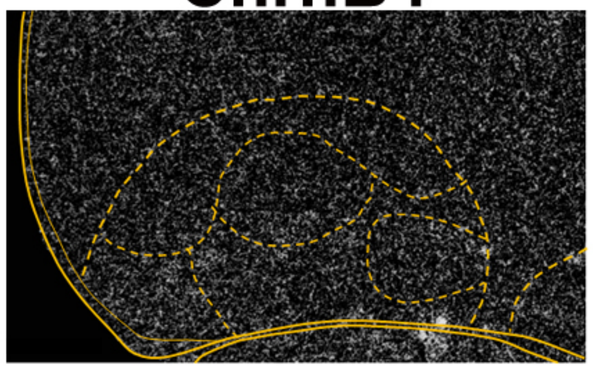

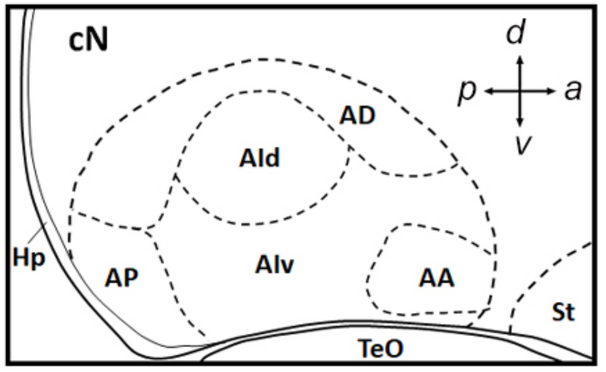

(b)

ChrnA8

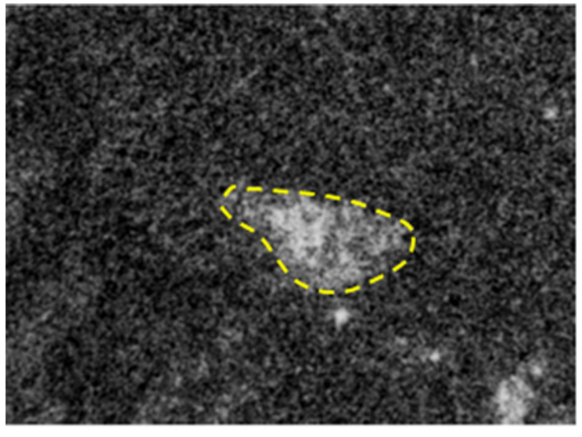

Nissl

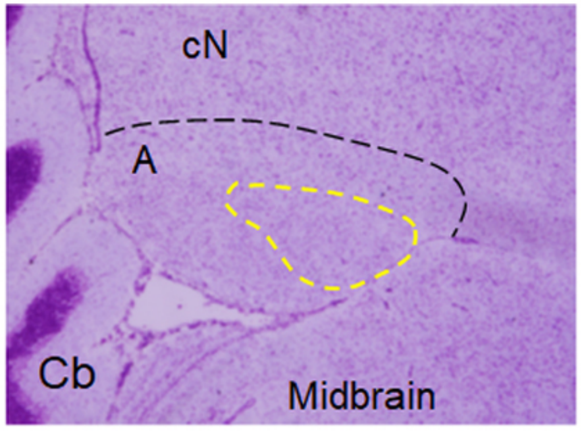

Merge

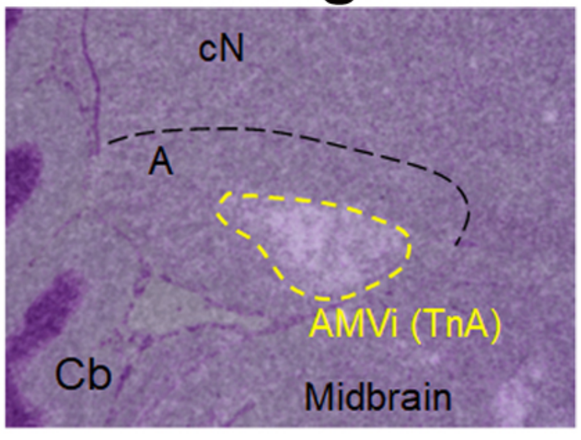

ChrnA2

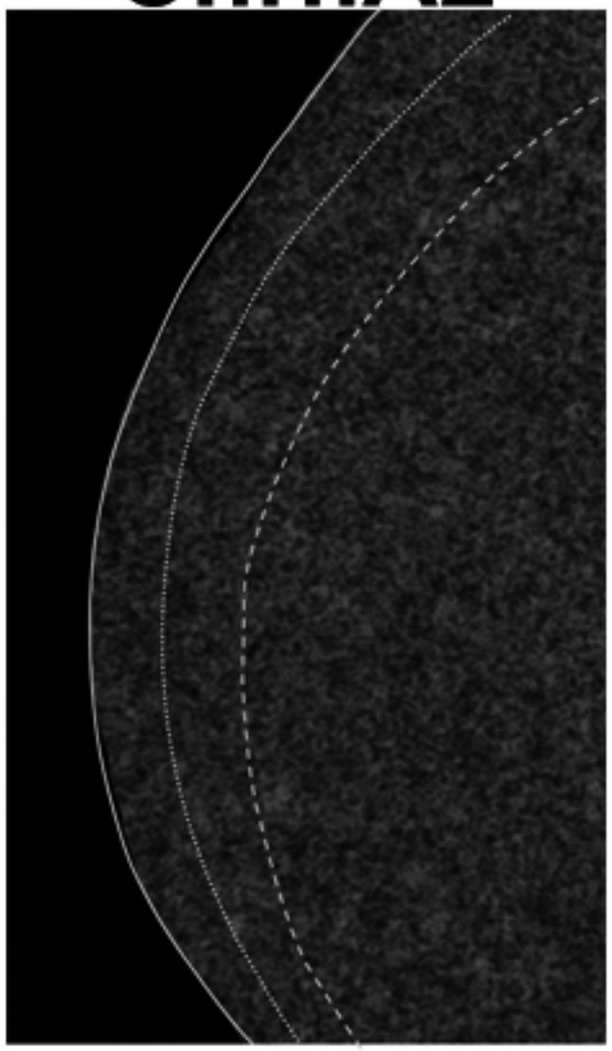

ChrnA3

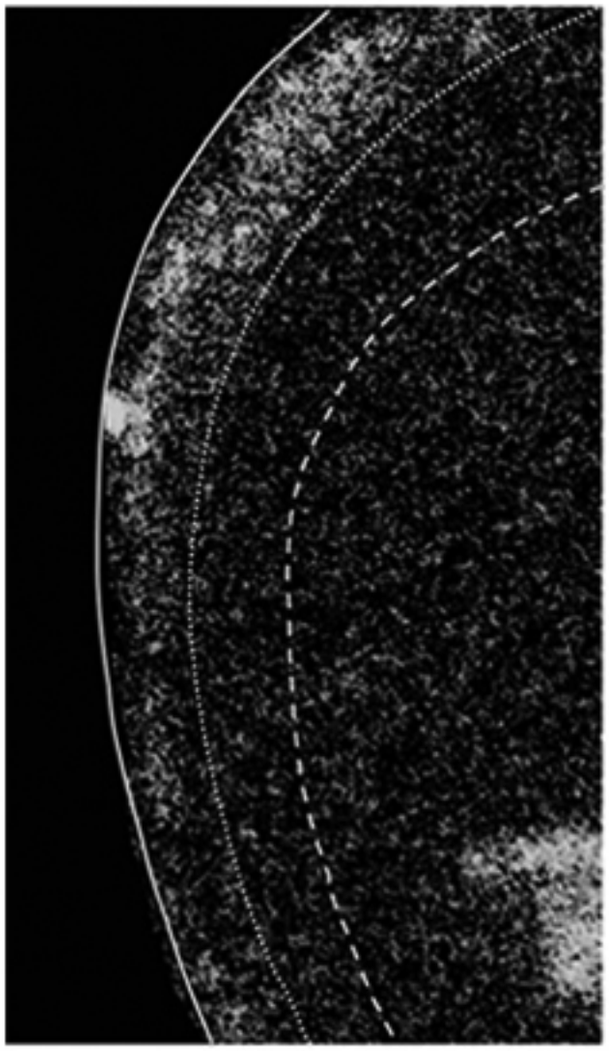

ChrnA4

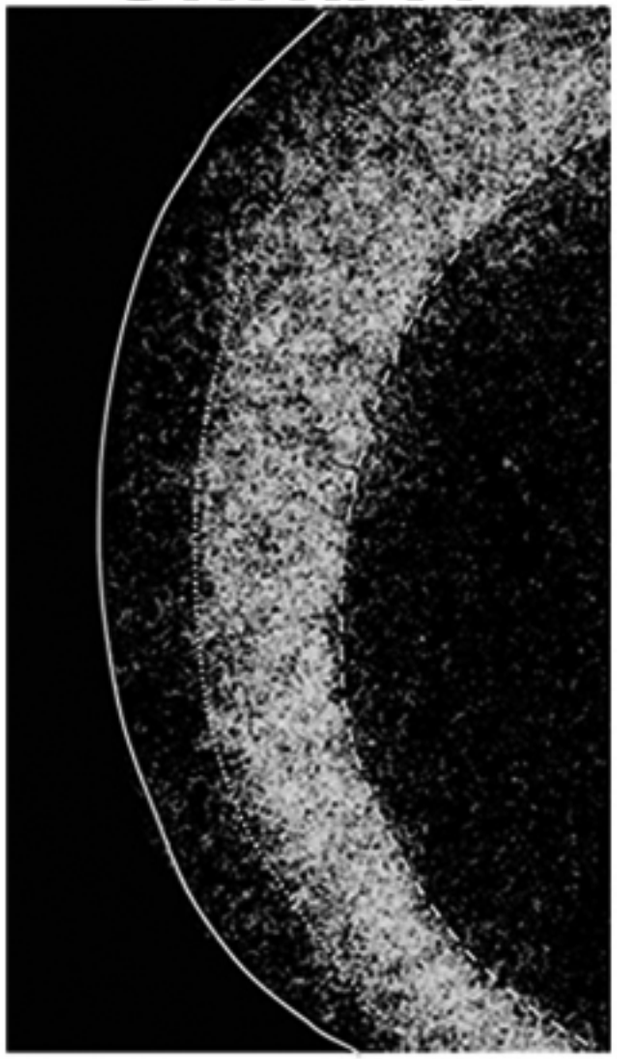

ChrnA5

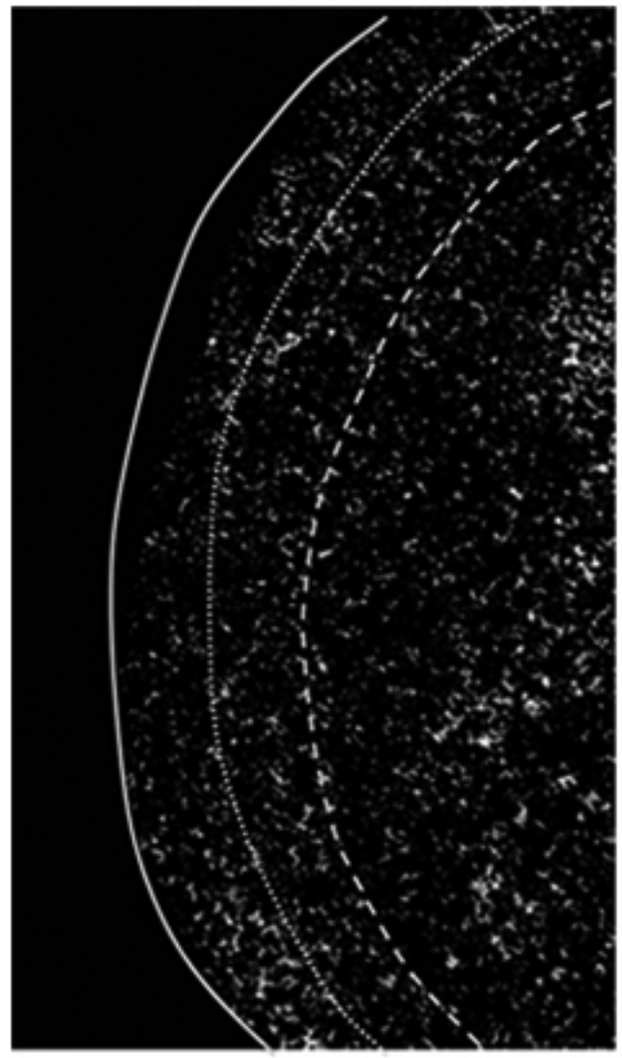

ChrnA7

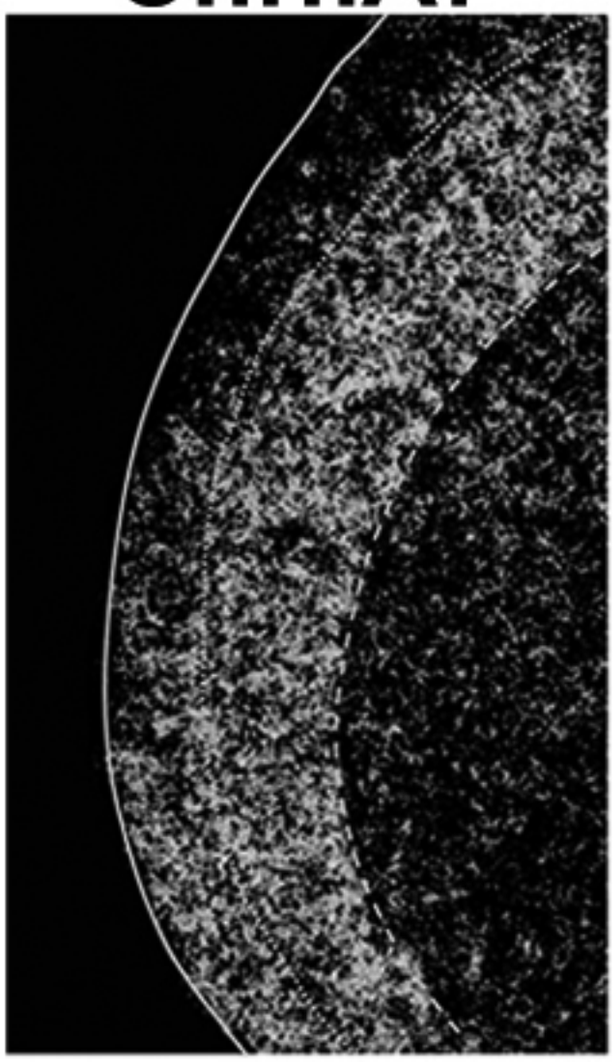

ChrnB2

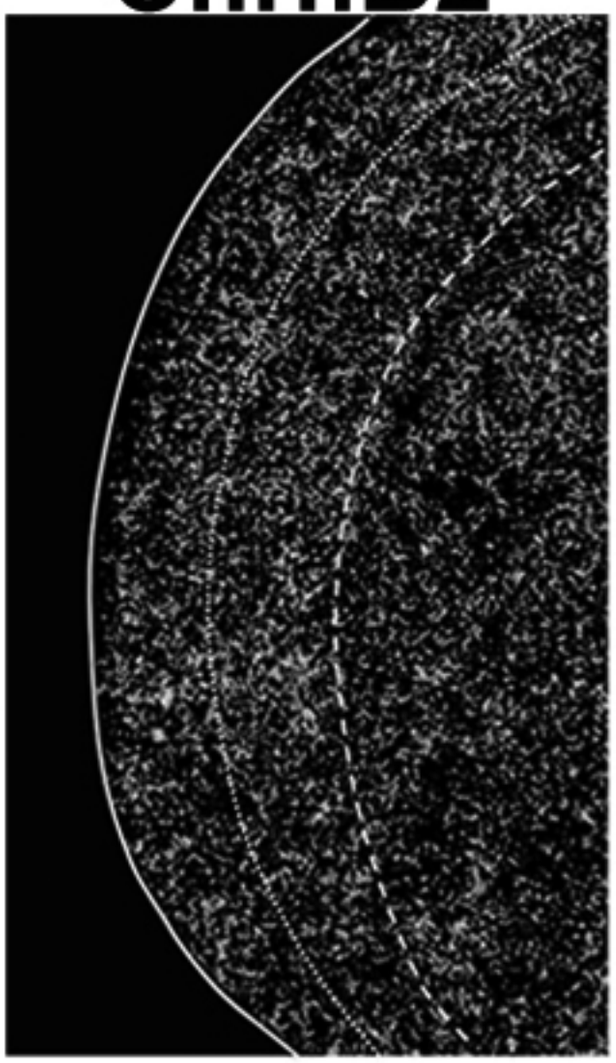

ChrnB4

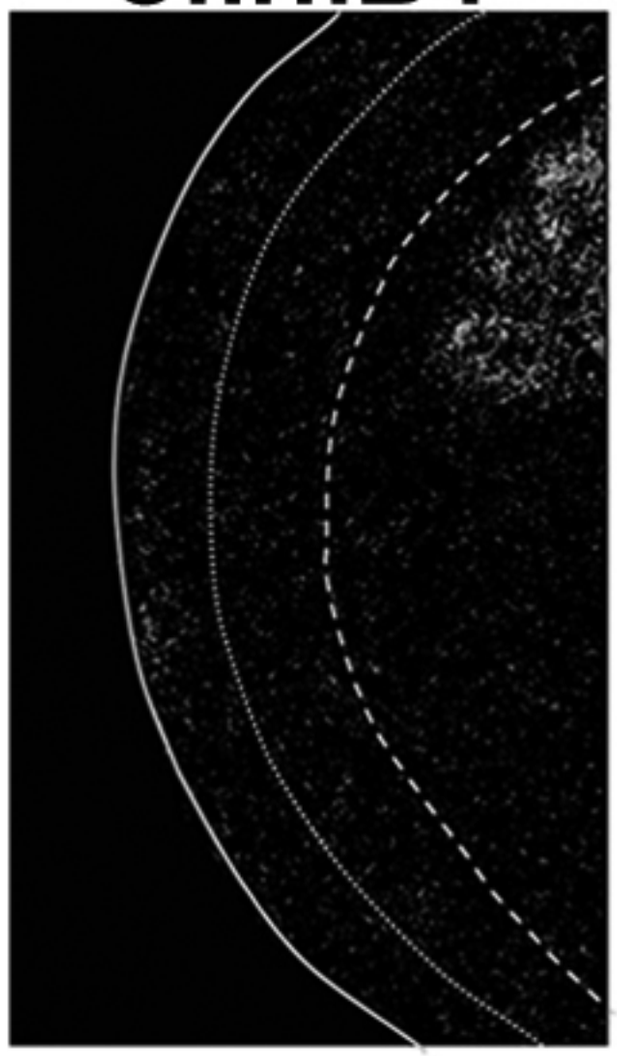

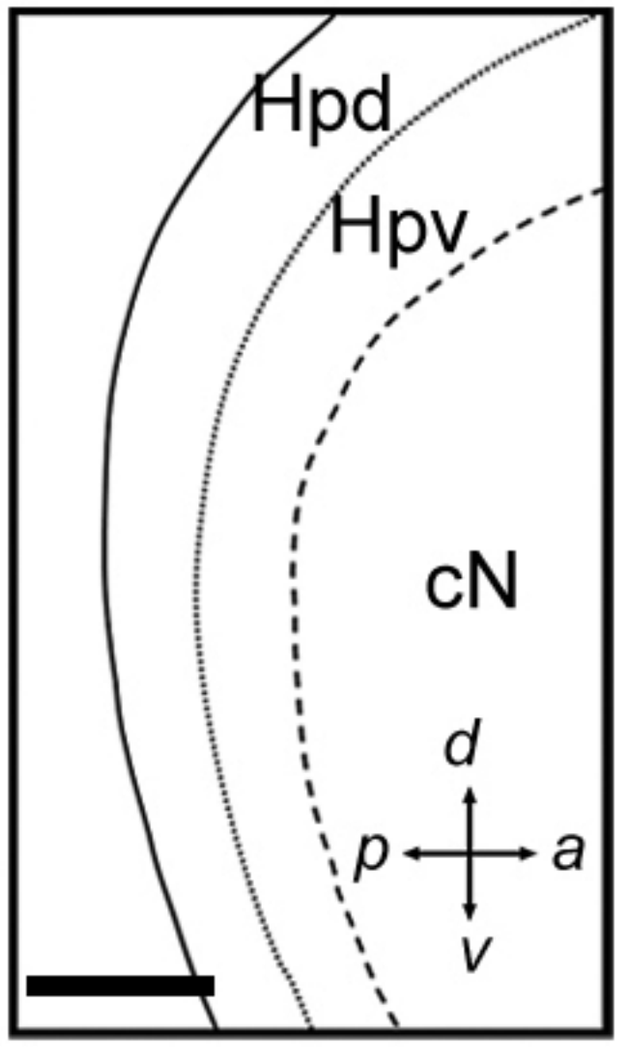

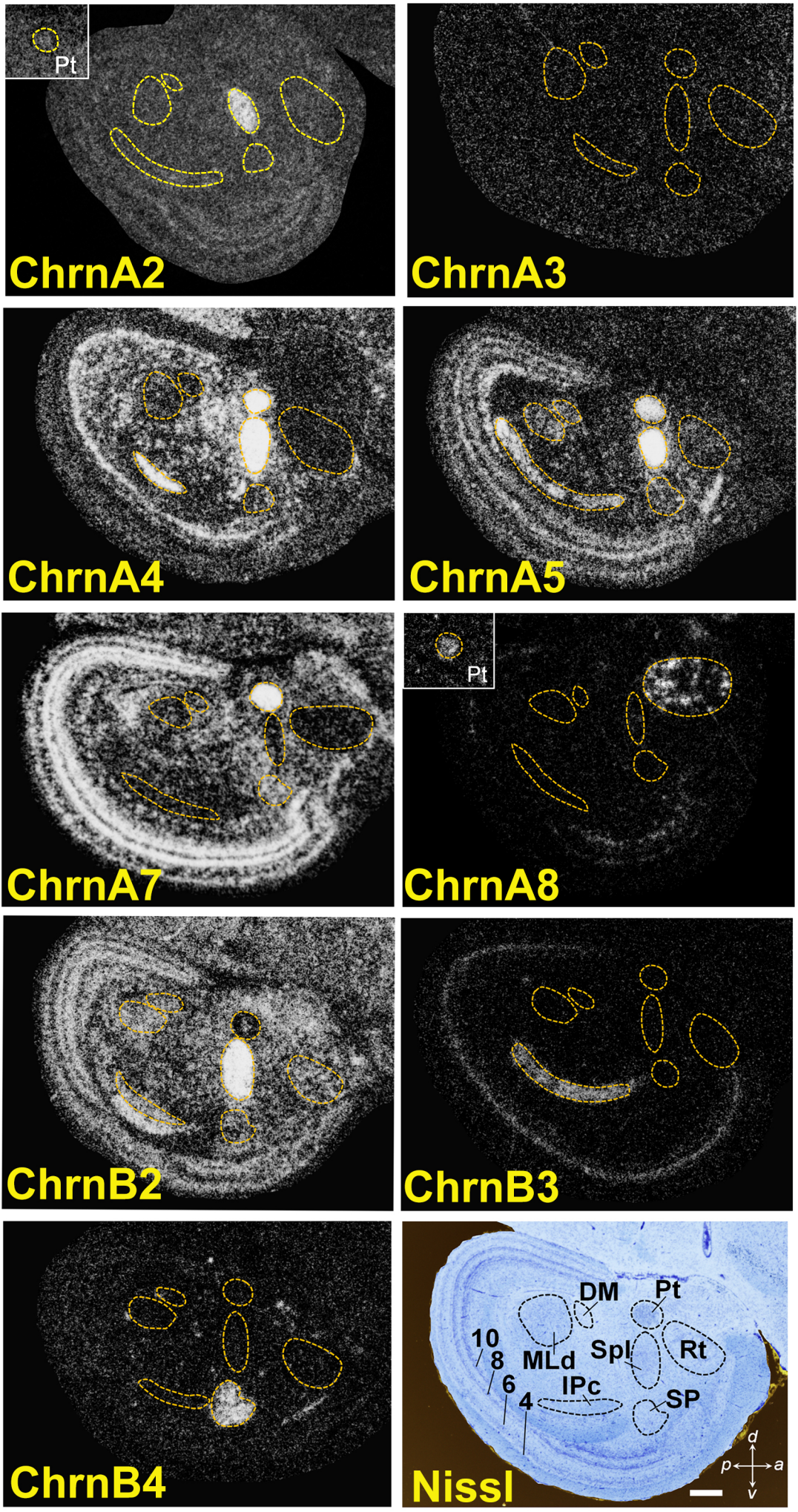
Pt
ChrnA2
ChrnA3
ChrnA4
ChrnA5
ChrnA7
Pt
ChrnA8
ChrnB2
ChrnB3
ChrnB4
DM
Pt
10
8
6
4
MLd
Spl
Rt
IPc
SP
Nissl
d
p
a
v

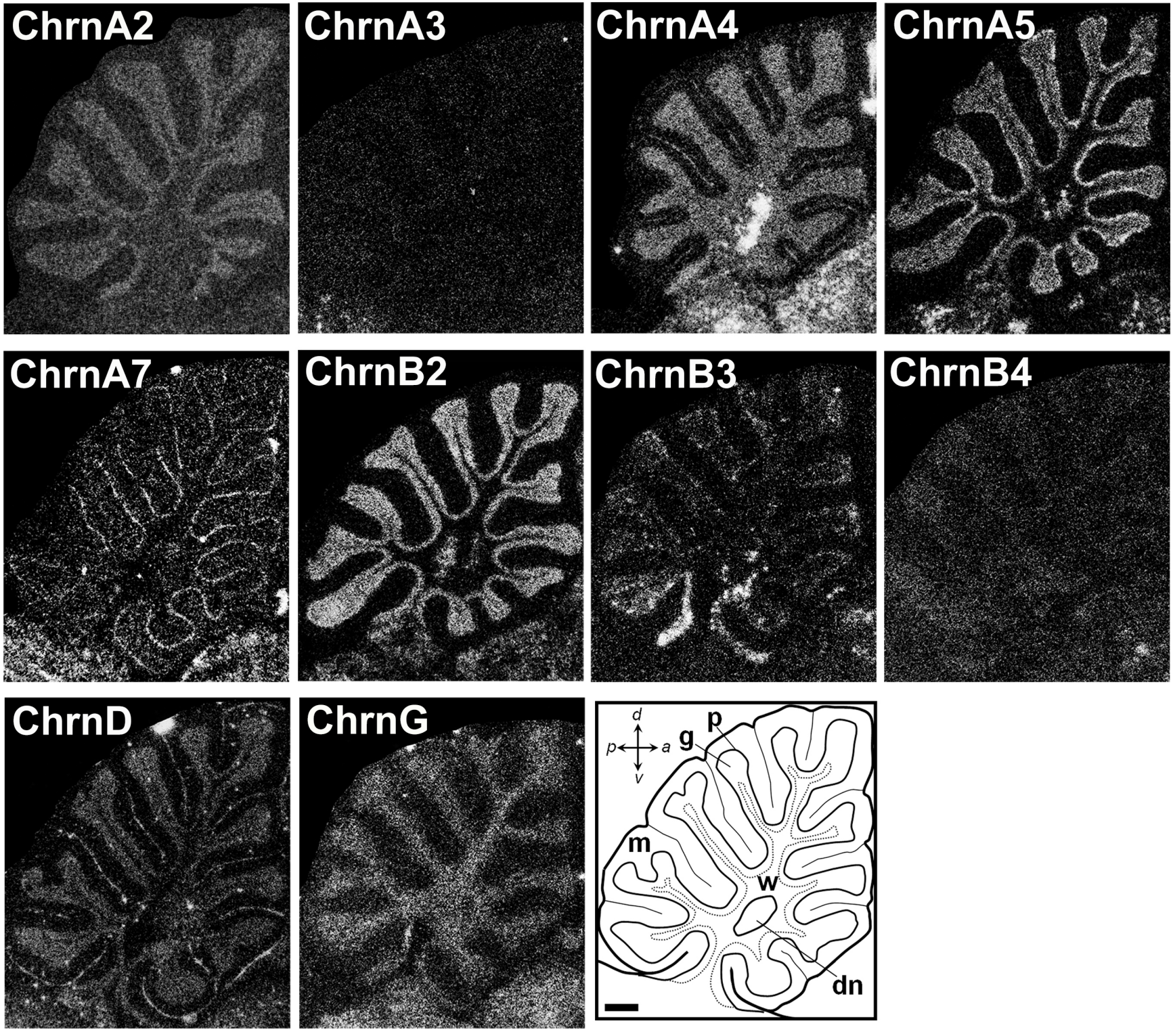
ChrnA2
ChrnA3
ChrnA4
ChrnA5
ChrnA7
ChrnB2
ChrnB3
ChrnB4
ChrnD
ChrnG
d
p
a
v
g
p
m
w
dn

Chrn

A

B

1 2 3 4 5 6 7 8 9 10 2 3 4 D G

Pallium

H M N NCM AId AIv AA AP AD AMVi Hpd Hpv L E B

Subpallium

Str P

Midbrain

Pt Rt Spl TeO SP IPc DM MLd

Cerebellum

pr m g w dn

mRNA expression level (pixel density)

0 80 200

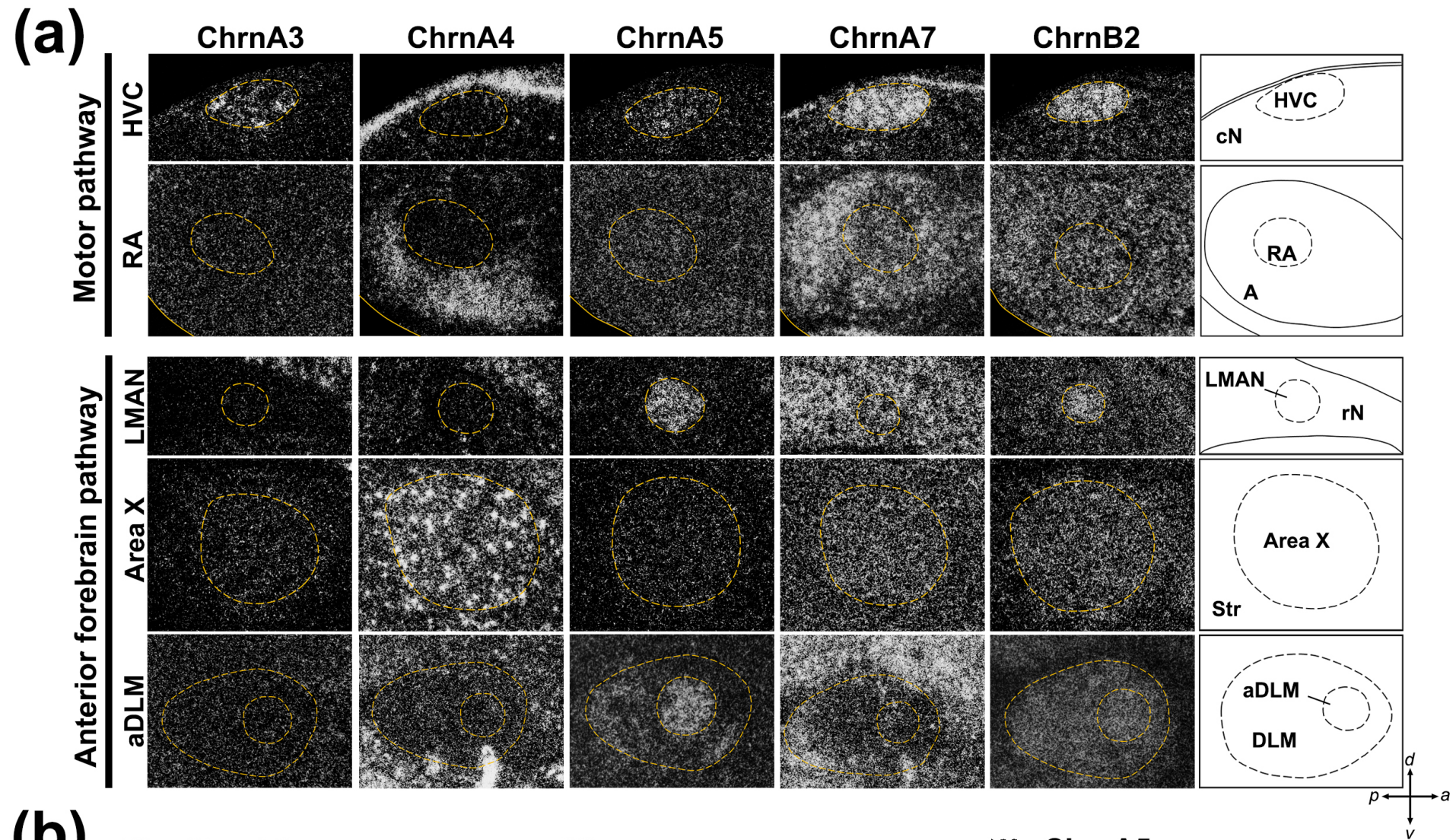
(a)
ChrnA3
ChrnA4
ChrnA5
ChrnA7
ChrnB2
Motor pathway
HVC
RA
Anterior forebrain pathway
LMAN
Area X
aDLM
HVC
cN
RA
A
LMAN
rN
Area X
Str
aDLM
DLM
d
p
a
v

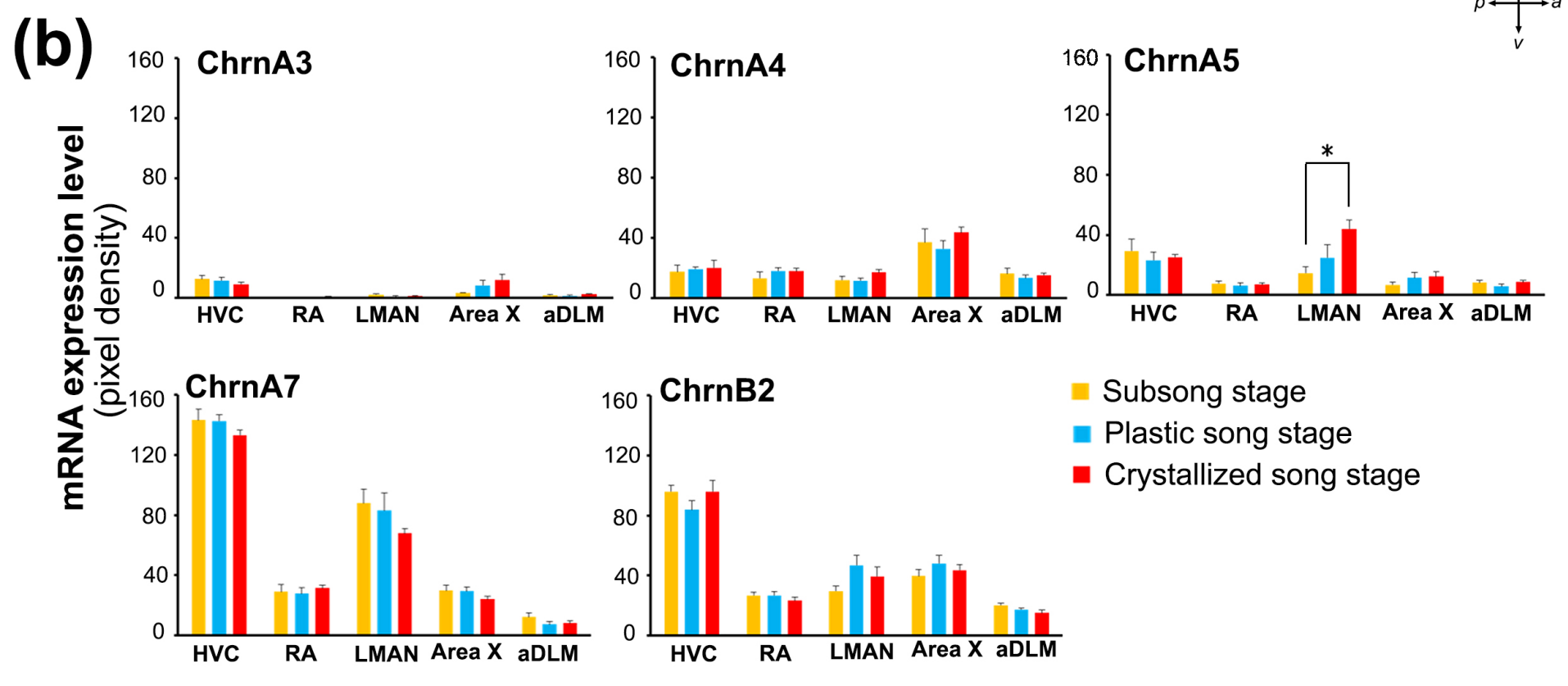
(b)
mRNA expression level
(pixel density)
ChrnA3
ChrnA4
ChrnA5
ChrnA7
ChrnB2
160
120
80
40
0
HVC
RA
LMAN
Area X
aDLM
*
Subsong stage
Plastic song stage
Crystallized song stage

(a)

Glutamatergic neuron

SLC17A6

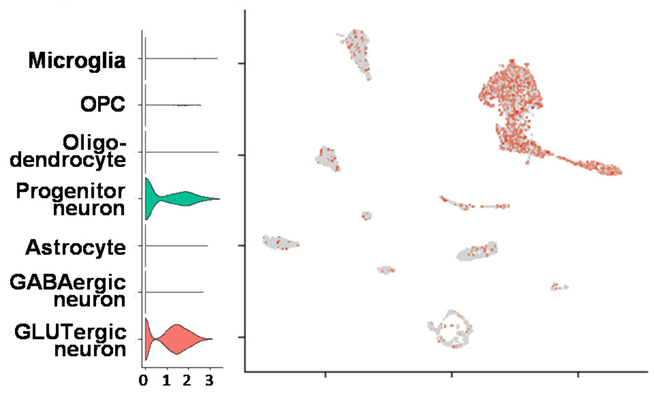

GABAergic neuron

GAD1

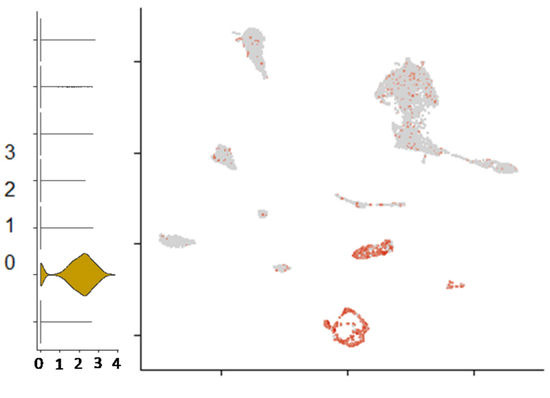

GAD2

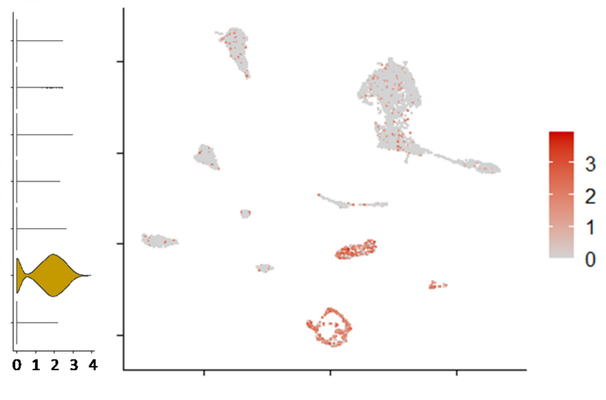

Oligodendrocyte

PLP1

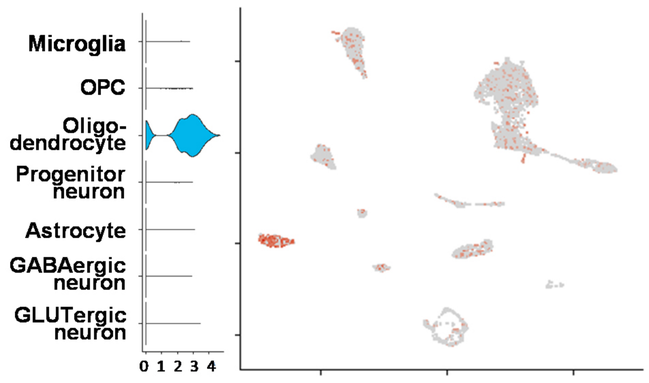

ST18

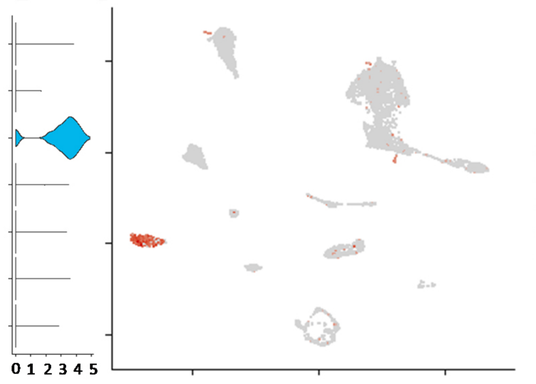

Microglia

CSF1R

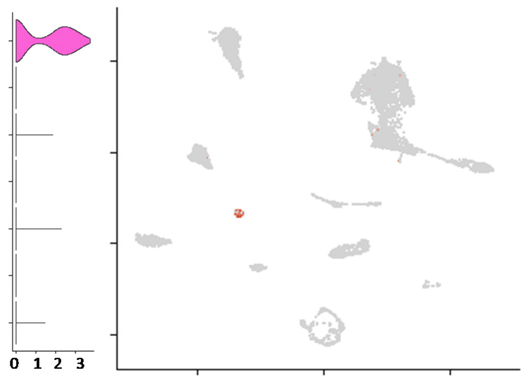

IKZF1

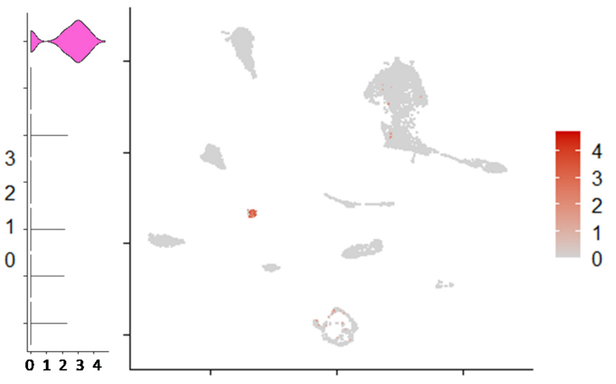

Astrocyte

SLC15A2

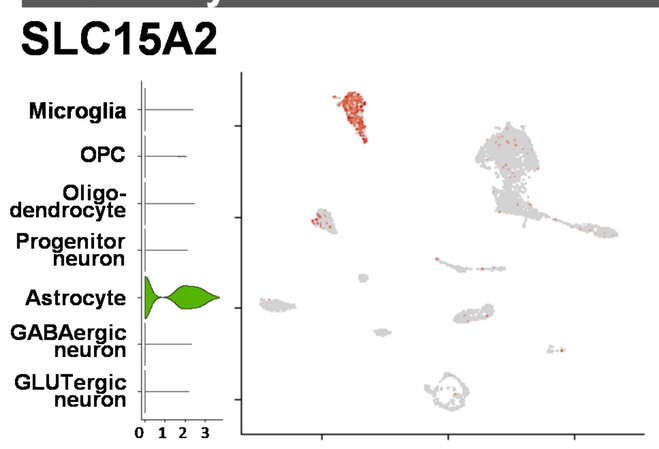

SLC1A2

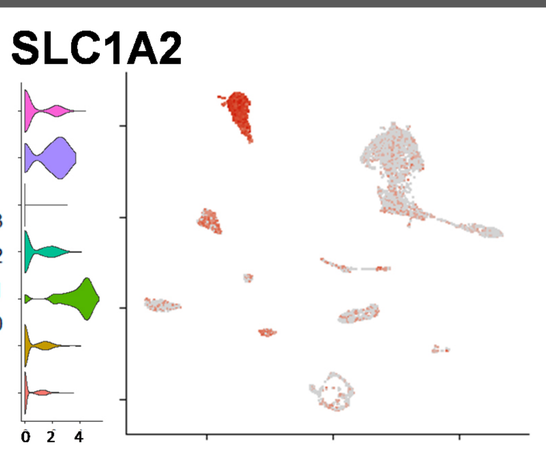

ASPA

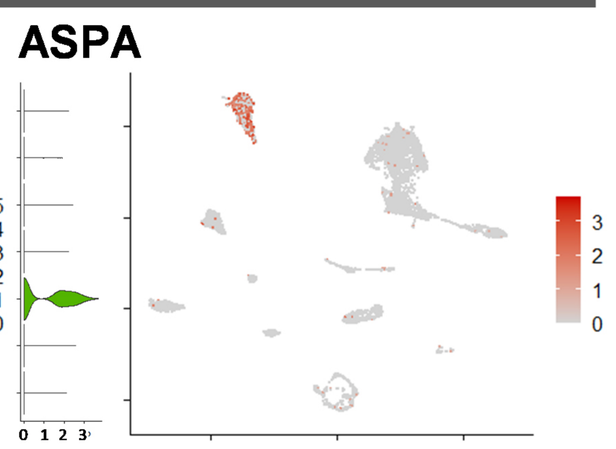

OPC

PDGFRA

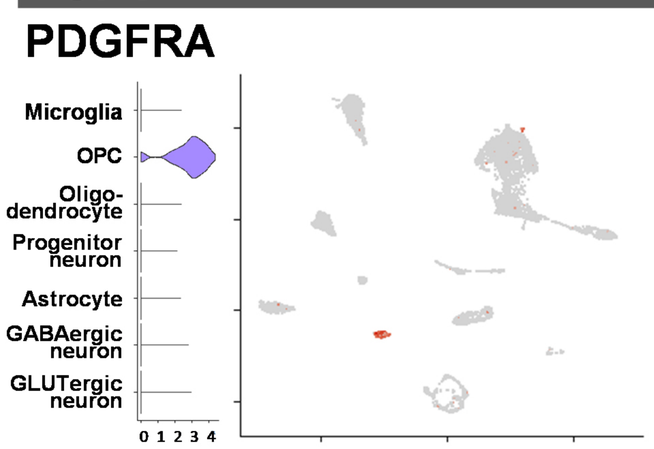

NKX2-2

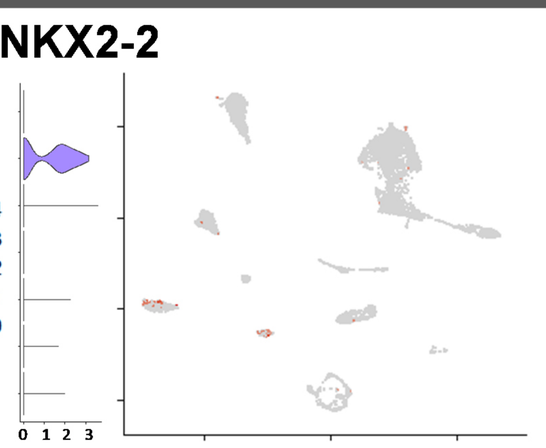

Progenitor neuron

SOX4

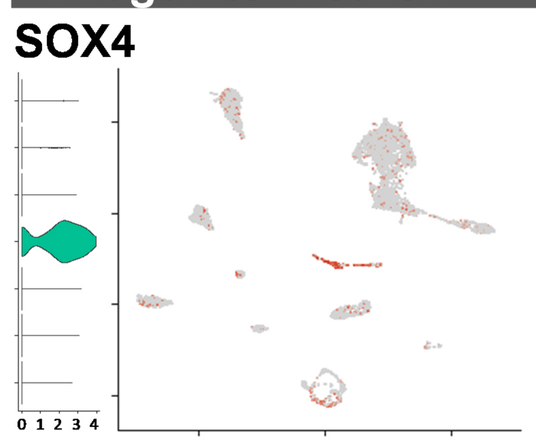

SOX11

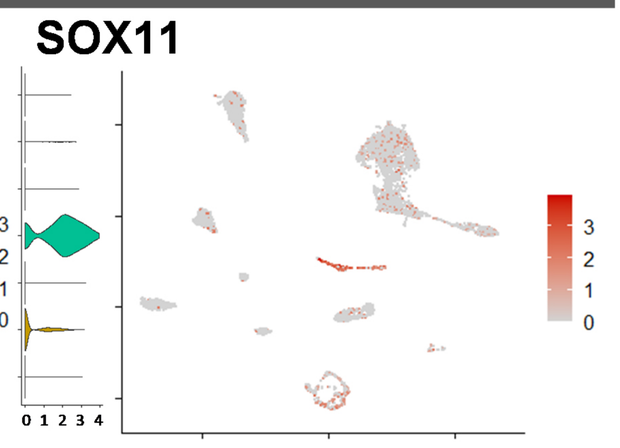

(b)

$HVC_{(RA)}$ neuron

UTS2B

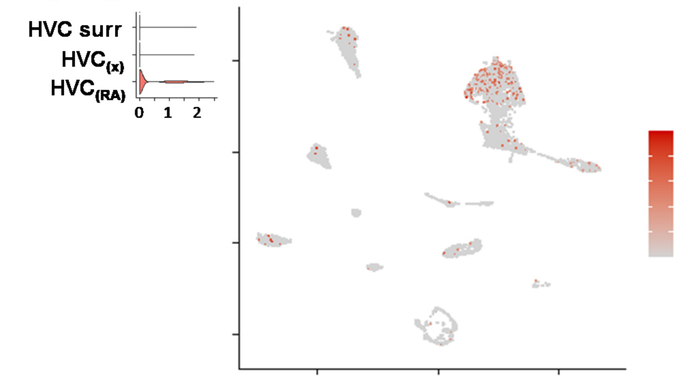

GFRA1

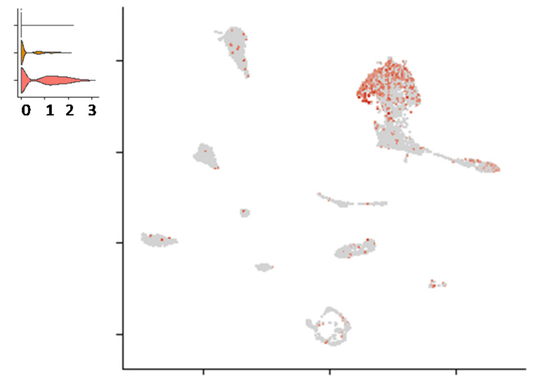

$HVC_{(x)}$ neuron

NTS

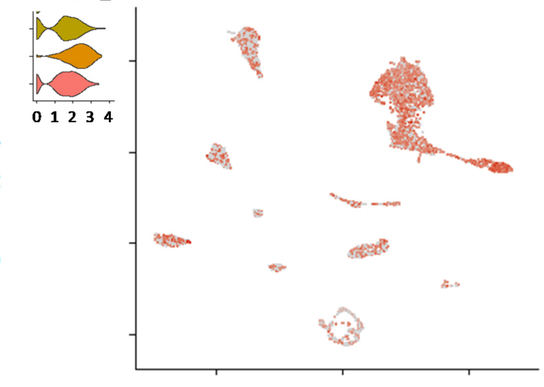

SCUBE1

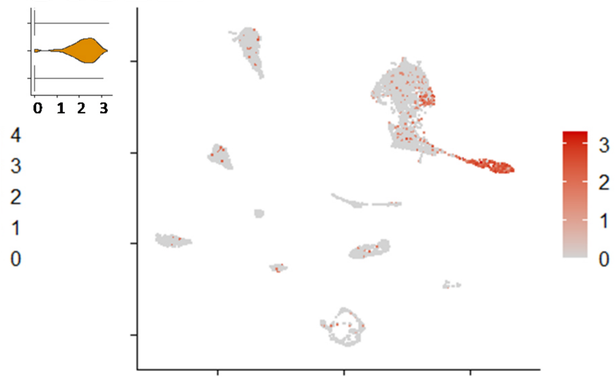

HVC surrounding neuron

GRIA4

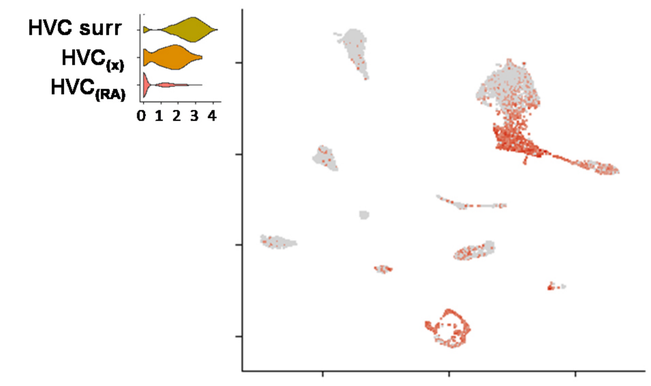

GRM1

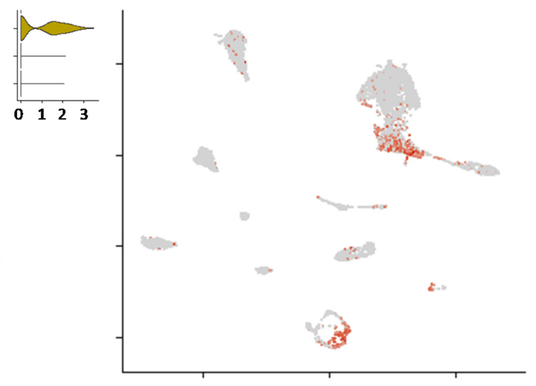

CACNA2D1

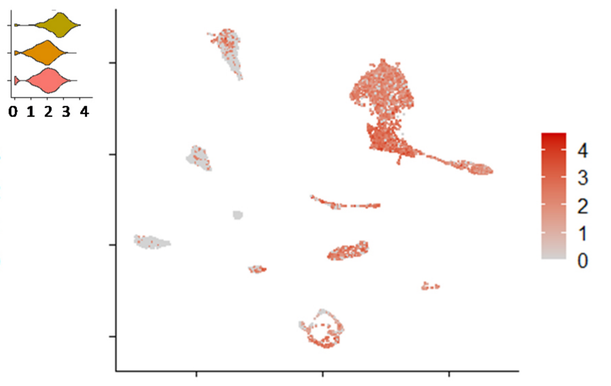

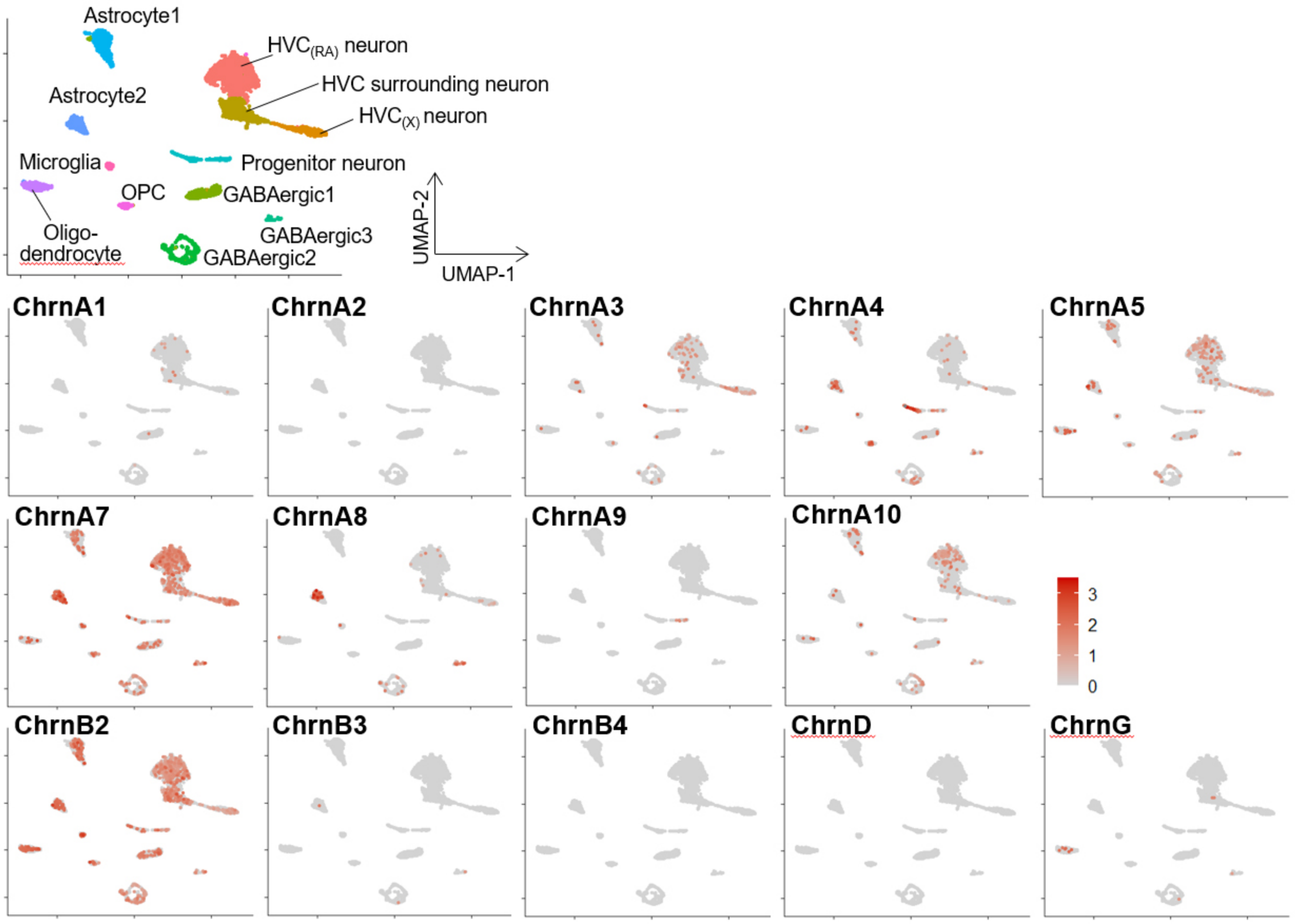
Astrocyte1
HVC(RA) neuron
HVC surrounding neuron
HVC(X) neuron
Astrocyte2
Microglia
Progenitor neuron
OPC
GABAergic1
Oligo-
dendrocyte
GABAergic3
GABAergic2
UMAP-2
UMAP-1
ChrnA1
ChrnA2
ChrnA3
ChrnA4
ChrnA5
ChrnA7
ChrnA8
ChrnA9
ChrnA10
3
2
1
0
ChrnB2
ChrnB3
ChrnB4
ChrnD
ChrnG

(a)

Glutamatergic neuron

SLC17A6

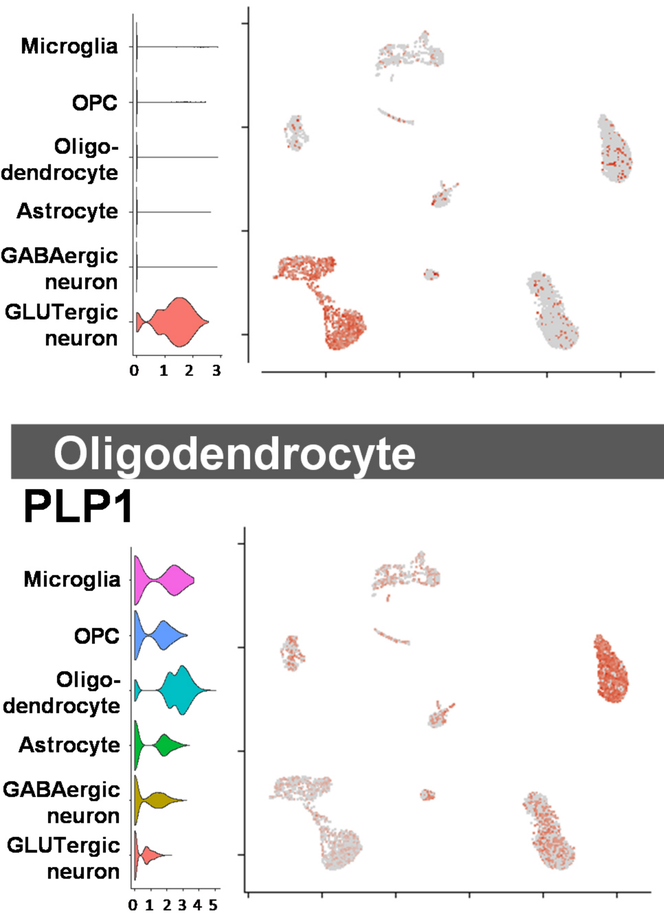

GABAergic neuron

GAD1

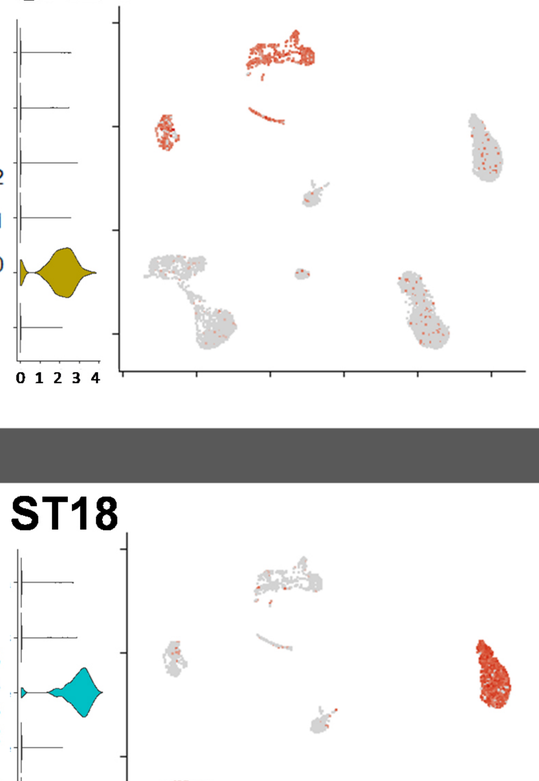

GAD2

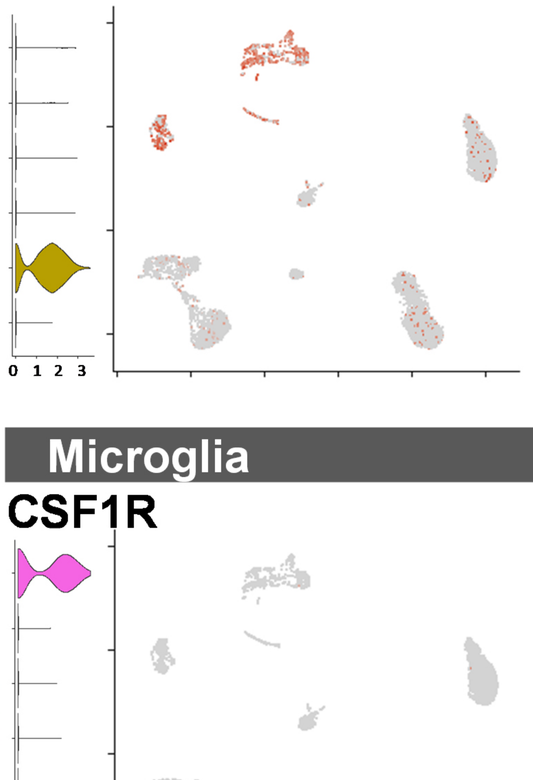

Oligodendrocyte

PLP1

ST18

Microglia

CSF1R

IKZF1

Astrocyte

SLC15A2

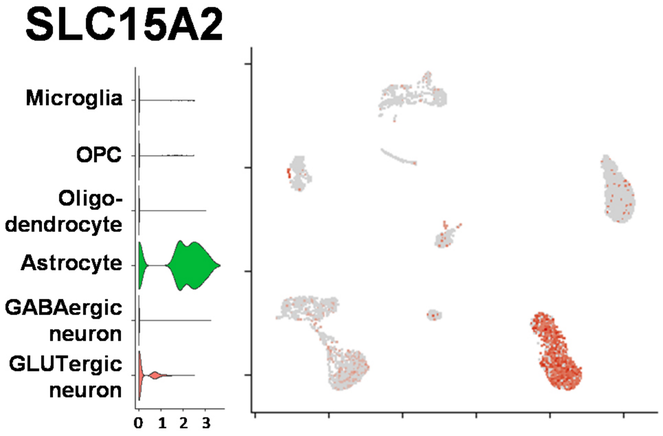

SLC1A2

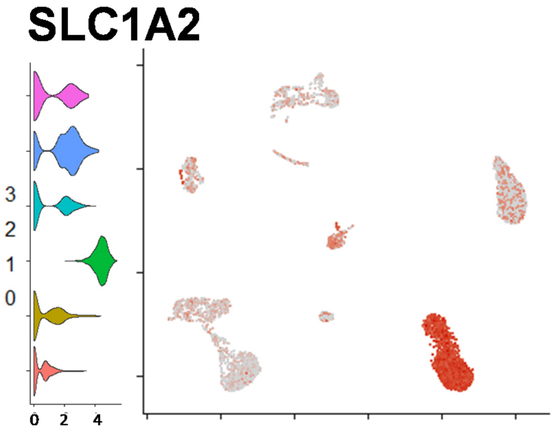

ASPA

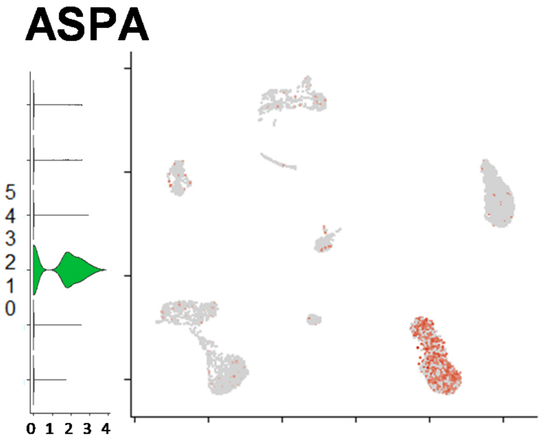

OPC

PDGFRA

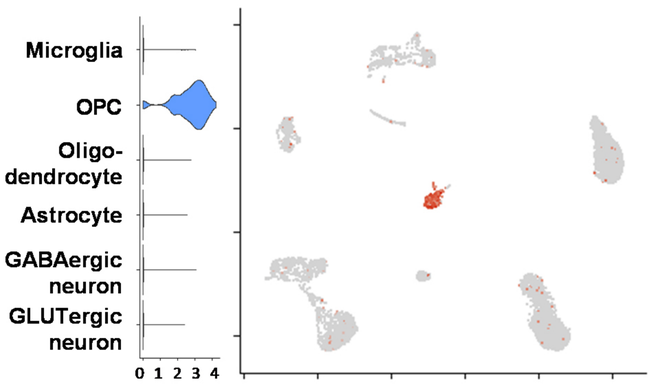

NKX2-2

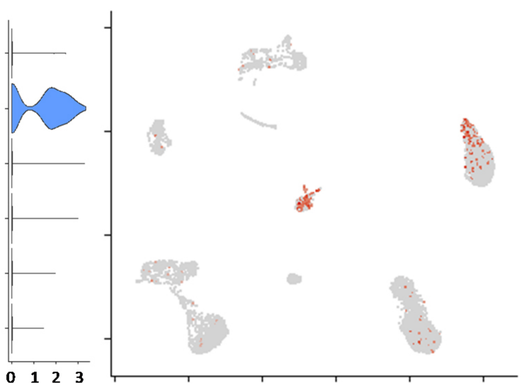

(b)

RA projecting neuron

SCUBE1

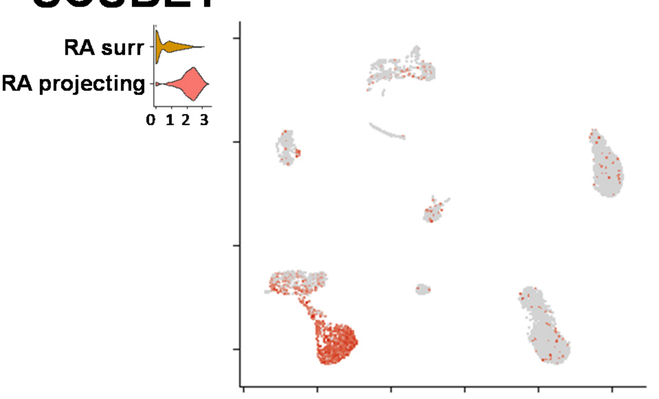

RA surrounding neuron

CACNA1H

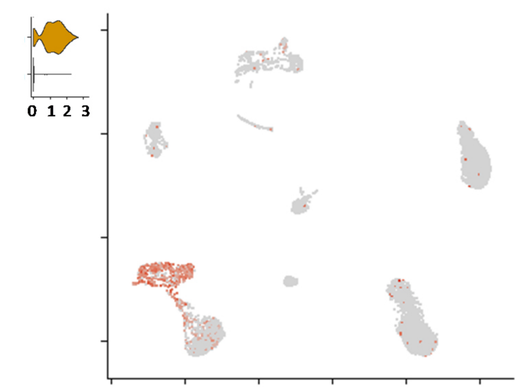

MGAT4C

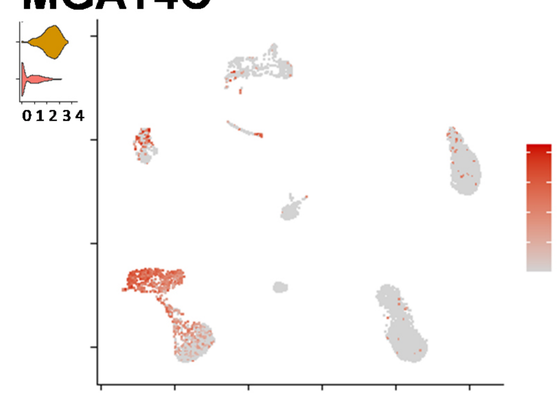

ADCYAP1

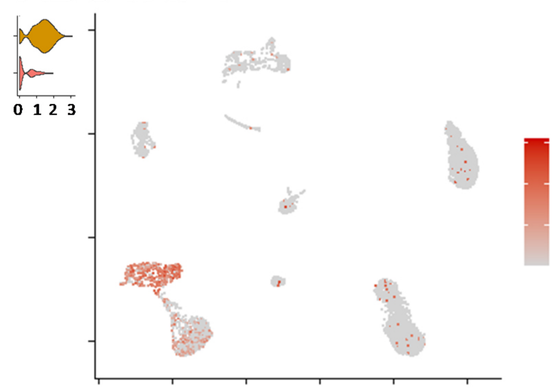

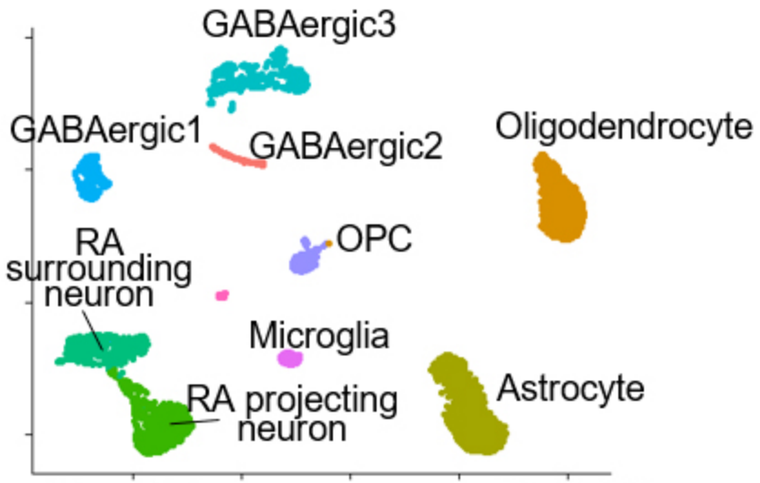
GABAergic3
GABAergic1
GABAergic2
Oligodendrocyte
OPC
RA surrounding neuron
Microglia
Astrocyte
RA projecting neuron

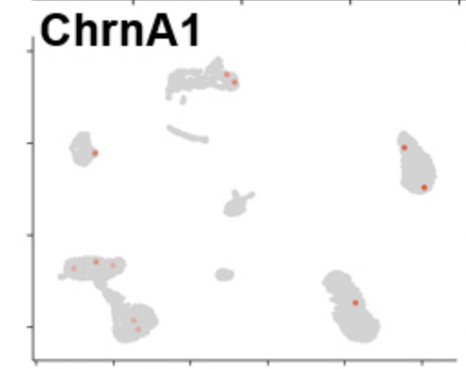
ChrnA1

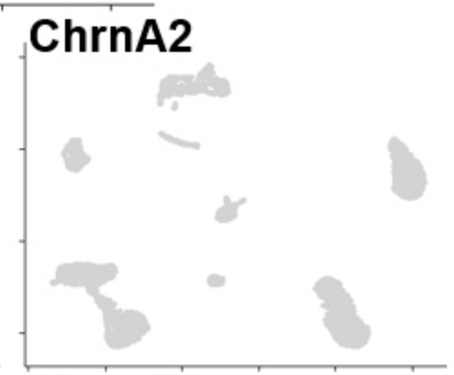
ChrnA2

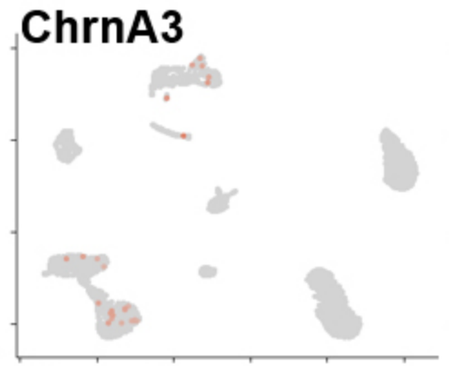
ChrnA3

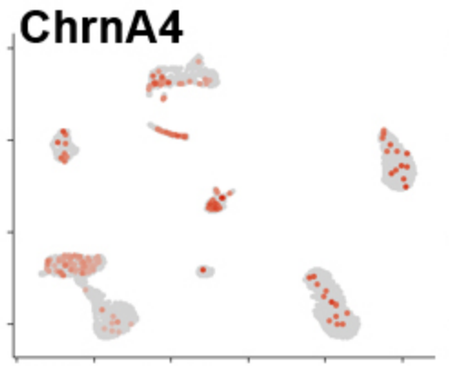
ChrnA4

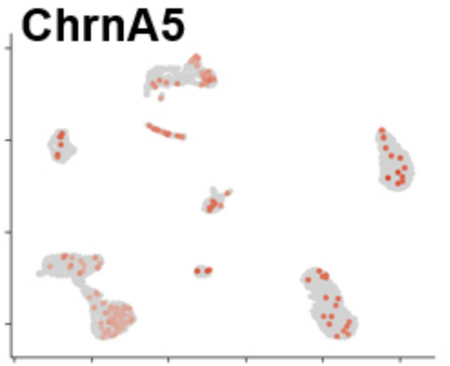
ChrnA5

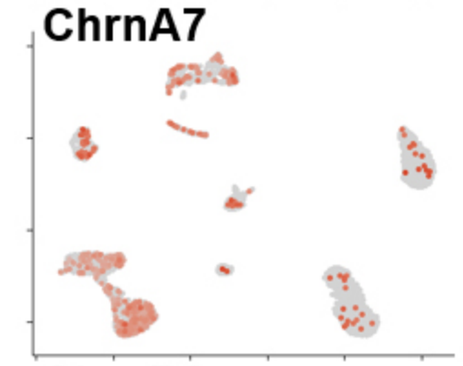
ChrnA7

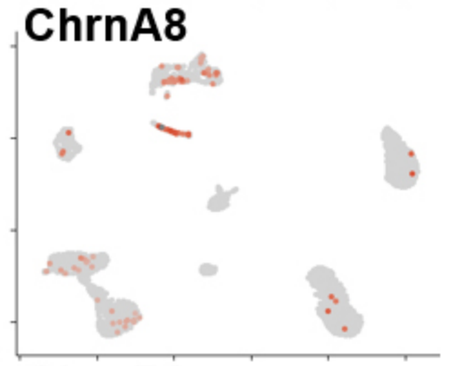
ChrnA8

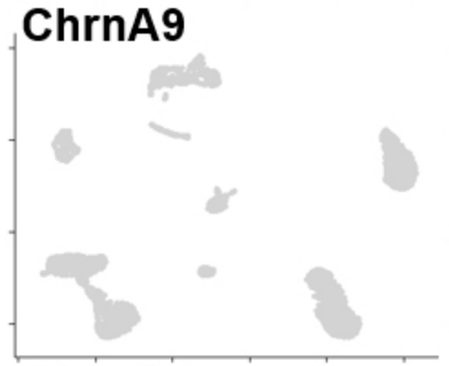
ChrnA9

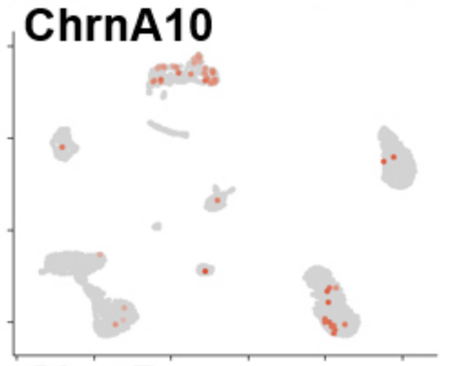
ChrnA10

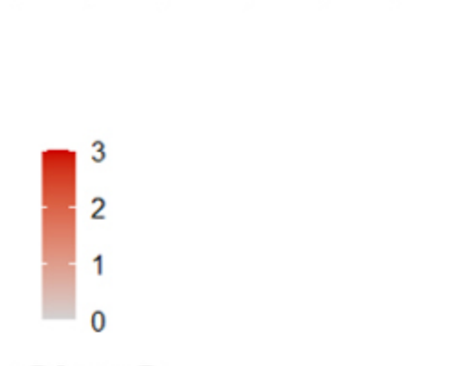
3
2
1
0

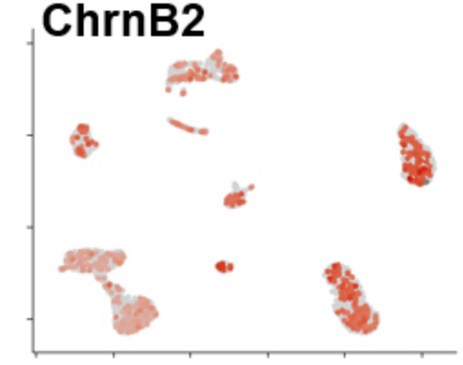
ChrnB2

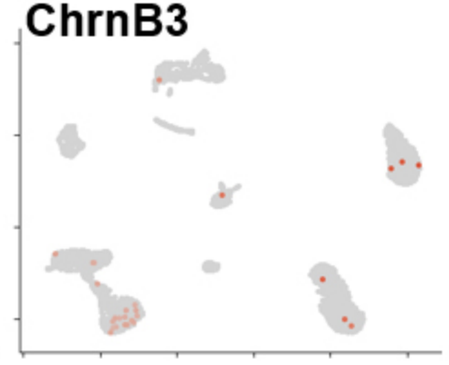
ChrnB3

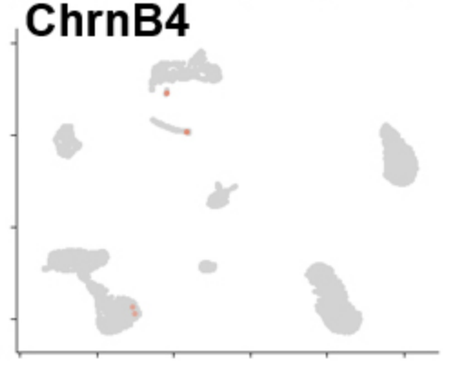
ChrnB4

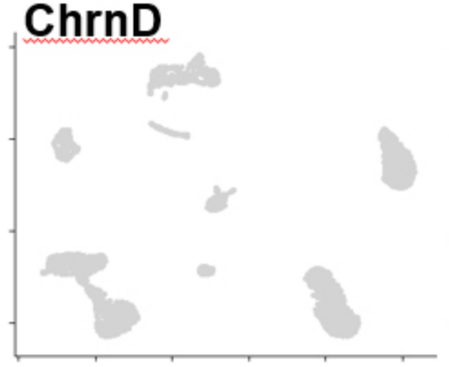
ChrnD

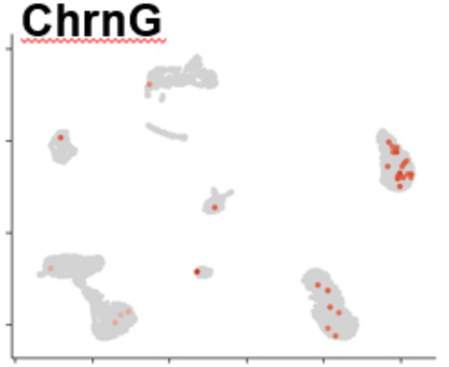
ChrnG

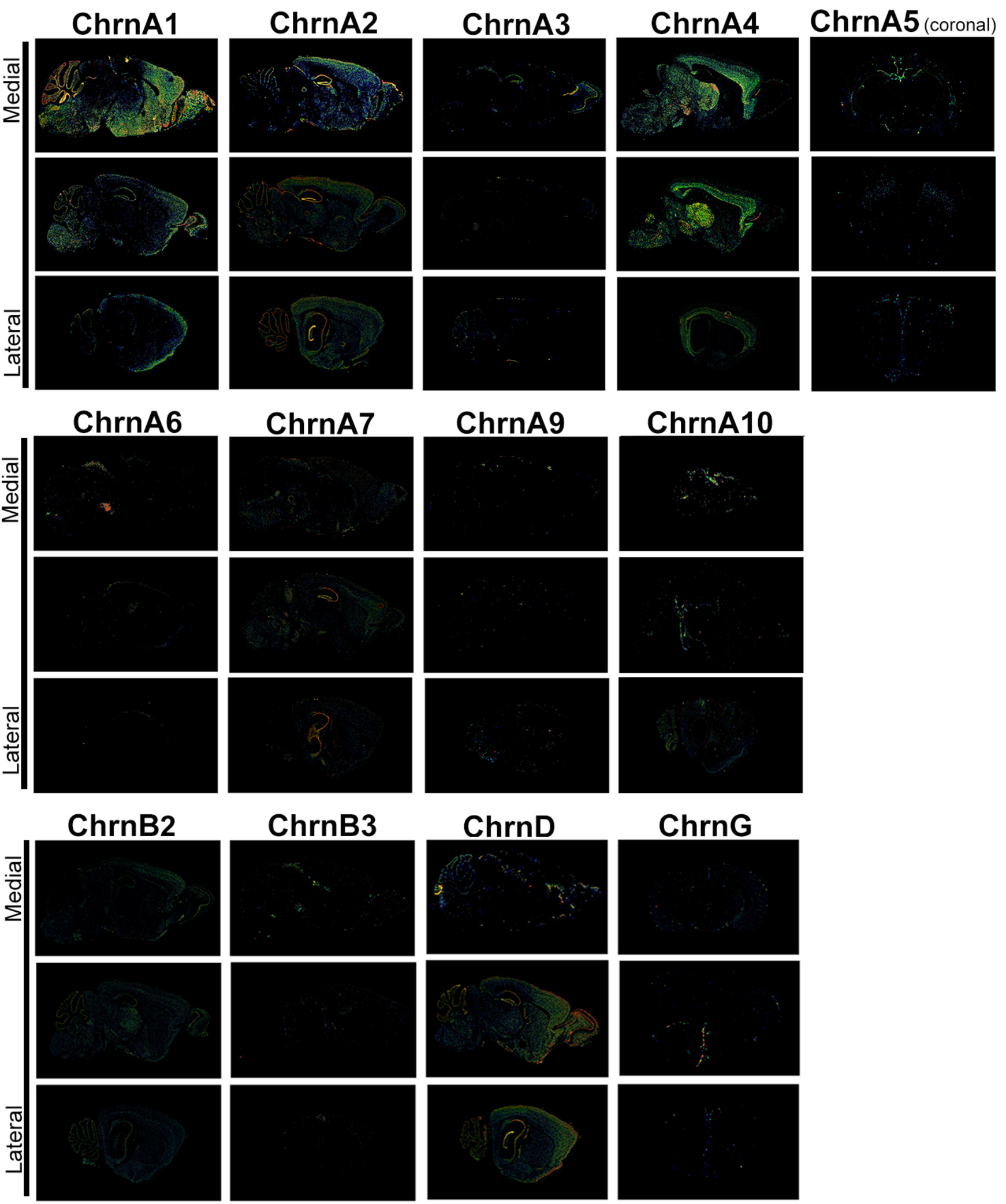
ChrnA1
ChrnA2
ChrnA3
ChrnA4
ChrnA5 (coronal)
Medial
Lateral
ChrnA6
ChrnA7
ChrnA9
ChrnA10
Medial
Lateral
ChrnB2
ChrnB3
ChrnD
ChrnG
Medial
Lateral

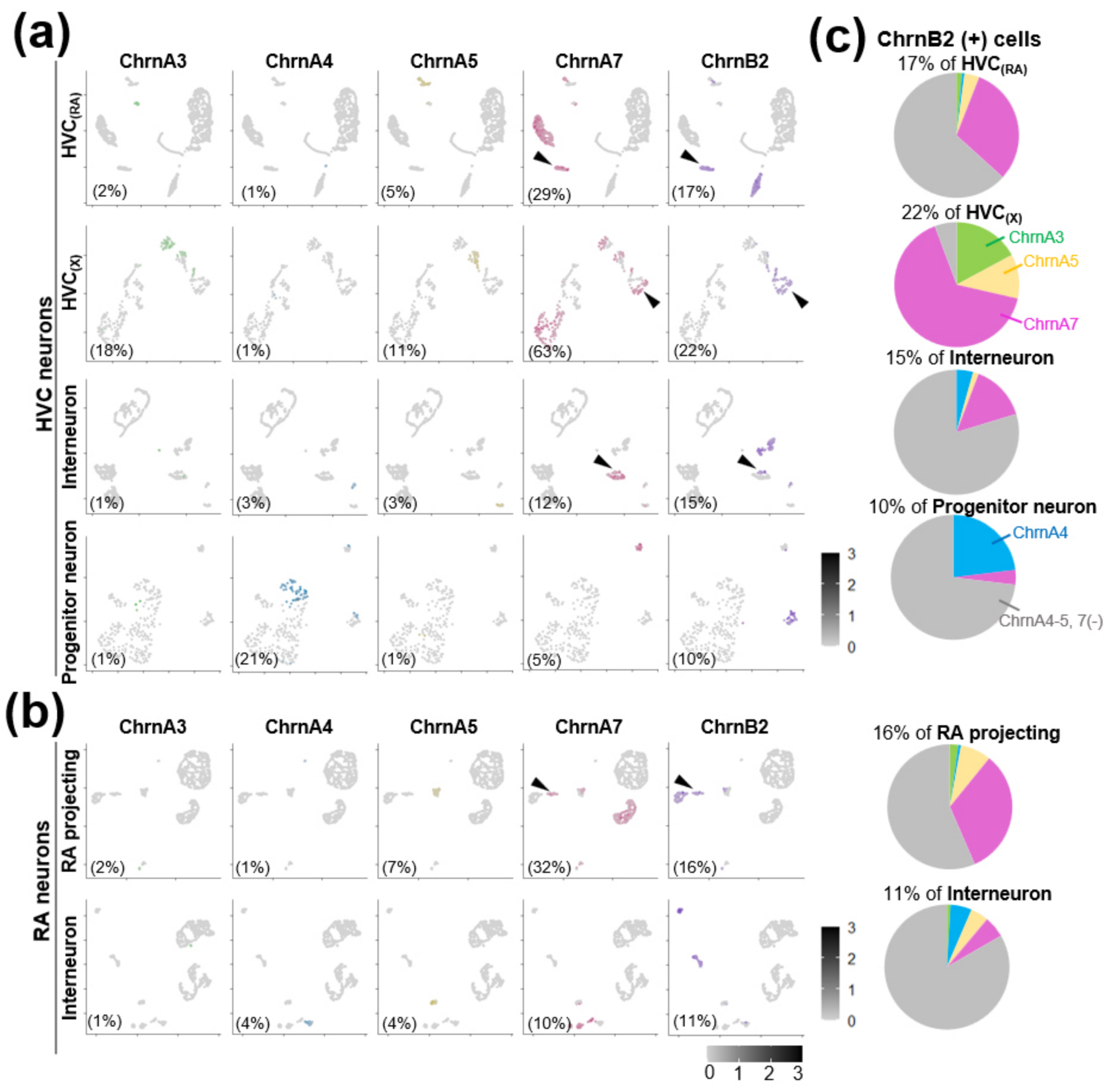
(a)
ChrnA3
ChrnA4
ChrnA5
ChrnA7
ChrnB2
HVC neurons
HVC(RA)
HVC(X)
Interneuron
Progenitor neuron
(2%)
(1%)
(5%)
(29%)
(17%)
(18%)
(1%)
(11%)
(63%)
(22%)
(1%)
(3%)
(3%)
(12%)
(15%)
(1%)
(21%)
(1%)
(5%)
(10%)
3
2
1
0
(b)
ChrnA3
ChrnA4
ChrnA5
ChrnA7
ChrnB2
RA neurons
RA projecting
Interneuron
(2%)
(1%)
(7%)
(32%)
(16%)
(1%)
(4%)
(4%)
(10%)
(11%)
0 1 2 3
(c)
ChrnB2 (+) cells
17% of HVC(RA)
22% of HVC(X)
ChrnA3
ChrnA5
ChrnA7
15% of Interneuron
10% of Progenitor neuron
ChrnA4
ChrnA4-5, 7(-)
16% of RA projecting
11% of Interneuron

(a)

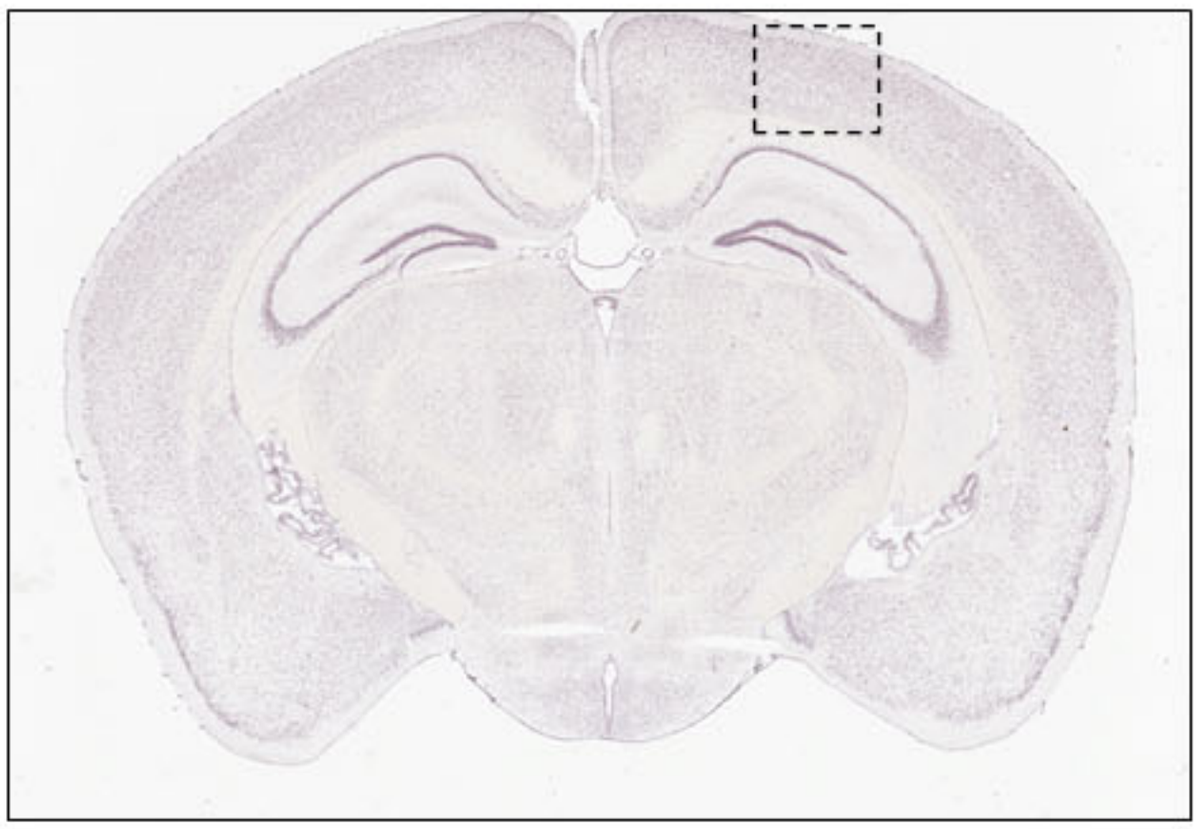

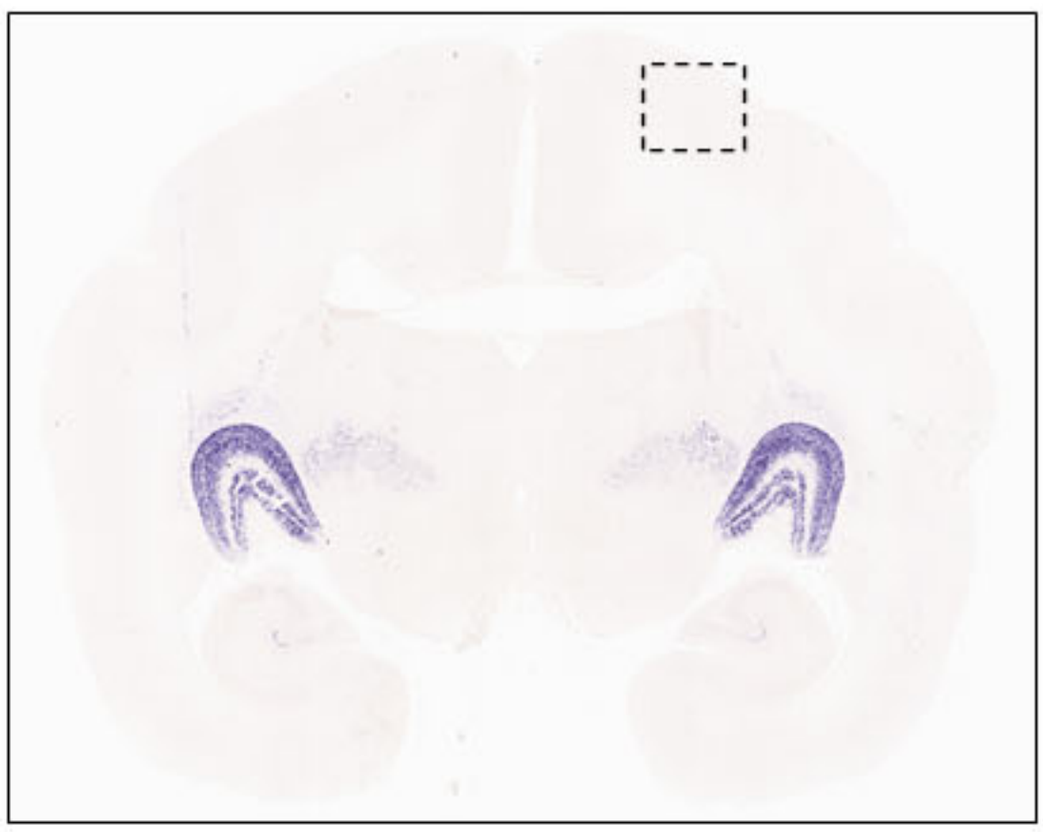

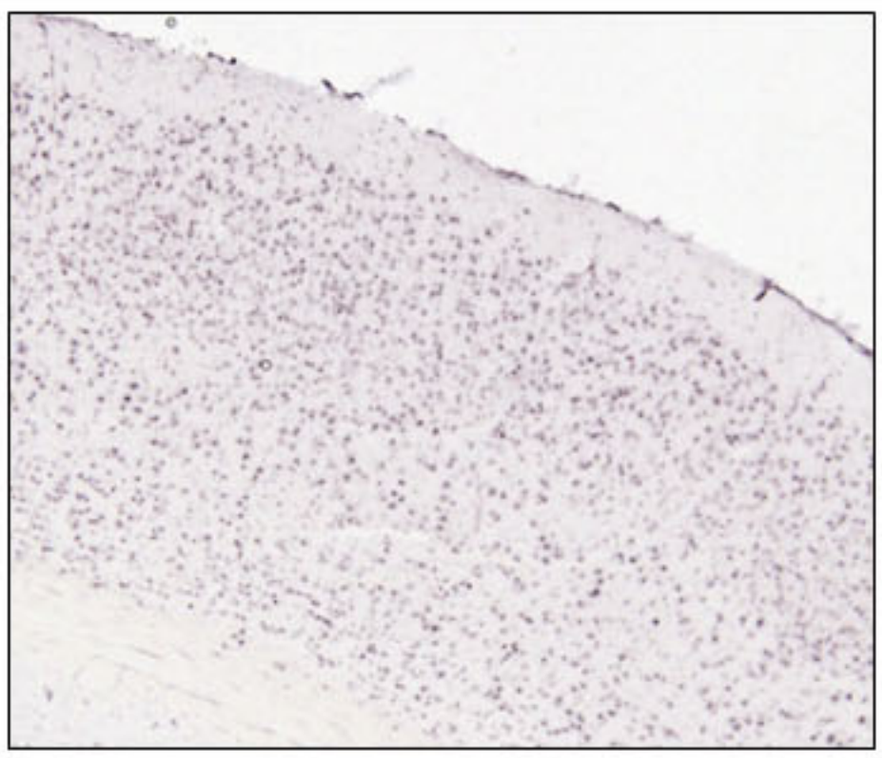

(b)

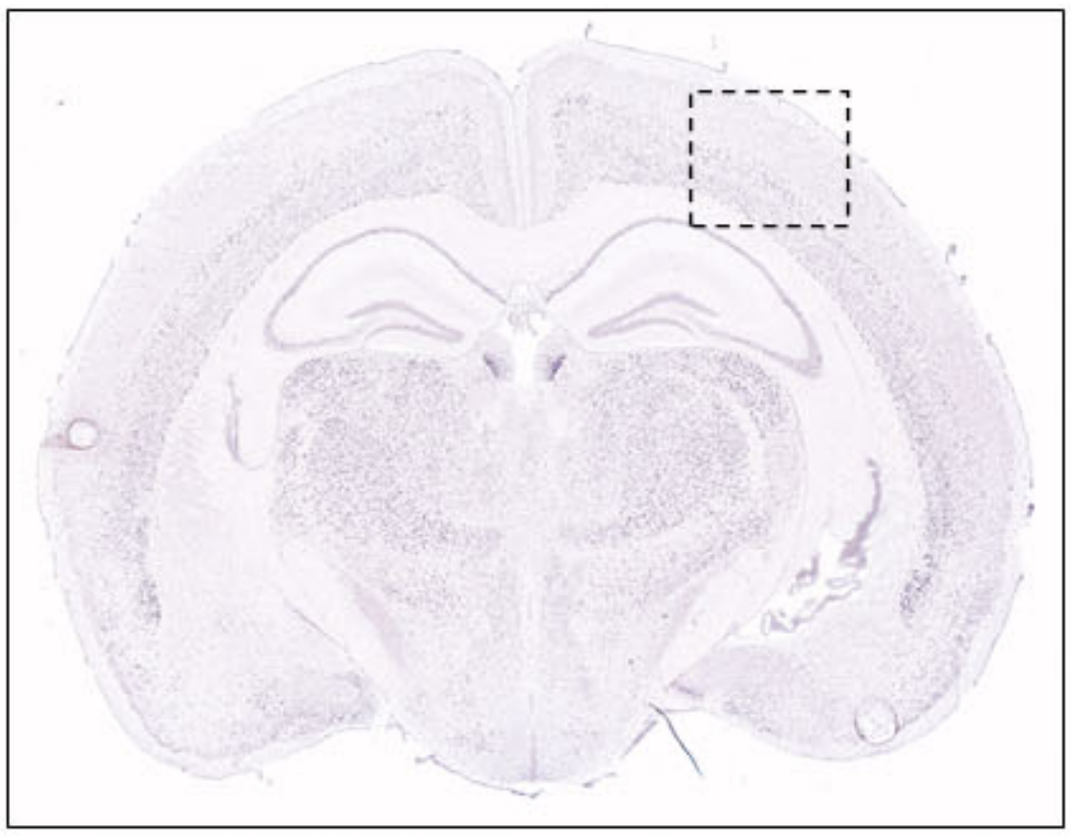

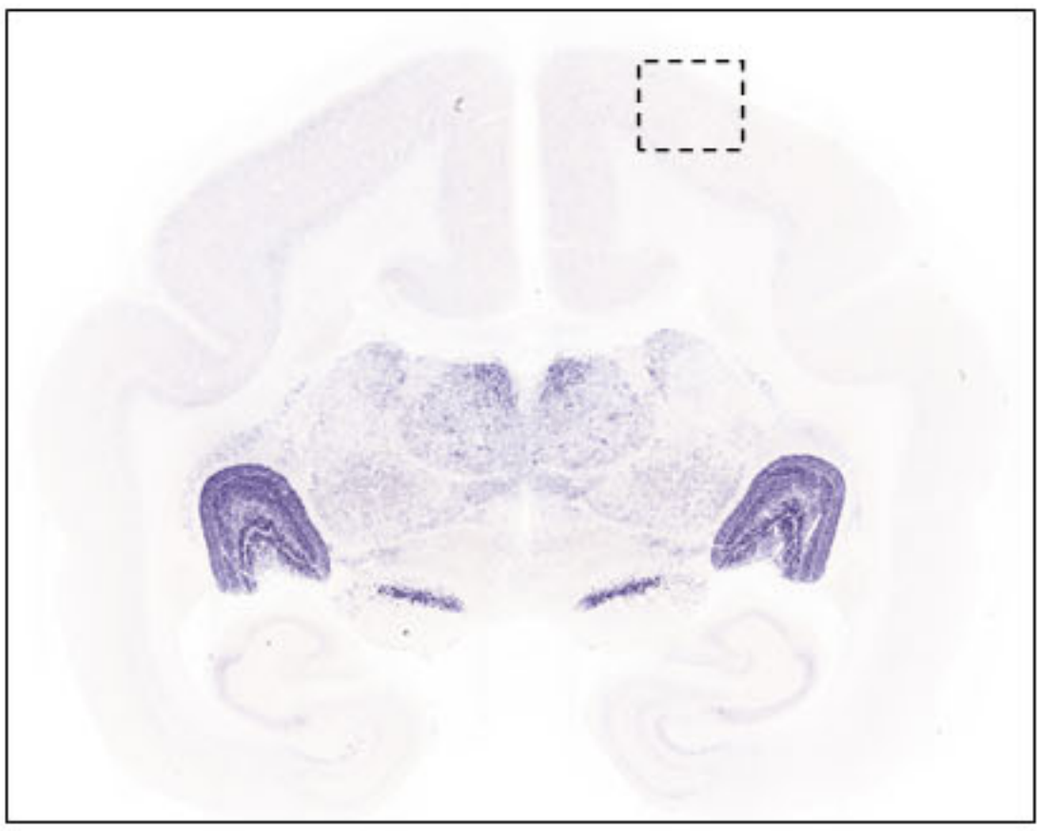

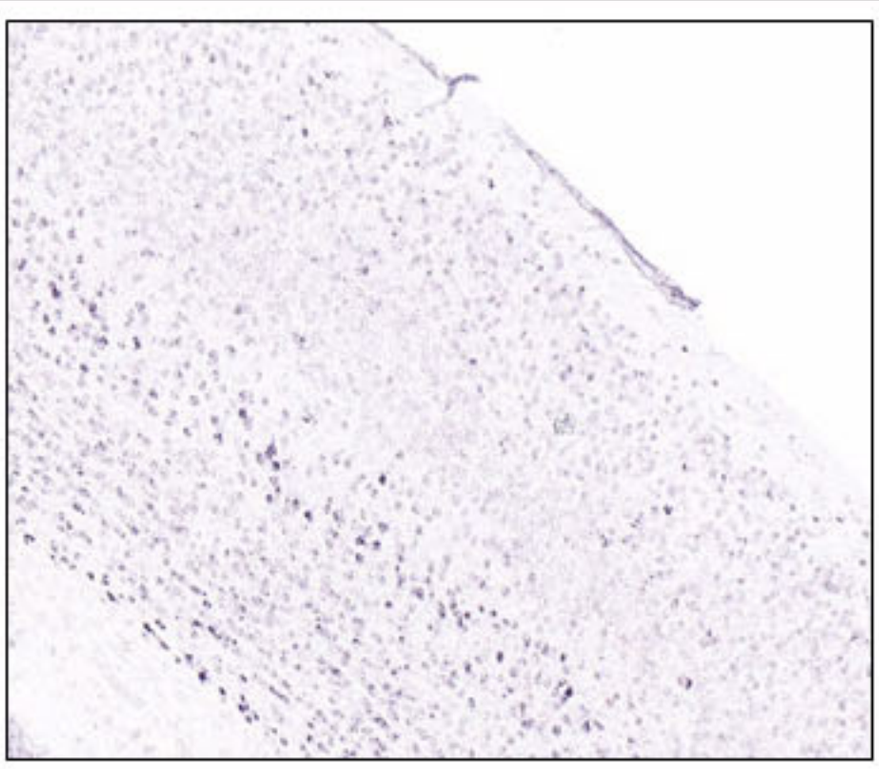

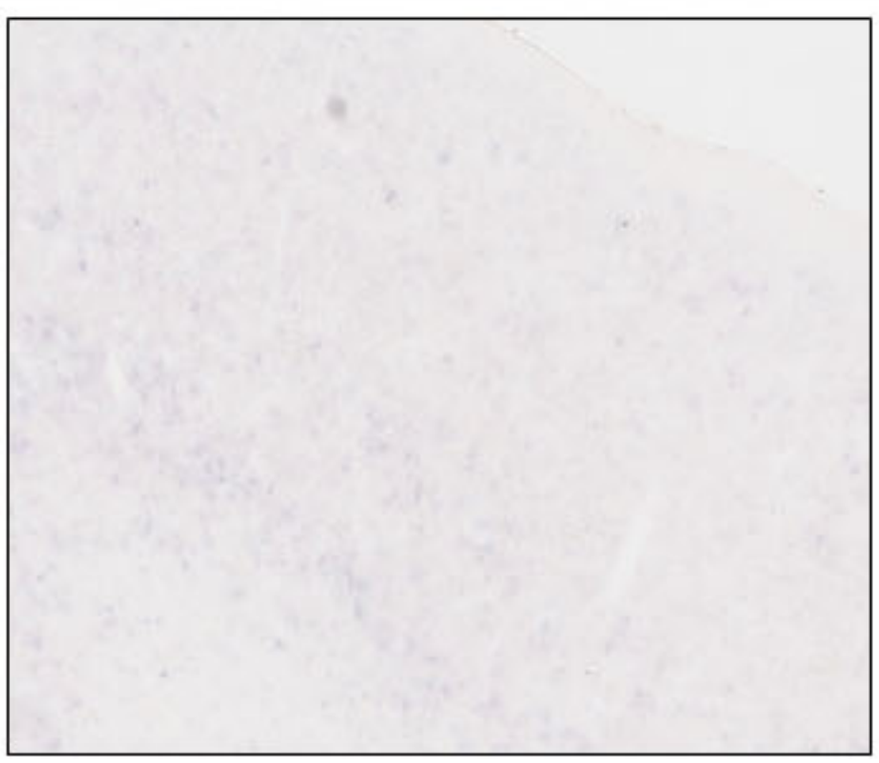

Cloned subunits in this study	Forward primer	Reverse primer	Cloned fragment length (bp)	Accession # of cloned subunits in this study	Accession # of zebra finch predicted nAChR mRNAs	Position at protein coding sequence	Similarity to zebra finch predicted nAChR proteins	Similarity to chicken nAChR proteins	Similarity to human nAChR proteisn
ChrnA1	5'- AATGGACAGACGTCAACCTC -3'	5'- CTGGAGGTGGAGGGAATCA -3'	592	OL679454	XM_002199046	86-282a.a./457a.a.	99% to XP_002199082	97% to NP_990147	89% to NP_000070
ChrnA2	5'- ACATCACCTTCTACTTCGTC- -3'	5'-CGATGATGAAGATCCAGAGG -3'	834	OL679455	XM_041715494	227-503a.a./522a.a.	100% to XP_041571428	73% to NP_990146	67% to NP_000733
ChrnA3	5'- AGTTGGGGATTTCCAGGTTG -3'	5'- GTTCCTAGAATACATACCAGG -3'	1,051	OL679456	XM_012569079	126-474a.a./496a.a.	100% to XP_012424533	96% to NP_989747	87% to NP_00073
ChrnA4	5'- TGATGACCACCAATGTGTGG -3'	5'- GCATGGACTCAATGAGCTTC -3'	842	OL679457	XM_012570240	84-363a.a./624a.a.	100% to XP_012425694	98% to NP_001384279	91% to NP_000735
ChrnA5	5'- TGGGTTCGTCCAGTGGAAC -3'	5'- GTGCAGAAATATCTTGCGAAC -3'	854	OL679458	XM_030281197	45-328a.a./445a.a.	100% to XP_030137058	99% to NP_989746	92% to NP_000736
ChrnA6	5'- CAAACTGCGATGGGATCCC -3'	5'- CTCTGTCTATCACCATAGCTA -3'	1,038	OL679459	XM_002188838	125-460a.a./493a.a.	99% to XP_002188874	93% to NP_990695	80% to NP_004189
ChrnA7	5'- CTGCAAGGAGAGTTCCAAAG -3'	5'- GAAGGCCATCAAGCAGAGC -3'	1,326	OL679460	XM_030281037	28-468a.a./502a.a.	100% to XP_030136897	98% to NP_989512	91% to NP_000737
ChrnA8 (7-like)	5'-GCTGCTTGTGGCTGAGATC-3'	5'-CAAACTTCCACTCACTGCAG-3'	563	OL679461	XM_002187662	285-471a.a./511a.a.	99% to XP_002187698	86% to NP_990532	N/A
ChrnA9	5'- TATGCTCACATGCTGTTTAATG -3'	5'- GAATCTCCCATTCCACATCTT -3'	486	OL679462	XM_030270964	6-166a.a./448a.a.	100% to XP_030126824	98% to NP_990091	91% to NP_060051
ChrnA10	5'- TTCGTGGAGAACGTGGAGTG-3'	5'- TGATCATGGTCATGGTGGCG-3'	303	OM201170	XM_030284731	203-302a.a./456a.a.	100% to XP_030140591	97% to NP_001094506	83% to NP_065135
ChrnB2	5'- AGCGGGAGCAGATCATGAC -3'	5'- CGCTGGTGACGATGGAGAA-3'	694	OL679463	XM_030291667	72-302a.a./491a.a.	99% to XP_030147527	99% to NP_990144	98% to NP_000739
ChrnB3	5'- TTACCATCCCATGGCACCC -3'	5'- CAAAGTGTTGTTCAGCCACAT -3'	354	OL679464	XM_002189012	331-448a.a./455a.a.	99% to XP_002189048	91% to NP_990143	79% to NP_000740
ChrnB4	5'- GGAAGCATGGCAGCAGATG -3'	5'- CTGGTAACTATTGAGAAGGTC -3'	730	OL679465	XM_030281195	26-298a.a.(spliced out 83-120a.a.)/489a.a.	100% to XP_030137055	99% to NP_990150	89% to NP_000741
ChrnD	5'- ATAGTCCTGGAGAACAACAATG -3'	5'- GCTTGTTCTCCTCCCGGTA -3'	1,169	OL679466	XM_030280650	121-509a.a./518a.a.	99% to XP_030136510	85% to NP_001026488	67% to NP_001298125
ChrnG	5'- ATCTCTGCCATGGCTGTGC -3'	5'- GCCTGGTTGAAGTGAGCCA -3'	690	OL679467	XM_030280649	258-487a.a./509a.a.	99% to XP_030136509	91% to NP_001026739	60% to NP_005190

Predicted zebra finch nAChR subunits		Cloned partial cDNAs to make *in-situ* hybridization probes														
Genbank accession#	nAChR subunits	ChrnA1	ChrnA2	ChrnA3	ChrnA4	ChrnA5	ChrnA6	ChrnA7	ChrnA8	ChrnA9	ChrnA10	ChrnB2	ChrnB3	ChrnB4	ChrnD	ChrnG
XM_002199046	ChrnA1	99.7	30.3	16.1	58.0	20.3	23.3	0.0	0.0	0.0	0.0	31.6	12.0	30.2	0.0	0.0
XM_041715494	ChrnA2	61.4	100.0	38.4	76.8	45.0	0.0	1.7	0.0	0.0	62.0	68.9	8.8	7.0	26.7	0.0
XM_012569079	ChrnA3	30.0	25.3	99.9	66.8	51.6	54.0	0.0	0.0	5.1	0.0	34.2	0.0	11.1	8.9	0.0
XM_012570240	ChrnA4	60.0	47.9	42.2	99.1	48.4	42.5	4.7	2.6	27.0	0.0	66.9	9.7	42.3	29.7	0.0
XM_030281197	ChrnA5	13.2	19.9	33.1	36.4	100.0	36.7	12.5	0.0	30.3	0.0	14.0	0.0	18.5	3.3	0.0
XM_002188838	ChrnA6	37.2	0.0	53.4	56.0	61.6	99.8	0.0	4.0	27.1	0.0	12.0	0.0	33.4	4.8	0.0
XM_030281037	ChrnA7	0.0	2.5	0.0	1.9	19.7	0.0	99.7	30.2	0.0	0.0	0.0	4.3	0.0	0.0	0.0
XM_002187662	ChrnA8 (7-like)	0.0	0.0	1.0	5.3	22.6	1.0	53.3	99.1	0.0	0.0	4.5	0.0	11.9	0.0	0.0
XM_030270964	ChrnA9	9.2	0.0	0.0	15.5	16.9	8.2	0.0	6.9	100.0	67.9	1.9	0.0	12.1	0.0	0.0
XM_030284731	ChrnA10	0.0	24.5	0.0	46.5	0.0	0.0	0.0	0.0	64.5	99.0	39.9	0.0	0.0	16.6	0.0
XM_030291667	ChrnB2	30.5	44.2	25.8	58.4	19.6	18.3	0.0	0.0	0.0	37.4	99.3	0.0	67.0	21.1	19.7
XM_002189012	ChrnB3	34.9	3.7	35.6	57.1	70.9	0.0	1.0	0.0	0.0	0.0	0.0	99.7	0.0	4.5	0.0
XM_030281195	ChrnB4	24.8	0.0	10.4	49.7	22.2	29.6	0.0	0.0	0.0	0.0	72.9	0.0	100.0	14.0	0.0
XM_030280650	ChrnD	0.0	29.3	9.6	12.9	4.1	5.6	0.0	0.0	0.0	43.9	46.3	0.0	21.9	99.4	22.7
XM_030280649	ChrnG	4.1	0.0	2.5	0.0	0.0	0.0	0.0	0.0	0.0	0.0	63.1	0.0	4.2	40.2	98.6